Title
Mechanisms of Action of Kinase Inhibitors in Chronic Myeloid Leukemia

Author
Gajan, Jennifer

Publication Date
2013

Mechanisms of Action of Kinase Inhibitors
in Chronic Myeloid Leukemia

by

Jennifer Kay Elizabeth Gajan

DISSERTATION

Submitted in partial satisfaction of the requirements for the degree of

DOCTOR OF PHILOSOPHY

in

Pharmaceutical Sciences and Pharmacogenomics

in the

GRADUATE DIVISION

of the

[redacted]

This dissertation is dedicated to my wonderful Neil and faithful Wendy.

Thanks for standing by me, walking with me, and for all the tail wagging every step of the way.

Acknowledgements

I would first like to thank Neil Shah for all of his support and guidance throughout my time here at UCSF. Neil has been an amazing mentor, particularly because he is a caring, understanding, and a patient physician-scientist. He has challenged me to see the smallest of details as well as the greater picture in every experiment I propose and perform. As a scientist, he has taught me not to be overwhelmed or intimidated by what might seem difficult initially, but instead to persevere and to move forward one step at a time. Thank you for challenging me to be independent and creative, for this I will always be grateful.

I would also like to thank the current and past members of the Shah lab for all of their support and understanding: Corynn Kasap, Chris Weier, Cathy Smith, Doris Kim, Bianca Lee, Beth Lasater, Gabe Reyes, Kimberly Lin, Whitney Stewart, and Ana Markovic. Without all of the streets we have biked, the pathways we have hiked, the songs we danced and sang, the chair races in the hall, the boxes we climbed into, the volleyball we played, the Sour Patch kids we ate, the yodeling pickle, and the laughs we have shared, graduate school would have been long, difficult, and lonely.

I would like to thank my family and friends for their love and support while I completed my graduate studies. My mom and Brooks, my dad and Hope, as well as my brother Joe and step-sisters, Katie and Laurie, for making holidays and extended weekends a wonderful way to take a break from the lab. I would also like to acknowledge my sweetheart Neil and our dog Wendy. Without the two of you, I would not be the woman and scientist I am today.

I would also like to thank my extended family here at UCSF, my fellow students as well as other postdoctoral fellows and faculty who have guided me, in many big and small ways, to the finish line. In particular, my fellow PSPG students for making the first few years in San Francisco feel like home, the members of the Passagué lab, Burlingame lab, Loh lab, and Müschen lab for always lending their ears and hands with new techniques and experiments, and the faculty members of the joint hematology group meeting on Fridays for their positive and constructive criticism throughout my time in the Shah lab.

Finally, I would like to thank my thesis committee members for all of their support and guidance: Kevin Shannon, Mike McManus and Al Burlingame. Thanks for all of the helpful scientific feedback, suggestions, and career advice. I feel lucky to have had the guidance and support of such inspiring scientists throughout the dissertation process.

Contributions to presented work

Chapter 2 of this dissertation contains material that is currently under revision at Cancer Discovery:

Gajan J., Tajon C., Oses-Prieto J., Lasater E., Jun Y., Taylor B.S., Burlingame A., Craik C., and Shah N.P. MEK-Dependent Negative Feedback Facilitates BCR-ABL-Mediated Oncogene Addiction. (Under revision).

I performed the studies described in chapter 2 under the guidance of Neil Shah (MD, PhD). Cheryl Tajon, Young-wook Jun (PhD), and Charles Craik (PhD) designed and analyzed the plasmonic nanosensor technique responsible for the detection of single molecule caspase-3 cleavage events. Juan Oses-Prieto (PhD) and Alma Burlingame (PhD) aided in the design and interpretation of the quantitative phosphoproteomic analysis. Elisabeth Lasater provided general experimental guidance and technical assistance in these studies. Barry Taylor provided experimental guidance and bioinformatic interpretation of the Illumina gene expression analysis.

Chapter 3 of this dissertation contains unpublished material:

Gajan J., Horng H., Benet L., Shah NP. High Dose Pulse-Mediated Apoptosis of CML Cells Results from the Intracellular Accumulation and Retention of BCR-ABL Kinase Inhibitors.

I performed the studies described in chapter 3 under the guidance of Neil Shah (MD, PhD). Howard Horng (PhD) and Les Benet (PhD) are responsible for the LC-MS/MS experimental design and analysis of extracellular and intracellular inhibitor concentrations following high dose pulse treatment.

Chapter 4 of this dissertation contains unpublished material that is currently in preparation:

Gajan J., Shah NP. Aurora B is the Critical Kinase Target of Dual ABL/Aurora Inhibitors in Chronic Myeloid Leukemia Cells. (In preparation).

I performed the studies described in chapter 4 under the guidance of Neil Shah (MD, PhD).

Abstract

Mechanisms of Action of Kinase Inhibitors

in Chronic Myeloid Leukemia

Jennifer Kay Elizabeth Gajan

Oncogene addiction refers to a cancer cell's reliance upon the continued activity of a particular oncogene for survival. This concept has been clinically validated by the success of tyrosine kinase inhibitor (TKI) therapy in chronic myeloid leukemia (CML). CML is a clonal myeloproliferative neoplasm that is initiated by a single chromosomal translocation event, which results in the formation and expression of the *BCR-ABL* fusion gene. This gene encodes a protein also called BCR-ABL that exhibits constitutive tyrosine kinase activity, thereby promoting increased cellular proliferation. TKI therapy results in the inhibition of BCR-ABL kinase activity and induces deep and durable responses in the majority of patients with the chronic phase of the disease. In contrast, kinase inhibitor therapies in other activated kinase driven malignancies, although successful, have failed to achieve the same extent of durable disease remissions observed in CML. Here, we have sought to investigate the mechanism(s) responsible for the exquisite sensitivity of CML cells to TKI therapy. Using an isogenic system and patient-derived CML cell lines we have discovered that BCR-ABL-dependent negative feedback is responsible for the attenuation of growth factor-receptor (GF-R) signaling in CML cells. Furthermore, we have found that BCR-ABL-dependent negative feedback persists for an extended period of time following the initiation of dasatinib or imatinib treatment, during which CML cells commit to apoptosis. Experiments performed using a selective MEK inhibitor revealed BCR-ABL-mediated

negative feedback to be largely MEK-dependent. Our findings are in contrast to what has been observed in BRAF-V600E-dependent malignancies, where MEK-dependent negative feedback is rapidly attenuated following BRAF inhibitor treatment. This work has also validated the importance of the RAS/MAPK, STAT5A/B, and S6 signaling pathways in BCR-ABL-mediated oncogene addiction. Additional studies investigating the mechanism of apoptosis in CML cells treated transiently with potent concentrations of BCR-ABL inhibitors revealed that intracellular accumulation of the BCR-ABL kinase inhibitors imatinib and dasatinib results in prolonged BCR-ABL kinase inhibition. Interestingly, apoptosis following transient kinase inhibitor therapy *in vitro* has been described for epidermal growth factor receptor (EGFR) and Fms-like tyrosine kinase 3 (FLT3) inhibitors, suggesting that this phenomenon is not restricted to BCR-ABL kinase inhibitors. In contrast to the BCR-ABL tyrosine kinase inhibitors imatinib and dasatinib, the dual ABL/Aurora kinase inhibitors XL228, danusertib (PHA-739358), and MK-0457 appear to mediate cytotoxicity through inhibition of the Aurora kinases, namely Aurora B. We have shown that expression of BCR-ABL in a cell line harboring a drug resistant mutation in Aurora B confers biochemical cross-resistance to dual ABL/Aurora inhibitors. However, the clinical efficacy of dual ABL/Aurora kinase inhibitors in CML patients suggests that Aurora B may represent an adjunctive therapeutic target in CML. In conclusion, the work presented here provides novel insight into the mechanisms of action BCR-ABL kinase inhibitors in CML by providing a potential explanation for why BCR-ABL-expressing cells are exquisitely sensitive to TKI therapy, proposing a mechanistic explanation for the effectiveness of transient kinase inhibitor therapy, and identifying the critical cellular target of clinically active dual ABL/Aurora kinase inhibitors in CML cells.

Table of Contents

List of Tables

Chapter 2

Chapter 4

List of Figures

Chapter 2

Chapter 3

Chapter 4

Chapter 1

Introduction

Part I: Chronic Myeloid Leukemia

1. Molecular Pathogenesis

Chronic myeloid leukemia (CML) is a myeloproliferative neoplasm characterized by the expansion of committed myeloid progenitors and terminally differentiated myeloid lineage cell types (1). Identifying the molecular mechanism responsible for the development of CML spanned several decades, but a chromosomal translocation was determined to be the initiating leukemic event (2, 3). CML represents a unique human malignancy in that one genetic abnormality appears to be responsible for disease initiation and maintenance, whereas other cancers are heterogenous in nature and can be comprised of polyclonal cell populations containing many different genetic abnormalities and mutations.

Clinically, CML is characterized by three disease phases. Chronic phase is the initial phase of the disease and is characterized by the presence of increased, differentiated myeloid cell populations (1). Chronic phase typically lasts for several years before transitioning into an accelerated phase, which is believed to be initiated by the acquisition of additional cytogenetic abnormalities and mutations (4). The final phase of the disease is blast crisis, which is characterized by increased immature, undifferentiated myeloid or lymphoid cells proliferating in an unrestricted manner (1). Prior to the discovery of the tyrosine kinase inhibitor imatinib the only curative therapy available for CML patients was an allogeneic bone marrow transplant (5). However, the discovery and clinical use of imatinib and other tyrosine kinase inhibitors has transformed CML into a manageable

disease in most cases. Patients treated with imatinib in the chronic phase of CML typically exhibit sustained clinical responses without disease progression (6).

CML is initiated by a chromosomal translocation involving the long arms of chromosome 9 (9;34) and chromosome 22 (22;11). This rearrangement fuses the end of the long arm of chromosome 9 to the long arm of chromosome 22 and is commonly referred to as the Philadelphia chromosome (Ph) (2, 3). The tyrosine kinase *c-ABL* resides at the translocated region of chromosome 9 and the region of chromosome 22 where *c-ABL* is transposed is termed the breakpoint cluster region (*BCR*) because of its involvement in the Ph chromosome translocation (7, 8). The fusion gene and corresponding protein that is generated as a result of the reciprocal translocation is therefore referred to as BCR-ABL.

The location of the breakpoint between *c-ABL* and *BCR* determines the allele type and molecular weight of the expressed BCR-ABL fusion protein. In CML, *c-ABL* is typically translocated to the major breakpoint cluster region (M-*bcr*) between exon b2 and b3 of *BCR* resulting in a fusion kinase with a molecular weight of 210 kilodaltons (kDa) in the majority of patients (9). However, in ≥ 50% of Ph positive acute lymphoblastic leukemia (ALL) patients, *c-ABL* is fused to *BCR* at the minor breakpoint cluster region (m-*bcr*) resulting in a smaller 190kDa allele of BCR-ABL (9). Subsequent discussion will focus on the 210kDa allele of BCR-ABL, as this allele is more relevant for the initiation and maintenance of CML.

2. BCR-ABL Structure

The N-terminal portion of the 210kDa BCR-ABL allele is typically comprised of exon 1 through exon 13 or 14 of *BCR* (9). Protein domains within this portion of *BCR* include a

coiled-coiled (CC) domain, a serine/theronine kinase domain, and a RAC/CDC42 GTPase domain (10-12). The functional importance of each protein domain in the setting of CML has been extensively interrogated. In particular, the CC-domain of BCR is critical for BCR-ABL activation and transforming abilities, both *in vitro* and *in vivo* (13, 14). Mechanistically, the CC-domain is responsible for the homotetramerization of BCR-ABL molecules in the cell, which subsequently allows for BCR-ABL transphosphorylation and kinase activation. Tyrosine 177 (Y177) of the N-terminal BCR region plays a critical role in BCR-ABL-mediated activation of downstream signaling pathways. Mutation of this tyrosine to phenylalanine (Y177F) has been found to inhibit BCR-ABL-mediated transformation of cell lines and primary cells *in vitro*, as well as alter disease phenotype and delay disease onset *in vivo* (14, 15).

The C-terminal portion of BCR-ABL contains nearly the entire c-ABL protein, usually exons 2 through 11 (4). The *c-ABL* gene encodes a non-receptor, cytoplasmic tyrosine kinase that is a member of the ABL family of kinases, which also includes c-ABL-related gene (*ARG*). The ABL kinases are structurally similar to Src family kinases (SFK) and contain an N-terminal Src-homology 3 (SH3) domain capable of binding proline rich protein sequences, a Src-homolgy 2 (SH2) domain capable of binding consensus phosphotyrosine motifs, and a Src-homology 1 (SH1) or tyrosine kinase domain (16). The ABL kinases also possess an extended C-terminal region that contains F-actin binding motifs allowing the ABL kinases to participate in regulation of cytoskeleton dynamics. Normal c-ABL kinase activity is tightly regulated through various intramolecular interactions involving an N-terminal myristoylation modification located within the first exon of *c-ABL* and the C-terminal lobe of the c-ABL kinase domain (17, 18). Loss of the first

exon and N-terminal myristoylation in the BCR-ABL fusion protein is believed to interrupt these critical autoinhibitory interactions, promoting constitutive kinase activation.

3. CML Signaling Pathways

The constitutive kinase activity of BCR-ABL activates a number of signaling pathways in the cell that are typically activated by growth factor-receptors (GF-R) and receptor tyrosine kinases (RTK) following ligand stimulation. These include the RAS/MAPK, PI3K/AKT, and STAT5 signaling pathways. Deregulation of these pathways as a result of mutation or upstream kinase activation is implicated in a broad range of human malignancies (19). For the purpose of this discussion, these three pathways will be referred to as the "canonical" BCR-ABL signaling pathways in CML.

The RAS/MAPK signaling pathway is one of the major mitogenic pathways activated by BCR-ABL kinase activity. RAS is a GTP-binding protein that cycles between the GTP-loaded ("on-state") and GDP-loaded ("off-state") with the help of guanine exchange factors (GEFs) like the son of sevenless homolog 1 and 2 proteins (SOS-1, SOS-2) and GTPase activating proteins (GAPs) like neurofibromin-1 (NF1) (20). RAS-GTP activates various cellular pathways, including the RAF/MEK/ERK and the PI3K/AKT signaling pathways (19). In CML, BCR-ABL expressing cell lines have been documented to exhibit growth factor-independent RAS-GTP loading *in vitro* (21). It was subsequently determined that recruitment of the adaptor protein growth factor receptor-bound protein 2 (GRB2) in complex with SOS-1 to phospho-Y177 in the N-terminal portion of BCR is necessary for BCR-ABL-mediated activation of the RAS/MAPK signaling pathway (15, 22).

The phosphatidylinositol-3 kinase (PI3K)/AKT pathway is the second major canonical pathway that is activated by BCR-ABL kinase activity. Traditionally, PI3K is activated following ligand stimulation of an RTK or GF-R via recruitment to phosphorylated tyrosine residues on the intracellular region of the activated receptor (23). Recruitment of PI3K to the receptor tail and plasma membrane is responsible for the generation of the second messenger phosphatidylinositol-3,4,5-triphosphate (PIP3), which results in the activation of AKT and its downstream pathway effectors. It has been documented that RNA silencing of the p85 regulatory subunit of PI3K inhibits the proliferation of BCR-ABL expressing cell lines and primary CML patient samples (24). BCR-ABL is proposed to activate the PI3K/AKT pathway by recruiting the p85 regulatory subunit to the tyrosine phosphorylated GRB2/GRB2-associated-binding protein 2 (GAB2) scaffolding complex, which is associated with BCR-ABL via phospho-Y177 in the N-terminal region of BCR (25).

Constitutive STAT5A/B signaling is the third canonical pathway upregulated by BCR-ABL kinase activity in CML cell lines and primary CML patient samples. STAT5A and STAT5B represent two of seven signal transducer and activation of transcription (STAT) mammalian family members that, like RAS and PI3K, are traditionally activated following GF-R or RTK stimulation (26). The phosphorylation of STAT5A/B was shown to be dependent on BCR-ABL kinase activity and STAT5A/B-DNA binding complexes have been observed in BCR-ABL expressing cell lines (27, 28). The SH2 and SH3 domains of BCR-ABL appear to be critical for STAT5A/B phosphorylation, as deletions or mutations in these regions prevent STAT5A/B activation and inhibit BCR-ABL-mediated leukemogenesis (29).

Whether STAT5A/B is a direct substrate of BCR-ABL or is phosphorylated by JAK2 in CML cells has been an ongoing topic of debate. Older studies suggest that JAK2 is

phosphorylated, is potentially responsible for the tyrosine phosphorylation of GAB2, but is not critically involved in the phosphorylation of STAT5A/B in BCR-ABL expressing cells (27, 28, 30, 31). However, recent experimental evidence has more clearly defined the importance of JAK2 in CML. Hantschel et al used a mouse model to conditionally delete JAK2 in the hematopoietic compartment and documented that JAK2 is dispensable for BCR-ABL-mediated transformation and disease maintenance in the myeloid lineage (32). In the same study the authors documented that any apoptotic effects mediated by JAK2 kinase inhibitors in CML cells are likely due to previously unappreciated, unintended BCR-ABL kinase inhibition.

The importance of RAS/MAPK, PI3K/AKT and STAT5A/B canonical signaling pathways in BCR-ABL-mediated leukemogenesis and CML cell survival has been interrogated using various experimental approaches. Expression of dominant negative (DN) alleles of RAS (N17), STAT5 (694F), and p85 (Δp85) in K562 cells, a patient-derived CML cell line, inhibited cellular proliferation and the inhibitory effect was increased when any of the two DN alleles were co-expressed in the same population (33). Expression of DN RAS (N17) alone induced a minimal degree of apoptosis, whereas co-expression with another DN allele increased the amount of apoptosis observed (33). Similar inhibitory effects on CML cell proliferation and viability have been replicated in other studies, which targeted various components of the three canonical BCR-ABL signaling pathways using different DN alleles and RNA-mediated gene silencing (34, 35).

4. Oncogene Addiction

Cancer has been postulated to be the result of a multi-step process resulting from the accumulation of mutations in oncogenes and tumor suppressors in the right cellular context. However, critical work performed using various transgenic, inducible gene expression systems *in vivo* and *in vitro* documented that an oncogene responsible for the initiation of disease could also retain importance in the process of disease maintenance (36-38). This concept of dependence is referred to as oncogene addiction. By definition, oncogene addiction refers to the state of dependency established by the expression of an oncogene such that the cell has become reliant on the continued activity of the expressed oncogene for survival (39). It is now appreciated that an oncogene responsible for this type of dependence does not have to be an initiating genetic event (40). The clinical implications of these findings suggest that under the right circumstances antagonizing the activity of an initiating oncogene may result in a substantial reduction in tumor burden. As will be discussed in more detail below, the discovery and success of tyrosine kinase inhibitor (TKI) therapy in CML represented the first clinical validation of oncogene addiction. Targeted inhibition of the initiating oncogene BCR-ABL induced rapid and sustained disease responses in CML patients and importantly, mutational reactivation of BCR-ABL resulted in disease progression documenting a continued dependence on BCR-ABL kinase activity for CML cell survival and disease pathogenesis.

Part II: Kinase Inhibitors in CML

1. BCR-ABL Tyrosine Kinase Inhibitors

The clinical success of the first-generation BCR-ABL tyrosine kinase inhibitor (TKI) imatinib initiated the era of targeted cancer therapy. Since the discovery of imatinib, a number of other clinically active kinase inhibitors have been developed for various types of malignancies. Although some targeted agents have come close in terms of initial disease response, like AC220 in FLT3-dependent acute myeloid leukemia (AML) and erlotinib in EGFR-dependent non-small cell lung cancer (NSCLC), the observed number of durable responses achieved with these inhibitors is only a fraction of those achieved by BCR-ABL inhibitors in chronic phase CML (40, 41). Additional BCR-ABL inhibitors have since been developed to circumvent imatinib resistance, including the second-generation inhibitor dasatinib and the third-generation inhibitor ponatinib.

Mechanistically, BCR-ABL inhibitors bind to the active site of the c-ABL kinase domain thereby preventing ATP-binding, substrate phosphorylation, and downstream pathway activation. The crystal structure c-ABL bound to imatinib revealed binding to an inactive confirmation of c-ABL, where the activation loop is unphosphorylated and folded into the kinase domain to prevent substrate binding (42). In contrast, the crystal structure of c-ABL bound to dasatinib revealed binding to an active confirmation, where the activation loop is phosphorylated and extended away from the active site (43). Differences in the chemical structure of imatinib and dasatinib affect which residues in c-ABL are critical for inhibitor binding, with one exception. The hydroxyl group of threonine 315 (T315) in the kinase domain of c-ABL creates a critical hydrogen bond with both inhibitors

and mutations at this residue confer resistance to all clinically relevant first- and second-generation BCR-ABL inhibitors

The observed clinical responses to front-line first- or second-generation BCR-ABL kinase inhibitor therapy in chronic phase CML are dramatic and durable. In the initial phase I clinical trial of imatinib, nearly every chronic phase CML patient enrolled achieved a complete hematological response (44). A similar response rate was observed in the phase I clinical trial of dasatinib (45). Long-term response rates to BCR-ABL inhibitor therapy are favorable, and in one 6-year follow-up study there was an 88% overall survival rate of CML patients treated with imatinib as front-line therapy (46). In conclusion, the discovery and successful use of BCR-ABL TKIs in the treatment of CML has changed how we envision targeted therapy and define disease response. Furthermore, the efficacy of TKI therapy in the treatment of CML was the first clinical demonstration of oncogene addiction and validated the importance of BCR-ABL kinase activity in the pathogenesis of this disease.

2. Pharmacokinetics of BCR-ABL Tyrosine Kinase Inhibitors

Since the discovery and clinical development of dasatinib, there has been an ongoing discussion about the necessity of continuous BCR-ABL kinase inhibition and disease remission. The half-life ($t_{1/2}$) of dasatinib is much shorter than all other approved BCR-ABL kinase inhibitors, yet dasatinib is no less effective clinically. This pharmacokinetic property of dasatinib raises an interesting question: is continuous BCR-ABL kinase inhibition necessary for a response to TKI therapy in CML?

The first clinical and pharmacokinetic assessment of once daily imatinib in CML patients documented that dephosphorylation of the adaptor protein CRKL correlated with disease response (44). CRKL is a direct substrate of BCR-ABL and the phosphorylation status of CRKL at tyrosine 207 (Y207) can be used as a pharmacodynamic measure of BCR-ABL kinase inhibition (47). Several studies have documented the $t_{1/2}$ of imatinib to be between 13-16 hours in patients treated with 400mg once daily (44, 48). Trough levels of imatinib have been approximated to be 1μM-1.46μM in patients treated with 350mg or 400mg of imatinib once daily, which is above the value necessary for the inhibition of primary CML cell colony growth *in vitro* (44, 49, 50). The metabolism of imatinib *in vivo* was also documented to produce an active metabolite with a long $t_{1/2}$ in CML patients (48). From these early clinical observations it was presumed that continuous BCR-ABL inhibition would be necessary to achieve disease remission in CML.

Similar to imatinib, the second and third generation BCR-ABL inhibitors nilotinib and ponatinib also exhibit an extended $t_{1/2}$ in CML patients. In the initial clinical trial of nilotinib, the $t_{1/2}$ was approximated to be 15 hours in patients treated with 400mg twice daily, while the trough plasma level of drug was measured near 1μM (51). The recorded trough level of nilotinib in CML patients is nearly 100-fold higher than the half-maximal inhibitory concentration (IC_{50}) of the patient-derived CML cell line, K562 (12nM) (52). CML patients treated with this dose of nilotinib should experience extended BCR-ABL kinase inhibition throughout the dosing regimen. Ponatinib, the third generation BCR-ABL inhibitor with activity against the T315I mutation, has a documented $t_{1/2}$ of 22 hours in CML patients treated with 30 mg once daily (53). The recorded trough level of ponatinib at this dose is ≥ 40nM, which is approximately 10-times the IC_{50} of K562 cells (4nM) (53, 54).

Again, CML patients treated with this dose of ponatinib should experience extended BCR-ABL kinase inhibition throughout the dosing regimen.

In contrast, the second-generation TKI dasatinib is unique amongst BCR-ABL kinase inhibitors. In preclinical models, dasatinib was documented to exhibit a short $t_{1/2}$ of only one to three hours *in vivo* (55, 56). Rats treated with an oral dose of 10mg/kg of dasatinib achieved a peak plasma concentration (C_{max}) of 500nM, which is well above the concentration necessary for the inhibition of imatinib resistant BCR-ABL expressing Ba/F3 cells *in vitro* (55, 57). It was also documented in a murine preclinical model that BCR-ABL inhibition, as monitored by phospho-CRKL, was achieved within one to three hours after oral dosing; however, kinase activity was restored within 12 to 24 hours post-dasatinib treatment (56, 57). Dasatinib treatment remained efficacious in these preclinical models despite restoration of BCR-ABL kinase activity during the dosing regimen (55, 57).

The pharmacokinetic properties of dasatinib were not described in the initial phase I clinical trial report; however, similar clinical outcomes were observed in patients treated with once-daily versus twice-daily dasatinib (45). A subsequent phase III clinical trial found no difference in the clinical outcome of CML patients treated with either 100mg once-daily or 70mg twice-daily dasatinib (58). Later pharmacokinetic studies in CML patients and healthy volunteers documented the $t_{1/2}$ of dasatinib to be approximately three to five hours (59, 60). The clinical efficacy of once-daily dasatinib treatment, despite its relative short $t_{1/2}$ in CML patients, suggested that continuous BCR-ABL inhibition is not necessary for disease response.

To investigate the molecular consequences of dasatinib's short $t_{1/2}$, several groups attempted to model transient inhibitor treatment using patient-derived CML cell lines and

primary CML patient samples *in vitro*. In most situations, CML cells were treated transiently with a concentration of dasatinib similar to the C_{max} observed *in vivo* followed by extensive washing to remove the inhibitor from the cells and culture medium. Similar to what was observed in preclinical murine models, CRKL phosphorylation in CML cells was only transiently inhibited by short-term dasatinib treatment *in vitro* (61-63). The kinetics of CRKL phosphorylation in cells harvested from peripheral blood mononuclear cells of several CML patients following dasatinib treatment was also found to be transiently inhibited, yet nearly fully restored eight hours post-drug treatment (63). These studies also documented that short-term dasatinib treatment was sufficient to inhibit CML cell viability and colony formation of CML progenitor cells (61-63). Collectively, these studies suggested that continuous BCR-ABL kinase inhibition was not necessary for response to TKI therapy in CML.

3. Resistance to TKI in CML

Clinical resistance to BCR-ABL tyrosine kinase inhibitors has been extensively studied. The majority of CML patients exhibiting TKI resistance harbor at least one point mutation in the kinase domain BCR-ABL that impairs drug binding. The scope of kinase domain mutations capable of conferring resistance has been defined *in vitro* for each clinically relevant BCR-ABL kinase inhibitor. At the moment, all clinically relevant single point mutations in BCR-ABL are successfully targeted by one or more of the following TKIs: imatinib, nilotinib, dasatinib, or ponatinib.

Early attempts to classify mechanisms of resistance to imatinib therapy were preformed *in vitro*. Mahon et al generated imatinib resistant cells by selecting patient-

derived CML cell lines and BCR-ABL expressing Ba/F3 cells in increasing concentrations of imatinib. In this study, cells exhibited two types of drug resistance, either BCR-ABL-dependent or BCR-ABL-independent imatinib resistance (64). BCR-ABL-dependent resistance involved *BCR-ABL* amplification at the genomic level and overexpression at the protein level (64). BCR-ABL-independent resistance involved overexpression of the multi-drug efflux pump P-glycoprotein 1 (Pgp) on the surface of CML cells. It has been documented that Pgp overexpression lowers the intracellular concentration of imatinib in CML cells, increasing the amount of drug necessary for apoptosis and growth inhibition (65, 66). Interestingly, Mahon et al failed to detect any point mutations in the kinase domain of *BCR-ABL* in imatinib resistant CML cells.

In contrast to early *in vitro* assessments of imatinib resistance, clinical resistance to imatinib therapy in CML patients who initially responded but subsequently relapsed was found to involve *BCR-ABL* kinase domain mutations in the majority of cases (67, 68). A portion of the kinase domain mutations identified directly interfere with drug binding by disrupting critical interactions between the active site of c-ABL and imatinib. Other mutations identified are predicted to prevent c-ABL from achieving the inactive confirmation necessary for imatinib binding, like mutations in the P-loop and activation loop of the c-ABL kinase domain (68). In both initial reports of clinical resistance to imatinib, *BCR-ABL* amplification at the genomic level was also cited as a relevant mechanism of resistance (67, 68). Interestingly, Shah et al identified imatinib resistant mutations in the kinase domain of *BCR-ABL* in chronic phase patients who were in remission at the time of sequencing analysis, prior to disease relapse (68). From this observation, the authors postulated that mutations in *BCR-ABL* accrue over time

throughout disease progression and that CML cells harboring drug resistant alleles of *BCR-ABL* are subsequently selected for upon TKI therapy (68). Importantly, the clinical observation that point mutations in BCR-ABL are sufficient for resistance to TKI therapy document that CML cells exhibit a critical dependence on BCR-ABL kinase activity for survival, thus validating the presence of oncogene addiction in CML.

An *in vitro* mutagenesis screen was used to further define the scope of *BCR-ABL* point mutations capable of conferring resistance to imatinib therapy (69, 70). Using this approach, Azam et al successfully identified 112 amino acid substitutions at 90 different residues in BCR-ABL and validated 59 of these residues as bona fide imatinib resistant alleles (69). Importantly, Azam et al identified mutations in *BCR-ABL* that were not previously predicted to confer drug resistance. These non-obvious resistant mutations presumably prevent BCR-ABL from achieving the structural confirmation associated with imatinib binding (42, 69). For example, mutations identified within the N-terminal cap of c-ABL, the SH3 domain, the SH2 domain, and the SH2-kinase domain linker regions were not appreciated as imatinib-resistant *BCR-ABL* alleles prior to this screen (69).

The same *in vitro* mutagenesis technique was used to define the number of mutations in *BCR-ABL* capable of conferring dasatinib resistance. Resistance conferring mutations at 50nM dasatinib were restricted to ten different mutations at six amino acid residues in the kinase domain of BCR-ABL, four of which are directly involved in dasatinib binding (71). The difference in the magnitude of drug resistant mutations between imatinib and dasatinib is due to the fact that imatinib only binds an inactive confirmation of c-ABL, while dasatinib inhibits an active confirmation and is therefore less susceptible to mutations that alter the conformational state of BCR-ABL (71). Hence, mutations

associated with dasatinib resistance are directly involved with inhibitor binding and are fewer in number relative to imatinib resistance mutations.

To identify mutations capable of conferring resistance to the third generation BCR-ABL inhibitor ponatinib a slightly different *in vitro* mutagenesis approach was employed. O'Hare et al used N-ethyl-N-nitrosourea (ENU) mutagenesis to introduce random point mutations across the genome of BCR-ABL-expressing Ba/F3 cells prior to selecting for ponatinib resistance (54). At 20nM ponatinib, approximately 5-10-fold higher than the IC_{50} of primary CML patient samples and patient-derived CML cell lines, all single kinase domain resistance conferring mutations in *BCR-ABL* are suppressed except for mutations at E255 (E255V) and T315 (T315I) (54). No outgrowth of resistance conferring *BCR-ABL* alleles were detected at 40nM, which is below the reported C_{max} for CML patients treated with 30mg ponatinib (53, 54). From these observations, O'Hare et al conclude that ponatinib should sufficiently inhibit the outgrowth of all single point mutation, drug-resistant alleles of *BCR-ABL*.

4. Dual ABL/Aurora Kinase Inhibitors

Limited therapeutic options existed for T315I-positive CML patients in disease relapse prior to ponatinib. The first class of inhibitors that demonstrated activity against T315I BCR-ABL included a small group of dual ABL/Aurora kinase inhibitors. Preclinical and early clinical studies with dual ABL/Aurora kinase inhibitors in CML involved MK-0457 (VX-680), danusertib (PHA-739358), and XL228. All three dual ABL/Aurora inhibitors demonstrated some clinical efficacy in T315I-positive CML patients in early clinical trials.

The inhibitors MK-0457 and danusertib continue to have the most success clinically, while XL228 is no longer in clinical development.

The Aurora kinases are a family of serine/threonine kinases involved in the process of mitosis. There are three mammalian Aurora kinases: Aurora A (AURKA), Aurora B (AURKB), and Aurora C (AURKC). The Aurora kinases share a large degree of sequence identity in the catalytically active C-terminal region, but sequence identity diverges in the N-terminal region of the proteins (72). AURKA is involved in centrosome maturation and duplication, as well as spindle assembly, and is localized at opposing cellular poles during mitosis (73). It was initially believed that the N-terminal region was critical for the appropriate localization of AURKA and AURKB in mitosis, but it was recently shown that a single residue (glycine 198) in the catalytic region of AURKA switches the function of this kinase to mimic that of AURKB (74). AURKB is involved in chromosome biorientation, cytokinesis, and the spindle assembly checkpoint and is localized primarily to the equatorial region and midbody of the cell during mitosis (72). The function of AURKA and AURKB is critical for mitosis in all dividing cells and inhibitors of this family of kinases have not exhibited the same degree of tumor specificity as BCR-ABL kinase inhibitors in CML (75).

The Aurora kinase inhibitor MK-0457 was the first inhibitor of this class documented to exhibit activity against c-ABL and the drug-resistant T315I-c-ABL allele *in vitro* (76). The crystal structure of AURKA explains why MK-0457 tolerates the bulky isoleucine substitution at T315 in c-ABL; a leucine is present at the analogous residue in the kinase domain of AURKA (77, 78). T315I-c-ABL was subsequently crystallized with

both MK-0457 and danusertib, mechanistically documenting how dual ABL/Aurora inhibitors tolerate the large isoleucine substitution in c-ABL (79, 80).

Preclinical experiments with dual ABL/Aurora kinase inhibitors provided evidence for their activity in CML cells. Like MK-0457, danusertib was documented to inhibit both c-ABL and T315I-c-ABL in murine Ba/F3 cellular proliferation assays and *in vitro* kinase assays (81). The role of Aurora kinase inhibition for the activity of these compounds in CML has been previously investigated; however, evidence for the importance Aurora kinase inhibition was more correlative than definitive (82). Donato et al documented that inhibition of AURKB, as monitored by Histone H3 phosphorylation, was associated with MK-0457 treatment, but failed to show that inhibition of the Aurora kinases was necessary for the observed antiproliferative effects. Hematological responses have been achieved in CML patients treated with dual ABL/Aurora inhibitors; however, the discovery of ponatinib will most likely decrease the clinical use of these compounds (83-88). It has been suggested that these inhibitors could be used as a bridge to transplantation for some CML patients who are unresponsive to BCR-ABL kinase inhibitor therapy (84).

Part III: Other Clinically Relevant Kinase Inhibitors

1. Overview of Other Clinically Relevant Kinase Inhibitors

EGFR Kinase Inhibitors

Since the development of imatinib, a number of other clinically active kinase inhibitors have been approved for the treatment of various malignancies. For instance, the epidermal growth factor receptor (EGFR) has been identified as an oncogenic target in a subset of NSCLC patients (89). EGFR is a receptor tyrosine kinase expressed in a broad range of epithelial cell types and is capable of activating various proliferation and survival signaling pathways. There are two FDA approved EGFR inhibitors used in the treatment of NSCLC, erlotinib and gefitinib. Although the response to EGFR inhibitor therapy in various NSCLC patient populations is generally greater than the response to chemotherapy, no difference in the overall survival rate between the two treatments regimens was observed across a number of phase II and III clinical trails (90). It was later discovered that NSCLC patients harboring activating mutations in EGFR have a high chance of responding to gefitinib or erlotinib therapy (91, 92). However, the response to EGFR inhibitor treatment in this sensitive patient population is generally transient and response is typically lost due to the development of acquired drug resistance. In TKI-sensitive NSCLC, resistance to EGFR therapy can be mediated by both "on-target" and "off-target" mechanisms. On-target mechanisms of clinical resistance include an acquired methionine mutation at threonine 790 (T790M), which is analogous to mutations at T315 in BCR-ABL (93, 94). Similar to kinase domain mutations in BCR-ABL, mutations at T790M in EGFR are predicted to disrupt inhibitor binding. Off-target mechanisms of clinical resistance include genomic

amplification of the hepatocyte growth factor receptor, the gene encoding the MET receptor, which allows for the reactivation of prosurvival and proliferative signaling pathways necessary for disease progression (95, 96).

FLT3 Kinase Inhibitors

FMS-like tyrosine kinase 3 (FLT3) has been identified as an oncogenic target in acute myeloid leukemia (AML) and is overexpressed or mutationally activated in a large portion of AML patients. FLT3 is a receptor tyrosine kinase that is expressed in hematopoietic progenitor populations and is normally stimulated by the addition of exogenous ligand (97). The early FLT3 inhibitors CEP-701 and PKC-412 demonstrated activity in preclinical studies (98, 99). However, clinical trials with CEP-701 and PKC-412 demonstrated only modest activity in FLT3 positive, relapse, chemotherapy refractory AML patients and the best response to therapy was a transient reduction in the number of leukemic blast cells in the peripheral blood and bone marrow (100-102).

In contrast to the clinical responses observed with CEP-701 and PKC-412, the second-generation FLT3 inhibitor AC220 has achieved large responses in the majority of FLT3-mutant AML patients (40). AC220 exhibited activity against FLT3-dependent cell lines and murine models of leukemia in preclinical studies and responses to AC220 treatment in early phase I/II clinical trials were dramatic relative to what had been achieved by previous FLT3 inhibitors (103). The composite complete remission rate in FLT3-ITD (+) and –ITD(-) patients was 44% and 34% in the phase II clinical trail of AC220 as monotherapy in relapsed and refractory AML patients (104). Although deep clinical responses have been achieved with AC220 in this cohort of AML patients, the median

duration of response is short (11 weeks in ITD(+), 5 weeks in ITD (-)) (104). Similar to BCR-ABL and EGFR, acquired resistance to first- and second-generation FLT3 inhibitors has been documented. Thus far, clinical resistance has been characterized by "on-target" point mutations in the kinase domain of FLT3 (40, 105). *In vitro* studies have also described "off-target" mechanisms of acquired resistance to the FLT3 inhibitors CEP-5214 and CEP-701, where patient-derived AML cell lines were documented to harbor an activating mutation in *NRAS* (106).

BRAF-V600E Kinase Inhibitors

Malignant melanoma is a form of skin cancer with a poor prognosis. A number of oncogenes have been identified in malignant melanoma patient samples, including NRAS, BRAF, and cKIT among others (107). Of these oncogenes, BRAF is mutated in nearly 60% of melanoma (108). Most mutations occur at valine 600 (V600) in BRAF and a glutamic acid substitution is the most common type of mutation (V600E); however, other activating BRAF point mutations have been identified (108). Not surprisingly, significant effort has been directed toward identifying a clinically active BRAF kinase inhibitor for this subset of patients.

The first BRAF kinase inhibitor to exhibit mutant BRAF-selective preclinical activity was PLX4720. In preclinical studies, PLX4720 inhibited BRAF-V600E kinase activity and BRAF-V600E-dependent cell line proliferation *in vitro*, as well as delayed tumor growth in BRAF-V600E-dependent xenografts (109). The BRAF inhibitor PLX4032 was derived from PLX4720 following further clinical development and optimization. PLX4032, also known as vemurafenib, was the first BRAF inhibitor to exhibit a large clinical response rate in

melanoma patients (41). Like PLX4720, PLX4032 has been documented to inhibit BRAF-V600E-dependent cell line proliferation and exhibited efficacy in various preclinical models (110-112). Clinically, partial responses were achieved in 81% of patients (26/32) in the extension arm of the PLX4032 phase I clinical trial, while two of the 26 patients achieved a complete response on therapy (41). However, in contrast to BCR-ABL inhibitors in CML, the overall median progression free survival for all patients in the phase I PLX4032 clinical trial was only seven months (41).

The historical experience with BCR-ABL inhibitors has established that loss of response is associated with reactivation of signaling pathways that are critical for CML cell survival. The same phenomenon holds true in the setting of BRAF-V600E melanoma, where reactivation of the MAPK pathway is associated with resistance to BRAF inhibitor therapy. Surprisingly, no secondary kinase domain mutations in BRAF-V600E have been detected in relapsed patient samples (113). However, mutations upstream of RAF have been documented to confer clinical resistance, including overexpression of the platelet-derived growth factor receptor-β (PDGFRβ) and mutational activation of NRAS (113). Upregulation of MAP3K8 (COT) and mutational activation of MEK1 have also been documented to confer clinical resistance to PLX4032 (114, 115). Finally, alternative splicing of BRAF-V600E was documented to confer resistance to PLX4032 in 6/19 patient tumors that initially responded but relapsed with acquired resistance (116). The last mechanism of resistance sheds light on basic BRAF-V600E biology by suggesting that BRAF-V600E activates MEK as a monomer in the cell. Consequently, it has been postulated BRAF inhibitor sensitivity is dependent on low basal levels of activated RAS in melanoma cells (116). This is a major biological observation and, as will be discussed in more detail

below, potentially explains why various BRAF-V600E malignancies exhibit differential sensitivity to BRAF inhibitor treatment.

Summary

The success of TKI therapy in CML laid the foundation for the clinical development of targeted agents in other types of cancers. Kinase inhibitors in non-small cell lung cancer (NSCLC), acute myeloid leukemia (AML), and metastatic melanoma have exhibited various degrees of clinical success. However, in contrast to BCR-ABL inhibitors these kinase inhibitors have failed to achieve the same degree of durable disease remission rates across each patient population. Differences in response to kinase inhibitor therapy may reflect inherent differences in the state of oncogene addiction established by each respective oncogenic kinase. Identifying the critical components of BCR-ABL-mediated oncogene addiction may help to develop better, targeted therapy regimens for other malignancies such as NSCLC, AML and metastatic melanoma.

2. Negative Feedback

The rapid induction of physiologic negative feedback is the cell's normal response to growth factor-receptor (GF-R) activation. Negative feedback acts a safeguard against unwanted, excess proliferative signaling, but also as an integral component of normal biological development. A number of molecular components responsible for negative feedback signaling have been identified for some of the major proliferative and survival pathways in the cell, including the RAS/MAPK and JAK/STAT signaling cascades.

Functional redundancy exists among the proteins involved in the negative feedback regulation of each signaling pathway in the cell. This is exemplified by the types of negative feedback molecules involved in the attenuation of the RAS/MAPK signaling pathway. For instance, expression of dual-specificity MAPK phosphatase proteins (DUSPs) are rapidly induced upon MAPK activation (117-120). These molecules have the ability to dephosphorylate the activation loop of MAPKs in order to attenuate MAPK activity in the cell (121). There are 10 catalytically active DUSPs found within the nucleus and/or cytoplasm of mammalian cells, each of which has the ability to recognize and dephosphorylate a subset of MAPK enzymes (121). Other proteins involved in the attenuation of RAS/MAPK signaling include the sprouty (SPRY) and the sprouty-related *protein* with an EVH1 domain (SPRED) proteins. There are 4 SPRY isoforms (SPRY1-4) and 4 SPRED isoforms (SPRED1-3 and EVE-3) in mammalian cells (122). The SPRY1, -2, and -4 isoforms are widely expressed, while SPRY3 is highly expressed in the brain and germ cells (122). In contrast to DUSPs, SPRY and SPRED molecules harbor no catalytic activity. Instead, it has been proposed that SPRY molecules attenuate GF-R signaling by sequestering the adaptor molecule GRB2, which is important for the coordination of GF-R-mediated RAS pathway activation (123). SPRED molecules are proposed to interfere directly with pathway activation. Experimental evidence suggests that SPRED molecules form a complex between RAS and RAF to prevent RAF-mediated activation of its downstream kinase target MEK (124). Collectively, RAS pathway activation can be attenuated directly through the dephosphorylation of MEK and ERK by DUSPs, or pathway attenuation can be achieved at more upstream locations by preventing GF-R-mediated activation of RAS or RAF-mediated activation of MEK. The multi-tiered nature of

RAS/MAPK-directed negative feedback illustrates both the complexity and redundancy of negative feedback in this one particular cellular pathway.

Similar to the negative feedback network associated with RAS/MAPK signaling, JAK/STAT pathway negative feedback is both complex and redundant. Various tyrosine phosphatases dephosphorylate the activation loop of JAK kinases, leading to kinase inactivation. This includes the protein tyrosine phosphatase 1B (PTP1B) and the T-cell protein tyrosine phosphatase, among others (125). The suppressors of cytokine signaling (SOCS) molecules are an additional family of proteins involved in the attenuation of JAK/STAT signaling. There are eight SOCS molecules (SOCS1-7 and CIS) in mammalian cells, all of which contain a highly conserved SH2 domain for binding specificity (125). Expression of the SOCS molecules are induced upon STAT activation and SOCS proteins inhibit JAK/STAT signaling by either directly inhibiting JAK kinase activity (SOCS1 and -3) or by competing with various STAT molecules for receptor binding sites (CIS, SOCS2) (125).

3. BRAF-V600E-Dependent Negative Feedback

The importance of negative feedback on cancer cell biology and its effect on the efficacy of cancer therapy has been an area of interest in recent years. For instance, BRAF-V600E-expressing melanoma cells have been documented to exhibit constitutively high levels of negative feedback. Pratilas et al documented a rapid transcriptional downregulation of a number of RAS/MAPK pathway negative feedback molecules in BRAF-V600E-expressing melanoma cell lines following MEK inhibitor treatment (126). The response to MEK inhibitor treatment was unique to BRAF-V600E expressing cells as no

common expression change in negative feedback molecules was observed in RTK-dependent cell lines under the same experimental conditions. The RAS/MAPK negative feedback mediators DUSP4, DUSP6, SPRY4 and SPRED2 were included among those genes transcriptionally downregulated by MEK inhibitor treatment in BRAF-V600E melanoma cell lines (126). The same effect was replicated when a similar panel of BRAF-V600E-expressing melanoma cell lines was treated with PLX4032 (110).

The consequences of negative feedback upon the biology of BRAF-V600E-expressing cancer cells have been recently appreciated. Beyond melanoma, BRAF-V600E has been documented as a genetic lesion in a subset of thyroid cancers and colorectal carcinomas (108, 127, 128). However in contrast to melanoma, in a phase I clinical trail of PLX4032 in BRAF-V600E-positive colorectal cancer, patients were relatively unresponsive to BRAF inhibition (129). Results from preclinical studies of BRAF inhibitors in BRAF-V600E-expressing thyroid cells were mixed, but generally suggest that BRAF-V600E-expressing thyroid patients will not exhibit the same clinical response to PLX4032 treatment as melanoma patients (130, 131). Indeed, low response rates were observed in early phase I/II clinical trials of BRAF inhibitors in thyroid cancer patients (132, 133). Mechanistically, the reason for the decreased efficacy of BRAF inhibitors in non-melanoma V600E-expressing cancers appears to be associated with the relief of MEK-dependent negative feedback. Similar to what was initially described by Pratilas et al, others have documented a loss of MEK-dependent negative feedback following PLX4032 treatment in BRAF-V600E colorectal cell lines. It has been proposed that constitutive BRAF-V600E-mediated activation of MEK and ERK results in ERK-mediated inhibition of EGFR kinase activity (134). Following PLX4032 treatment, ERK-mediated inhibition of EGFR is relieved, and

EGFR-mediated activation of RAS/MAPK and PI3K/AKT signaling pathways proceeds to rescue colorectal cancer cell lines from BRAF inhibitor-mediated apoptosis (134). In this study, the authors also document that melanoma cell lines express low basal levels of EGFR in contrast to colorectal cancer cell lines, providing one potential explanation for the difference in BRAF inhibitor sensitivity between these two malignancies.

Relief of negative feedback in BRAF-V600E thyroid cell lines has also been described and proposed as a potential reason for reduced BRAF-inhibitor sensitivity in this disease. Treatment of thyroid cancer cell lines with BRAF-inhibitors resulted in the transient inhibition of MEK and ERK activity, followed by rapid reactivation of the signaling pathway (135). The reactivation of MEK and ERK following BRAF inhibitor treatment was determined to be dependent on the transcriptional upregulation and kinase activation of the RTKs HER2 and HER3. Autocrine secretion of the HER-family ligand NRGI was found to be necessary for pathway reactivation following BRAF-inhibitor treatment of thyroid cancer cell lines (135). The authors of this study document that autocrine secretion of NRG1 is absent in BRAF-V600E melanoma cell lines, providing a potential explanation for the difference in BRAF-inhibitor sensitivity.

Collectively, the differences in sensitivity to BRAF inhibitors between these three V600E-expressing malignancies illustrate a new and evolving concept in the current era of targeted cancer therapy. The loss of negative feedback, the basal expression or induction of RTKs, and the presence or absence of the appropriate RTK ligands may determine disease response to targeted therapy. Interestingly, V600E-expressing melanoma cells can be rescued by the addition of exogenous ligand due to the loss of negative feedback at the level of RTK signaling (136). It has also been documented that innate resistance to BRAF-

inhibitors is associated with high levels of the RTK ligand HGF (MET receptor) in the tumor microenvironment and plasma of melanoma patients (137, 138). Therefore, the same concepts that describe why BRAF-V600E colorectal and thyroid patients respond poorly to inhibitor treatment may help to explain why a subset of melanoma patients are innately resistant to PLX4032 therapy.

Part IV: Objectives of Thesis

Mutational activation or deregulation of kinase activity has been documented in a number of cancers and effective targeting of these lesions has been observed in a subset of these diseases. However, as discussed above, no other kinase inhibitor has achieved the long-term clinical success as BCR-ABL inhibitors in CML. Although CML represents a unique situation where BCR-ABL appears to be solely responsible for disease initiation and maintenance, the mechanistic reason for the success of inhibitors like imatinib and dasatinib in CML are not well understood. A better understanding of how BCR-ABL establishes a state of oncogene addiction could explain why BCR-ABL inhibitors are so effective relative to other clinically relevant kinase inhibitors, and possibly identify adjunctive targets that will enhance oncogene addiction and thereby sensitivity to targeted therapeutics in other malignancies (e.g those associated with mutations in EGFR, FLT3, BRAF, etc).

In chapter 2 I will present work I performed to identify which pathways are critical for CML cell survival and BCR-ABL-mediated oncogene addiction. I will describe how the "high-dose pulse" model of dasatinib treatment was used to identify these pathways in CML cells using quantitative phosphoproteomics; how these findings were validated using an *in vitro* isogenic cell line model; and how the duration of BCR-ABL-mediated negative feedback determines cytokine responsiveness and the commitment to apoptosis following inhibitor treatment in CML cells.

In chapter 3 I will present work I performed describing how intracellular drug retention was determined to be responsible for "high-dose pulse" mediated apoptosis of

CML cells; how the removal of intracellular tyrosine kinase inhibitor restored CML cell viability and the activation of BCR-ABL canonical signaling pathways.

In chapter 4 I will present work I performed to delineate the contribution of Aurora and BCR-ABL kinase inhibition in the observed cytotoxicity of CML cells following treatment with the dual ABL/Aurora kinase inhibitors XL228, danusertib, and MK-0457; how a drug resistant allele of *AURKB* confers biochemical resistance to dual ABL/Aurora inhibitor treatment; and how BCR-ABL expression in the AURKB mutant cell line documents that AURKB is the critical kinase target of dual ABL/Aurora kinase inhibitors.

In chapter 5 I will discuss the major conclusions derived from this work and future directions.

References

1. Kurzrock R, Gutterman JU, Talpaz M. The molecular genetics of Philadelphia chromosome-positive leukemias. *N Engl J Med* 1988 Oct 13; **319**(15)**:** 990-998.

2. National Academy of Sciences. Abstracts of Papers Presented at the Autumn Meeting, 14-16 November 1960, Philadelphia, Pennsylvania. *Science* 1960; **132**(3438)**:** 1488-1501.

3. Rowley JD. Letter: A new consistent chromosomal abnormality in chronic myelogenous leukaemia identified by quinacrine fluorescence and Giemsa staining. *Nature* 1973 Jun 1; **243**(5405)**:** 290-293.

4. Faderl S, Talpaz M, Estrov Z, O'Brien S, Kurzrock R, Kantarjian HM. The biology of chronic myeloid leukemia. *N Engl J Med* 1999 Jul 15; **341**(3)**:** 164-172.

5. Sawyers CL. Chronic myeloid leukemia. *N Engl J Med* 1999 Apr 29; **340**(17)**:** 1330-1340.

6. Deininger M, Buchdunger E, Druker BJ. The development of imatinib as a therapeutic agent for chronic myeloid leukemia. *Blood* 2005 Apr 1; **105**(7)**:** 2640-2653.

7. Groffen J, Stephenson JR, Heisterkamp N, de Klein A, Bartram CR, Grosveld G. Philadelphia chromosomal breakpoints are clustered within a limited region, bcr, on chromosome 22. *Cell* 1984 Jan; **36**(1)**:** 93-99.

8. de Klein A, van Kessel AG, Grosveld G, Bartram CR, Hagemeijer A, Bootsma D*, et al.* A cellular oncogene is translocated to the Philadelphia chromosome in chronic myelocytic leukaemia. *Nature* 1982 Dec 23; **300**(5894)**:** 765-767.

9. Melo JV. The diversity of BCR-ABL fusion proteins and their relationship to leukemia phenotype. *Blood* 1996 Oct 1; **88**(7)**:** 2375-2384.

10. Diekmann D, Brill S, Garrett MD, Totty N, Hsuan J, Monfries C*, et al.* Bcr encodes a GTPase-activating protein for p21rac. *Nature* 1991 May 30; **351**(6325)**:** 400-402.

11. Maru Y, Witte ON. The BCR gene encodes a novel serine/threonine kinase activity within a single exon. *Cell* 1991 Nov 1; **67**(3)**:** 459-468.

12. Chuang TH, Xu X, Kaartinen V, Heisterkamp N, Groffen J, Bokoch GM. Abr and Bcr are multifunctional regulators of the Rho GTP-binding protein family. *Proc Natl Acad Sci U S A* 1995 Oct 24; **92**(22)**:** 10282-10286.

13. McWhirter JR, Galasso DL, Wang JY. A coiled-coil oligomerization domain of Bcr is essential for the transforming function of Bcr-Abl oncoproteins. *Mol Cell Biol* 1993 Dec; **13**(12)**:** 7587-7595.

14. Zhang X, Subrahmanyam R, Wong R, Gross AW, Ren R. The NH(2)-terminal coiled-coil domain and tyrosine 177 play important roles in induction of a myeloproliferative disease in mice by Bcr-Abl. *Mol Cell Biol* 2001 Feb; **21**(3)**:** 840-853.

15. Pendergast AM, Quilliam LA, Cripe LD, Bassing CH, Dai Z, Li N*, et al.* BCR-ABL-induced oncogenesis is mediated by direct interaction with the SH2 domain of the GRB-2 adaptor protein. *Cell* 1993 Oct 8; **75**(1)**:** 175-185.

16. Panjarian S, Iacob RE, Chen S, Engen JR, Smithgall TE. Structure and dynamic regulation of Abl kinases. *J Biol Chem* 2013 Feb 22; **288**(8)**:** 5443-5450.

17. Nagar B, Hantschel O, Young MA, Scheffzek K, Veach D, Bornmann W*, et al.* Structural basis for the autoinhibition of c-Abl tyrosine kinase. *Cell* 2003 Mar 21; **112**(6)**:** 859-871.

18. Hantschel O, Nagar B, Guettler S, Kretzschmar J, Dorey K, Kuriyan J*, et al.* A myristoyl/phosphotyrosine switch regulates c-Abl. *Cell* 2003 Mar 21; **112**(6)**:** 845-857.

19. Shaw RJ, Cantley LC. Ras, PI(3)K and mTOR signalling controls tumour cell growth. *Nature* 2006 May 25; **441**(7092)**:** 424-430.

20. Buday L, Downward J. Many faces of Ras activation. *Biochim Biophys Acta* 2008 Dec; **1786**(2)**:** 178-187.

21. Mandanas RA, Leibowitz DS, Gharehbaghi K, Tauchi T, Burgess GS, Miyazawa K*, et al.* Role of p21 RAS in p210 bcr-abl transformation of murine myeloid cells. *Blood* 1993 Sep 15; **82**(6)**:** 1838-1847.

22. Puil L, Liu J, Gish G, Mbamalu G, Bowtell D, Pelicci PG*, et al.* Bcr-Abl oncoproteins bind directly to activators of the Ras signalling pathway. *EMBO J* 1994 Feb 15; **13**(4)**:** 764-773.

23. Vivanco I, Sawyers CL. The phosphatidylinositol 3-Kinase AKT pathway in human cancer. *Nat Rev Cancer* 2002 Jul; **2**(7)**:** 489-501.

24. Skorski T, Kanakaraj P, Nieborowska-Skorska M, Ratajczak MZ, Wen SC, Zon G*, et al.* Phosphatidylinositol-3 kinase activity is regulated by BCR/ABL and is required for the growth of Philadelphia chromosome-positive cells. *Blood* 1995 Jul 15; **86**(2)**:** 726-736.

25. Sattler M, Mohi MG, Pride YB, Quinnan LR, Malouf NA, Podar K*, et al.* Critical role for Gab2 in transformation by BCR/ABL. *Cancer Cell* 2002 Jun; **1**(5)**:** 479-492.

26. Reich NC, Liu L. Tracking STAT nuclear traffic. *Nat Rev Immunol* 2006 Aug; **6**(8)**:** 602-612.

27. Carlesso N, Frank DA, Griffin JD. Tyrosyl phosphorylation and DNA binding activity of signal transducers and activators of transcription (STAT) proteins in hematopoietic cell lines transformed by Bcr/Abl. *J Exp Med* 1996 Mar 1; **183**(3)**:** 811-820.

28. Ilaria RL, Jr., Van Etten RA. P210 and P190(BCR/ABL) induce the tyrosine phosphorylation and DNA binding activity of multiple specific STAT family members. *J Biol Chem* 1996 Dec 6; **271**(49)**:** 31704-31710.

29. Nieborowska-Skorska M, Wasik MA, Slupianek A, Salomoni P, Kitamura T, Calabretta B*, et al.* Signal transducer and activator of transcription (STAT)5 activation by BCR/ABL is dependent on intact Src homology (SH)3 and SH2 domains of BCR/ABL and is required for leukemogenesis. *J Exp Med* 1999 Apr 19; **189**(8)**:** 1229-1242.

30. Samanta A, Perazzona B, Chakraborty S, Sun X, Modi H, Bhatia R*, et al.* Janus kinase 2 regulates Bcr-Abl signaling in chronic myeloid leukemia. *Leukemia* Mar; **25**(3)**:** 463-472.

31. Xie S, Wang Y, Liu J, Sun T, Wilson MB, Smithgall TE*, et al.* Involvement of Jak2 tyrosine phosphorylation in Bcr-Abl transformation. *Oncogene* 2001 Sep 27; **20**(43)**:** 6188-6195.

32. Hantschel O, Warsch W, Eckelhart E, Kaupe I, Grebien F, Wagner KU*, et al.* BCR-ABL uncouples canonical JAK2-STAT5 signaling in chronic myeloid leukemia. *Nat Chem Biol* Mar; **8**(3)**:** 285-293.

33. Sonoyama J, Matsumura I, Ezoe S, Satoh Y, Zhang X, Kataoka Y*, et al.* Functional cooperation among Ras, STAT5, and phosphatidylinositol 3-kinase is required for full oncogenic activities of BCR/ABL in K562 cells. *J Biol Chem* 2002 Mar 8; **277**(10)**:** 8076-8082.

34. Scherr M, Chaturvedi A, Battmer K, Dallmann I, Schultheis B, Ganser A*, et al.* Enhanced sensitivity to inhibition of SHP2, STAT5, and Gab2 expression in chronic myeloid leukemia (CML). *Blood* 2006 Apr 15; **107**(8)**:** 3279-3287.

35. Sillaber C, Gesbert F, Frank DA, Sattler M, Griffin JD. STAT5 activation contributes to growth and viability in Bcr/Abl-transformed cells. *Blood* 2000 Mar 15; **95**(6)**:** 2118-2125.

36. Felsher DW, Bishop JM. Reversible tumorigenesis by MYC in hematopoietic lineages. *Mol Cell* 1999 Aug; **4**(2)**:** 199-207.

37. Chin L, Tam A, Pomerantz J, Wong M, Holash J, Bardeesy N*, et al.* Essential role for oncogenic Ras in tumour maintenance. *Nature* 1999 Jul 29; **400**(6743)**:** 468-472.

38. Pelengaris S, Littlewood T, Khan M, Elia G, Evan G. Reversible activation of c-Myc in skin: induction of a complex neoplastic phenotype by a single oncogenic lesion. *Mol Cell* 1999 May; **3**(5)**:** 565-577.

39. Weinstein IB. Cancer. Addiction to oncogenes--the Achilles heal of cancer. *Science* 2002 Jul 5; **297**(5578)**:** 63-64.

40. Smith CC, Wang Q, Chin CS, Salerno S, Damon LE, Levis MJ*, et al.* Validation of ITD mutations in FLT3 as a therapeutic target in human acute myeloid leukaemia. *Nature* May 10; **485**(7397)**:** 260-263.

41. Flaherty KT, Puzanov I, Kim KB, Ribas A, McArthur GA, Sosman JA*, et al.* Inhibition of mutated, activated BRAF in metastatic melanoma. *N Engl J Med* Aug 26; **363**(9)**:** 809-819.

42. Schindler T, Bornmann W, Pellicena P, Miller WT, Clarkson B, Kuriyan J. Structural mechanism for STI-571 inhibition of abelson tyrosine kinase. *Science* 2000 Sep 15; **289**(5486)**:** 1938-1942.

43. Tokarski JS, Newitt JA, Chang CY, Cheng JD, Wittekind M, Kiefer SE*, et al.* The structure of Dasatinib (BMS-354825) bound to activated ABL kinase domain elucidates its inhibitory activity against imatinib-resistant ABL mutants. *Cancer Res* 2006 Jun 1; **66**(11)**:** 5790-5797.

44. Druker BJ, Sawyers CL, Kantarjian H, Resta DJ, Reese SF, Ford JM*, et al.* Activity of a specific inhibitor of the BCR-ABL tyrosine kinase in the blast crisis of chronic myeloid leukemia and acute lymphoblastic leukemia with the Philadelphia chromosome. *N Engl J Med* 2001 Apr 5; **344**(14)**:** 1038-1042.

45. Talpaz M, Shah NP, Kantarjian H, Donato N, Nicoll J, Paquette R*, et al.* Dasatinib in imatinib-resistant Philadelphia chromosome-positive leukemias. *N Engl J Med* 2006 Jun 15; **354**(24)**:** 2531-2541.

46. Hochhaus A, O'Brien SG, Guilhot F, Druker BJ, Branford S, Foroni L*, et al.* Six-year follow-up of patients receiving imatinib for the first-line treatment of chronic myeloid leukemia. *Leukemia* 2009 Jun; **23**(6)**:** 1054-1061.

47. Oda T, Heaney C, Hagopian JR, Okuda K, Griffin JD, Druker BJ. Crkl is the major tyrosine-phosphorylated protein in neutrophils from patients with chronic myelogenous leukemia. *J Biol Chem* 1994 Sep 16; **269**(37)**:** 22925-22928.

48. le Coutre P, Kreuzer KA, Pursche S, Bonin M, Leopold T, Baskaynak G*, et al.* Pharmacokinetics and cellular uptake of imatinib and its main metabolite CGP74588. *Cancer Chemother Pharmacol* 2004 Apr; **53**(4)**:** 313-323.

49. Peng B, Hayes M, Resta D, Racine-Poon A, Druker BJ, Talpaz M*, et al.* Pharmacokinetics and pharmacodynamics of imatinib in a phase I trial with chronic myeloid leukemia patients. *J Clin Oncol* 2004 Mar 1; **22**(5)**:** 935-942.

50. Deininger MW, Goldman JM, Lydon N, Melo JV. The tyrosine kinase inhibitor CGP57148B selectively inhibits the growth of BCR-ABL-positive cells. *Blood* 1997 Nov 1; **90**(9)**:** 3691-3698.

51. Kantarjian H, Giles F, Wunderle L, Bhalla K, O'Brien S, Wassmann B*, et al.* Nilotinib in imatinib-resistant CML and Philadelphia chromosome-positive ALL. *N Engl J Med* 2006 Jun 15; **354**(24)**:** 2542-2551.

52. Weisberg E, Manley PW, Breitenstein W, Bruggen J, Cowan-Jacob SW, Ray A*, et al.* Characterization of AMN107, a selective inhibitor of native and mutant Bcr-Abl. *Cancer Cell* 2005 Feb; **7**(2)**:** 129-141.

53. Cortes JE, Kantarjian H, Shah NP, Bixby D, Mauro MJ, Flinn I*, et al.* Ponatinib in refractory Philadelphia chromosome-positive leukemias. *N Engl J Med* 2012 Nov 29; **367**(22)**:** 2075-2088.

54. O'Hare T, Shakespeare WC, Zhu X, Eide CA, Rivera VM, Wang F*, et al.* AP24534, a pan-BCR-ABL inhibitor for chronic myeloid leukemia, potently inhibits the T315I mutant and overcomes mutation-based resistance. *Cancer Cell* 2009 Nov 6; **16**(5)**:** 401-412.

55. Lombardo LJ, Lee FY, Chen P, Norris D, Barrish JC, Behnia K*, et al.* Discovery of N-(2-chloro-6-methyl- phenyl)-2-(6-(4-(2-hydroxyethyl)- piperazin-1-yl)-2-methylpyrimidin-4- ylamino)thiazole-5-carboxamide (BMS-354825), a dual Src/Abl kinase inhibitor with potent antitumor activity in preclinical assays. *J Med Chem* 2004 Dec 30; **47**(27)**:** 6658-6661.

56. Luo FR, Yang Z, Camuso A, Smykla R, McGlinchey K, Fager K*, et al.* Dasatinib (BMS-354825) pharmacokinetics and pharmacodynamic biomarkers in animal models predict optimal clinical exposure. *Clin Cancer Res* 2006 Dec 1; **12**(23)**:** 7180-7186.

57. Shah NP, Tran C, Lee FY, Chen P, Norris D, Sawyers CL. Overriding imatinib resistance with a novel ABL kinase inhibitor. *Science* 2004 Jul 16; **305**(5682)**:** 399-401.

58. Shah NP, Kantarjian HM, Kim DW, Rea D, Dorlhiac-Llacer PE, Milone JH*, et al.* Intermittent target inhibition with dasatinib 100 mg once daily preserves efficacy

and improves tolerability in imatinib-resistant and -intolerant chronic-phase chronic myeloid leukemia. *J Clin Oncol* 2008 Jul 1; **26**(19)**:** 3204-3212.

59. Christopher LJ, Cui D, Wu C, Luo R, Manning JA, Bonacorsi SJ*, et al.* Metabolism and disposition of dasatinib after oral administration to humans. *Drug Metab Dispos* 2008 Jul; **36**(7)**:** 1357-1364.

60. Steinberg M. Dasatinib: a tyrosine kinase inhibitor for the treatment of chronic myelogenous leukemia and philadelphia chromosome-positive acute lymphoblastic leukemia. *Clin Ther* 2007 Nov; **29**(11)**:** 2289-2308.

61. Hiwase DK, White DL, Powell JA, Saunders VA, Zrim SA, Frede AK*, et al.* Blocking cytokine signaling along with intense Bcr-Abl kinase inhibition induces apoptosis in primary CML progenitors. *Leukemia* Apr; **24**(4)**:** 771-778.

62. Snead JL, O'Hare T, Adrian LT, Eide CA, Lange T, Druker BJ*, et al.* Acute dasatinib exposure commits Bcr-Abl-dependent cells to apoptosis. *Blood* 2009 Oct 15; **114**(16)**:** 3459-3463.

63. Shah NP, Kasap C, Weier C, Balbas M, Nicoll JM, Bleickardt E*, et al.* Transient potent BCR-ABL inhibition is sufficient to commit chronic myeloid leukemia cells irreversibly to apoptosis. *Cancer Cell* 2008 Dec 9; **14**(6)**:** 485-493.

64. Mahon FX, Deininger MW, Schultheis B, Chabrol J, Reiffers J, Goldman JM*, et al.* Selection and characterization of BCR-ABL positive cell lines with differential sensitivity to the tyrosine kinase inhibitor STI571: diverse mechanisms of resistance. *Blood* 2000 Aug 1; **96**(3)**:** 1070-1079.

65. Mahon FX, Belloc F, Lagarde V, Chollet C, Moreau-Gaudry F, Reiffers J*, et al.* MDR1 gene overexpression confers resistance to imatinib mesylate in leukemia cell line models. *Blood* 2003 Mar 15; **101**(6)**:** 2368-2373.

66. Illmer T, Schaich M, Platzbecker U, Freiberg-Richter J, Oelschlagel U, von Bonin M*, et al.* P-glycoprotein-mediated drug efflux is a resistance mechanism of chronic myelogenous leukemia cells to treatment with imatinib mesylate. *Leukemia* 2004 Mar; **18**(3)**:** 401-408.

67. Gorre ME, Mohammed M, Ellwood K, Hsu N, Paquette R, Rao PN*, et al.* Clinical resistance to STI-571 cancer therapy caused by BCR-ABL gene mutation or amplification. *Science* 2001 Aug 3; **293**(5531)**:** 876-880.

68. Shah NP, Nicoll JM, Nagar B, Gorre ME, Paquette RL, Kuriyan J*, et al.* Multiple BCR-ABL kinase domain mutations confer polyclonal resistance to the tyrosine kinase inhibitor imatinib (STI571) in chronic phase and blast crisis chronic myeloid leukemia. *Cancer Cell* 2002 Aug; **2**(2)**:** 117-125.

69. Azam M, Latek RR, Daley GQ. Mechanisms of autoinhibition and STI-571/imatinib resistance revealed by mutagenesis of BCR-ABL. *Cell* 2003 Mar 21; **112**(6)**:** 831-843.

70. Azam M, Raz T, Nardi V, Opitz SL, Daley GQ. A screen to identify drug resistant variants to target-directed anti-cancer agents. *Biol Proced Online* 2003; **5:** 204-210.

71. Burgess MR, Skaggs BJ, Shah NP, Lee FY, Sawyers CL. Comparative analysis of two clinically active BCR-ABL kinase inhibitors reveals the role of conformation-specific binding in resistance. *Proc Natl Acad Sci U S A* 2005 Mar 1; **102**(9)**:** 3395-3400.

72. Carmena M, Earnshaw WC. The cellular geography of aurora kinases. *Nat Rev Mol Cell Biol* 2003 Nov; **4**(11)**:** 842-854.

73. Marumoto T, Zhang D, Saya H. Aurora-A - a guardian of poles. *Nat Rev Cancer* 2005 Jan; **5**(1)**:** 42-50.

74. Hans F, Skoufias DA, Dimitrov S, Margolis RL. Molecular distinctions between Aurora A and B: a single residue change transforms Aurora A into correctly localized and functional Aurora B. *Mol Biol Cell* 2009 Aug; **20**(15)**:** 3491-3502.

75. Kollareddy M, Zheleva D, Dzubak P, Brahmkshatriya PS, Lepsik M, Hajduch M. Aurora kinase inhibitors: progress towards the clinic. *Invest New Drugs* 2012 Dec; **30**(6)**:** 2411-2432.

76. Carter TA, Wodicka LM, Shah NP, Velasco AM, Fabian MA, Treiber DK*, et al.* Inhibition of drug-resistant mutants of ABL, KIT, and EGF receptor kinases. *Proc Natl Acad Sci U S A* 2005 Aug 2; **102**(31)**:** 11011-11016.

77. Cheetham GM, Knegtel RM, Coll JT, Renwick SB, Swenson L, Weber P*, et al.* Crystal structure of aurora-2, an oncogenic serine/threonine kinase. *J Biol Chem* 2002 Nov 8; **277**(45)**:** 42419-42422.

78. Nowakowski J, Cronin CN, McRee DE, Knuth MW, Nelson CG, Pavletich NP*, et al.* Structures of the cancer-related Aurora-A, FAK, and EphA2 protein kinases from nanovolume crystallography. *Structure* 2002 Dec; **10**(12)**:** 1659-1667.

79. Modugno M, Casale E, Soncini C, Rosettani P, Colombo R, Lupi R*, et al.* Crystal structure of the T315I Abl mutant in complex with the aurora kinases inhibitor PHA-739358. *Cancer Res* 2007 Sep 1; **67**(17)**:** 7987-7990.

80. Young MA, Shah NP, Chao LH, Seeliger M, Milanov ZV, Biggs WH, 3rd*, et al.* Structure of the kinase domain of an imatinib-resistant Abl mutant in complex with the Aurora kinase inhibitor VX-680. *Cancer Res* 2006 Jan 15; **66**(2)**:** 1007-1014.

81. Gontarewicz A, Balabanov S, Keller G, Colombo R, Graziano A, Pesenti E*, et al.* Simultaneous targeting of Aurora kinases and Bcr-Abl kinase by the small molecule

inhibitor PHA-739358 is effective against imatinib-resistant BCR-ABL mutations including T315I. *Blood* 2008 Apr 15; **111**(8)**:** 4355-4364.

82. Donato NJ, Fang D, Sun H, Giannola D, Peterson LF, Talpaz M. Targets and effectors of the cellular response to aurora kinase inhibitor MK-0457 (VX-680) in imatinib sensitive and resistant chronic myelogenous leukemia. *Biochem Pharmacol* 2010 Mar 1; **79**(5)**:** 688-697.

83. Giles FJ, Cortes J, Jones D, Bergstrom D, Kantarjian H, Freedman SJ. MK-0457, a novel kinase inhibitor, is active in patients with chronic myeloid leukemia or acute lymphocytic leukemia with the T315I BCR-ABL mutation. *Blood* 2007 Jan 15; **109**(2)**:** 500-502.

84. Giles FJ, Swords RT, Nagler A, Hochhaus A, Ottmann OG, Rizzieri DA*, et al.* MK-0457, an Aurora kinase and BCR-ABL inhibitor, is active in patients with BCR-ABL T315I leukemia. *Leukemia* 2013 Jan; **27**(1)**:** 113-117.

85. Shah NP, Kasap C, Paquette R, Cortes J, Pinilla J, Talpaz M*, et al.* Targeting Drug-Resistant CML and Ph+-ALL with the Spectrum Selective Protein Kinase Inhibitor XL228. *ASH Annual Meeting Abstracts* 2007 December 12, 2007; **110**(11)**:** 474.

86. Cortes J, Paquette R, Talpaz M, Pinilla J, Asatiani E, Wetzler M*, et al.* Preliminary Clinical Activity in a Phase I Trial of the BCR-ABL/IGF- 1R/Aurora Kinase Inhibitor XL228 in Patients with Ph++ Leukemias with Either Failure to Multiple TKI Therapies or with T315I Mutation. *ASH Annual Meeting Abstracts* 2008 December 5, 2008; **112**(11)**:** 3232.

87. Cortes-Franco J, Dombret H, Schafhausen P, Brummendorf TH, Boissel N, Latini F*, et al.* Danusertib Hydrochloride (PHA-739358), a Multi-Kinase Aurora Inhibitor, Elicits Clinical Benefit in Advanced Chronic Myeloid Leukemia and Philadelphia Chromosome Positive Acute Lymphoblastic Leukemia. *ASH Annual Meeting Abstracts* 2009 November 20, 2009; **114**(22)**:** 864-.

88. Paquette RL, Shah NP, Sawyers CL, Martinelli G, John N, Chalukya M*, et al.* PHA-739358, an Aurora Kinase Inhibitor, Induces Clinical Responses in Chronic Myeloid Leukemia Harboring T315I Mutations of BCR-ABL. *ASH Annual Meeting Abstracts* 2007 November 16, 2007; **110**(11)**:** 1030-.

89. Sharma SV, Bell DW, Settleman J, Haber DA. Epidermal growth factor receptor mutations in lung cancer. *Nat Rev Cancer* 2007 Mar; **7**(3)**:** 169-181.

90. Mok T, Yang JJ, Lam KC. Treating patients with EGFR-sensitizing mutations: first line or second line--is there a difference? *J Clin Oncol* 2013 Mar 10; **31**(8)**:** 1081-1088.

91. Paez JG, Janne PA, Lee JC, Tracy S, Greulich H, Gabriel S*, et al.* EGFR mutations in lung cancer: correlation with clinical response to gefitinib therapy. *Science* 2004 Jun 4; **304**(5676)**:** 1497-1500.

92. Lynch TJ, Bell DW, Sordella R, Gurubhagavatula S, Okimoto RA, Brannigan BW*, et al.* Activating mutations in the epidermal growth factor receptor underlying responsiveness of non-small-cell lung cancer to gefitinib. *N Engl J Med* 2004 May 20; **350**(21)**:** 2129-2139.

93. Kobayashi S, Boggon TJ, Dayaram T, Janne PA, Kocher O, Meyerson M*, et al.* EGFR mutation and resistance of non-small-cell lung cancer to gefitinib. *N Engl J Med* 2005 Feb 24; **352**(8)**:** 786-792.

94. Pao W, Miller VA, Politi KA, Riely GJ, Somwar R, Zakowski MF*, et al.* Acquired resistance of lung adenocarcinomas to gefitinib or erlotinib is associated with a second mutation in the EGFR kinase domain. *PLoS Med* 2005 Mar; **2**(3)**:** e73.

95. Bean J, Brennan C, Shih JY, Riely G, Viale A, Wang L*, et al.* MET amplification occurs with or without T790M mutations in EGFR mutant lung tumors with acquired resistance to gefitinib or erlotinib. *Proc Natl Acad Sci U S A* 2007 Dec 26; **104**(52)**:** 20932-20937.

96. Engelman JA, Zejnullahu K, Mitsudomi T, Song Y, Hyland C, Park JO*, et al.* MET amplification leads to gefitinib resistance in lung cancer by activating ERBB3 signaling. *Science* 2007 May 18; **316**(5827)**:** 1039-1043.

97. Gilliland DG, Griffin JD. The roles of FLT3 in hematopoiesis and leukemia. *Blood* 2002 Sep 1; **100**(5)**:** 1532-1542.

98. Levis M, Allebach J, Tse KF, Zheng R, Baldwin BR, Smith BD*, et al.* A FLT3-targeted tyrosine kinase inhibitor is cytotoxic to leukemia cells in vitro and in vivo. *Blood* 2002 Jun 1; **99**(11)**:** 3885-3891.

99. Weisberg E, Boulton C, Kelly LM, Manley P, Fabbro D, Meyer T*, et al.* Inhibition of mutant FLT3 receptors in leukemia cells by the small molecule tyrosine kinase inhibitor PKC412. *Cancer Cell* 2002 Jun; **1**(5)**:** 433-443.

100. Stone RM, DeAngelo DJ, Klimek V, Galinsky I, Estey E, Nimer SD*, et al.* Patients with acute myeloid leukemia and an activating mutation in FLT3 respond to a small-molecule FLT3 tyrosine kinase inhibitor, PKC412. *Blood* 2005 Jan 1; **105**(1)**:** 54-60.

101. Smith BD, Levis M, Beran M, Giles F, Kantarjian H, Berg K*, et al.* Single-agent CEP-701, a novel FLT3 inhibitor, shows biologic and clinical activity in patients with relapsed or refractory acute myeloid leukemia. *Blood* 2004 May 15; **103**(10)**:** 3669-3676.

102. Knapper S, Burnett AK, Littlewood T, Kell WJ, Agrawal S, Chopra R*, et al.* A phase 2 trial of the FLT3 inhibitor lestaurtinib (CEP701) as first-line treatment for older patients with acute myeloid leukemia not considered fit for intensive chemotherapy. *Blood* 2006 Nov 15; **108**(10)**:** 3262-3270.

103. Zarrinkar PP, Gunawardane RN, Cramer MD, Gardner MF, Brigham D, Belli B*, et al.* AC220 is a uniquely potent and selective inhibitor of FLT3 for the treatment of acute myeloid leukemia (AML). *Blood* 2009 Oct 1; **114**(14)**:** 2984-2992.

104. Levis MJ, Perl AE, Dombret H, Dohner H, Steffen B, Rousselot P*, et al.* Final Results of a Phase 2 Open-Label, Monotherapy Efficacy and Safety Study of Quizartinib (AC220) in Patients with FLT3-ITD Positive or Negative Relapsed/Refractory Acute Myeloid Leukemia After Second-Line Chemotherapy or Hematopoietic Stem Cell Transplantation. *ASH Annual Meeting Abstracts* 2012 December 6, 2012; **120**(21)**:** 673.

105. Heidel F, Solem FK, Breitenbuecher F, Lipka DB, Kasper S, Thiede MH*, et al.* Clinical resistance to the kinase inhibitor PKC412 in acute myeloid leukemia by mutation of Asn-676 in the FLT3 tyrosine kinase domain. *Blood* 2006 Jan 1; **107**(1)**:** 293-300.

106. Piloto O, Wright M, Brown P, Kim KT, Levis M, Small D. Prolonged exposure to FLT3 inhibitors leads to resistance via activation of parallel signaling pathways. *Blood* 2007 Feb 15; **109**(4)**:** 1643-1652.

107. Flaherty KT, Hodi FS, Fisher DE. From genes to drugs: targeted strategies for melanoma. *Nat Rev Cancer* 2012 May; **12**(5)**:** 349-361.

108. Davies H, Bignell GR, Cox C, Stephens P, Edkins S, Clegg S*, et al.* Mutations of the BRAF gene in human cancer. *Nature* 2002 Jun 27; **417**(6892)**:** 949-954.

109. Tsai J, Lee JT, Wang W, Zhang J, Cho H, Mamo S*, et al.* Discovery of a selective inhibitor of oncogenic B-Raf kinase with potent antimelanoma activity. *Proc Natl Acad Sci U S A* 2008 Feb 26; **105**(8)**:** 3041-3046.

110. Joseph EW, Pratilas CA, Poulikakos PI, Tadi M, Wang W, Taylor BS*, et al.* The RAF inhibitor PLX4032 inhibits ERK signaling and tumor cell proliferation in a V600E BRAF-selective manner. *Proc Natl Acad Sci U S A* 2010 Aug 17; **107**(33)**:** 14903-14908.

111. Sondergaard JN, Nazarian R, Wang Q, Guo D, Hsueh T, Mok S*, et al.* Differential sensitivity of melanoma cell lines with BRAFV600E mutation to the specific Raf inhibitor PLX4032. *J Transl Med*; **8:** 39.

112. Yang H, Higgins B, Kolinsky K, Packman K, Go Z, Iyer R*, et al.* RG7204 (PLX4032), a selective BRAFV600E inhibitor, displays potent antitumor activity in preclinical melanoma models. *Cancer Res* 2010 Jul 1; **70**(13)**:** 5518-5527.

113. Nazarian R, Shi H, Wang Q, Kong X, Koya RC, Lee H*, et al.* Melanomas acquire resistance to B-RAF(V600E) inhibition by RTK or N-RAS upregulation. *Nature* 2010 Dec 16; **468**(7326)**:** 973-977.

114. Johannessen CM, Boehm JS, Kim SY, Thomas SR, Wardwell L, Johnson LA*, et al.* COT drives resistance to RAF inhibition through MAP kinase pathway reactivation. *Nature* 2010 Dec 16; **468**(7326)**:** 968-972.

115. Wagle N, Emery C, Berger MF, Davis MJ, Sawyer A, Pochanard P*, et al.* Dissecting therapeutic resistance to RAF inhibition in melanoma by tumor genomic profiling. *J Clin Oncol* 2011 Aug 1; **29**(22)**:** 3085-3096.

116. Poulikakos PI, Persaud Y, Janakiraman M, Kong X, Ng C, Moriceau G*, et al.* RAF inhibitor resistance is mediated by dimerization of aberrantly spliced BRAF(V600E). *Nature* 2011 Dec 15; **480**(7377)**:** 387-390.

117. Zheng CF, Guan KL. Dephosphorylation and inactivation of the mitogen-activated protein kinase by a mitogen-induced Thr/Tyr protein phosphatase. *J Biol Chem* 1993 Aug 5; **268**(22)**:** 16116-16119.

118. Alessi DR, Smythe C, Keyse SM. The human CL100 gene encodes a Tyr/Thr-protein phosphatase which potently and specifically inactivates MAP kinase and suppresses its activation by oncogenic ras in Xenopus oocyte extracts. *Oncogene* 1993 Jul; **8**(7)**:** 2015-2020.

119. Sun H, Charles CH, Lau LF, Tonks NK. MKP-1 (3CH134), an immediate early gene product, is a dual specificity phosphatase that dephosphorylates MAP kinase in vivo. *Cell* 1993 Nov 5; **75**(3)**:** 487-493.

120. Rohan PJ, Davis P, Moskaluk CA, Kearns M, Krutzsch H, Siebenlist U*, et al.* PAC-1: a mitogen-induced nuclear protein tyrosine phosphatase. *Science* 1993 Mar 19; **259**(5102)**:** 1763-1766.

121. Caunt CJ, Keyse SM. Dual-specificity MAP kinase phosphatases (MKPs): shaping the outcome of MAP kinase signalling. *FEBS J* 2013 Jan; **280**(2)**:** 489-504.

122. Cabrita MA, Christofori G. Sprouty proteins, masterminds of receptor tyrosine kinase signaling. *Angiogenesis* 2008; **11**(1)**:** 53-62.

123. Hanafusa H, Torii S, Yasunaga T, Nishida E. Sprouty1 and Sprouty2 provide a control mechanism for the Ras/MAPK signalling pathway. *Nat Cell Biol* 2002 Nov; **4**(11)**:** 850-858.

124. Wakioka T, Sasaki A, Kato R, Shouda T, Matsumoto A, Miyoshi K*, et al.* Spred is a Sprouty-related suppressor of Ras signalling. *Nature* 2001 Aug 9; **412**(6847)**:** 647-651.

125. Murphy JM, Tannahill GM, Hilton DJ, Greenhalgh CJ, Ralph AB, Edward AD. Chapter 64 - The Negative Regulation of JAK/STAT Signaling. *Handbook of Cell Signaling (Second Edition)*. Academic Press: San Diego, 2010, pp 467-480.

126. Pratilas CA, Taylor BS, Ye Q, Viale A, Sander C, Solit DB*, et al.* (V600E)BRAF is associated with disabled feedback inhibition of RAF-MEK signaling and elevated transcriptional output of the pathway. *Proc Natl Acad Sci U S A* 2009 Mar 17; **106**(11)**:** 4519-4524.

127. Xu X, Quiros RM, Gattuso P, Ain KB, Prinz RA. High prevalence of BRAF gene mutation in papillary thyroid carcinomas and thyroid tumor cell lines. *Cancer Res* 2003 Aug 1; **63**(15)**:** 4561-4567.

128. Kimura ET, Nikiforova MN, Zhu Z, Knauf JA, Nikiforov YE, Fagin JA. High prevalence of BRAF mutations in thyroid cancer: genetic evidence for constitutive activation of the RET/PTC-RAS-BRAF signaling pathway in papillary thyroid carcinoma. *Cancer Res* 2003 Apr 1; **63**(7)**:** 1454-1457.

129. Kopetz S, Desai J, Chan E, Hecht JR, O'Dwyer PJ, Lee RJ*, et al.* PLX4032 in metastatic colorectal cancer patients with mutant BRAF tumors. *ASCO Meeting Abstracts* 2010 June 14, 2010; **28**(15_suppl)**:** 3534.

130. Sala E, Mologni L, Truffa S, Gaetano C, Bollag GE, Gambacorti-Passerini C. BRAF silencing by short hairpin RNA or chemical blockade by PLX4032 leads to different responses in melanoma and thyroid carcinoma cells. *Mol Cancer Res* 2008 May; **6**(5)**:** 751-759.

131. Nucera C, Nehs MA, Nagarkatti SS, Sadow PM, Mekel M, Fischer AH*, et al.* Targeting BRAFV600E with PLX4720 displays potent antimigratory and anti-invasive activity in preclinical models of human thyroid cancer. *Oncologist* 2011; **16**(3)**:** 296-309.

132. Kim K, Cabanillas M, Lazar AJ, Williams MD, Sanders DL, Ilagan JL*, et al.* Clinical Responses to Vemurafenib in Patients with Metastatic Papillary Thyroid Cancer Harboring V600EBRAF Mutation. *Thyroid* 2013 Mar 14.

133. Savvides P, Nagaiah G, Lavertu P, Fu P, Wright JJ, Chapman R*, et al.* Phase II trial of sorafenib in patients with advanced anaplastic carcinoma of the thyroid. *Thyroid* 2013 May; **23**(5)**:** 600-604.

134. Prahallad A, Sun C, Huang S, Di Nicolantonio F, Salazar R, Zecchin D*, et al.* Unresponsiveness of colon cancer to BRAF(V600E) inhibition through feedback activation of EGFR. *Nature* Mar 1; **483**(7387)**:** 100-103.

135. Montero-Conde C, Ruiz-Llorente S, Dominguez JM, Knauf JA, Viale A, Sherman EJ*, et al.* Relief of feedback inhibition of HER3 transcription by RAF and MEK inhibitors attenuates their antitumor effects in BRAF-mutant thyroid carcinomas. *Cancer Discov* 2013 May; **3**(5)**:** 520-533.

136. Lito P, Pratilas CA, Joseph EW, Tadi M, Halilovic E, Zubrowski M*, et al.* Relief of profound feedback inhibition of mitogenic signaling by RAF inhibitors attenuates their activity in BRAFV600E melanomas. *Cancer Cell* Nov 13; **22**(5)**:** 668-682.

137. Wilson TR, Fridlyand J, Yan Y, Penuel E, Burton L, Chan E*, et al.* Widespread potential for growth-factor-driven resistance to anticancer kinase inhibitors. *Nature* Jul 26; **487**(7408)**:** 505-509.

138. Straussman R, Morikawa T, Shee K, Barzily-Rokni M, Qian ZR, Du J*, et al.* Tumour micro-environment elicits innate resistance to RAF inhibitors through HGF secretion. *Nature* Jul 26; **487**(7408)**:** 500-504.

Chapter 2

MEK-Dependent Negative Feedback Facilitates BCR-ABL-Mediated Oncogene Addiction

Abstract

The clinical experience with BCR-ABL tyrosine kinase inhibitors (TKIs) for the treatment of chronic myeloid leukemia (CML) provides compelling evidence for oncogene addiction. Yet, the molecular basis of oncogene addiction remains elusive. Through unbiased quantitative phosphoproteomic analyses of CML cells transiently exposed to BCR-ABL TKI, we identified persistent downregulation of growth factor-receptor (GF-R) signaling pathways. We then established and validated a tissue-relevant isogenic model of BCR-ABL-mediated addiction, and found evidence for myeloid GF-R signaling pathway rewiring that profoundly and persistently dampens physiologic pathway activation. We demonstrate that eventual restoration of ligand-mediated GF-R pathway activation is insufficient to fully rescue cells from a competing apoptotic fate. In contrast to previous work with BRAFV600E in melanoma cells, feedback inhibition following BCR-ABL TKI treatment is markedly prolonged, extending beyond the time required to initiate apoptosis. Mechanistically, BCR-ABL-mediated oncogene addiction is facilitated by persistent high levels of MEK-dependent negative feedback.

Statement of Significance

We found that BCR-ABL kinase activity can confer addiction *in vitro* by rewiring myeloid growth factor receptor (GF-R) signaling pathways through establishment of a high level of MEK-dependent negative feedback that effectively dampens prosurvival ligand-mediated GF-R pathway activation. Our findings predict that deeper, more durable responses to targeted agents across a broad range of human malignancies may be facilitated by maintenance of negative feedback in the setting of oncoprotein inhibition.

Introduction

Translational studies with small molecule tyrosine kinase inhibitors (TKIs) in patients with chronic myeloid leukemia (CML) have convincingly demonstrated that the clinical activity of these agents is achieved through inhibition of the intended target BCR-ABL (1). To date, the high rate of success associated with BCR-ABL TKIs provides the most compelling clinical evidence for the phenomenon of oncogene addiction, the exquisite reliance of cancer cells upon a pathologically activated oncogene. Oncogene addiction enables targeted therapies to effect clinical responses and simultaneously cause little toxicity. Even in patients with the most advanced phases of CML, a substantial proportion can achieve deep responses with BCR-ABL TKIs (2).

Our understanding of the molecular basis of oncogene addiction is poor. Sharma et al proposed the term "oncogenic shock" to describe the effect that numerous activated oncogenes, including BCR-ABL and mutant EGFR, have on the balance between prosurvival and proapoptotic signals. The oncogenic shock model proposes that upon acute inhibition of oncogene activity, a more rapid decay in prosurvival signals leads to a state that favors apoptosis (3). While this model provides a useful conceptual framework in which to begin to understand the phenomenon of oncogene addiction, evidence to support the oncogenic shock model is largely circumstantial, and molecular mechanisms that lead to the proposed heightened levels of prosurvival and proapoptotic signals have not been well-characterized.

Over the past decade, numerous oncogenic kinases in a wide variety of cancers have been identified and clinically targeted, including EGFR and ALK in non-small cell lung cancer (NSCLC), BRAFV600E in melanoma and colorectal cancer, and FLT3-ITD in acute

myeloid leukemia (AML). However, efforts to extrapolate the clinical success of BCR-ABL TKI therapy in CML to other malignancies have failed; the majority of patients treated with other clinically active TKIs do not achieve responses of similar magnitude. For example, the selective BRAF inhibitor vemurafenib, which is approved for BRAFV600E-expressing metastatic melanoma, rarely effects deep reductions in tumor volume (4). Interestingly, MEK inhibitors are active in BRAFV600E cells *in vitro* but, unexpectedly, not in cells with activated receptor tyrosine kinases (RTKs) which have also been documented to activate the RAS/MEK/ERK pathway (5). Previous studies demonstrated that BRAFV600E establishes a high level of ERK transcriptional output and MEK-dependent negative feedback of growth factor-receptor (GF-R) signaling, whereas activated oncogenic RTKs do not. Additionally, in contrast to RTKs, BRAFV600E escapes MEK-dependent negative feedback (6).

It has been postulated that efficient bypass of BRAF kinase inhibition may allow melanoma cells to survive in the tumor microenvironment through GF-R-mediated re-activation of the RAS/MAPK signaling pathway despite target inhibition, thereby rendering BRAFV600E melanoma cells relatively insensitive to vemurafenib, although this concept has not been definitively confirmed. Recent experimental data has demonstrated that melanoma and colorectal cancer cells harboring BRAFV600E mutations are inherently primed to circumvent BRAF inhibition by vemurafenib through rapid relief of negative feedback of GF-R signaling (7-10).

Here, we sought to characterize the molecular mechanisms that underlie BCR-ABL-mediated oncogene addiction in an effort to understand what makes this kinase the best-validated target in human cancer. We applied an unbiased kinetic quantitative

phosphoproteomic analysis to CML cells transiently exposed to the BCR-ABL TKI dasatinib to identify candidate mediators of BCR-ABL-dependent cell survival. To test the importance of the observed signaling changes, we established a tissue and species-context relevant isogenic model system to interrogate BCR-ABL-mediated oncogene addiction and validated our findings in patient-derived cell lines.

Results

Phosphoproteomic Analysis of Pulsed Dasatinib-Treated CML Cells Reveals Durable Alterations in Growth-Factor Signaling Pathways.

Previous work demonstrated that transient exposure (20 minutes) of CML cell lines to clinically relevant concentrations of dasatinib elicits apoptosis with kinetics similar to continuous TKI exposure. This occurs despite evidence that BCR-ABL kinase activity is largely restored within four hours of drug washout when assessed by antiphosphotyrosine antibody western immunoblot assays (11-13). We hypothesized that the phosphorylation status of a subset of proteins must be durably altered, and critical mediators of BCR-ABL-mediated cell survival would be included amongst this group. We therefore undertook an unbiased kinetic, quantitative assessment of phosphotyrosine-containing proteins in the patient-derived CML cell line K562 transiently exposed to a high-dose pulse (HDP) of 100nM dasatinib using stable isotope labeling by amino acids in culture (SILAC). We successfully identified 184 phosphotyrosine residues in 126 different proteins, representing the most comprehensive kinetic analysis of TKI-treated CML patient-derived cells to date (**supplemental table 1**). We compared the quantified phosphotyrosine profile before TKI treatment, at the end of a 20-minute TKI exposure, and at three and six hours after TKI washout (**figure 1a**).

We subsequently grouped phosphotyrosine peptides based on the pattern of tyrosine modification following HDP dasatinib treatment. Twenty-four tyrosine residues were transiently dephosphorylated, 31 were gradually dephosphorylated, 46 were not appreciably altered, and seven were hyperphosphorylated. Notably, 55 tyrosine residues

were persistently dephosphorylated following TKI washout, and functional enrichment of these peptides revealed an over-representation of proteins involved in GF-R signaling pathways (**supplemental table 2**). Amongst these were tyrosine residues from STAT5A/B, ERK1/2, GAB1 and SHC1 (**figure 1b**). Phosphotyrosine peptides associated with PI3K/AKT pathway activation were either transiently dephosphorylated or not altered (**figure 1b**). Several of the signaling changes identified in the phosphoproteomic analysis were confirmed by western immunoblot in K562 and KU812 cells, a second independent patient-derived CML cell line (**figure 1c**). While tyrosine residues within the PI3K/AKT pathway were not durably altered in the phosphoproteomic (or western immunoblot) analysis, serine phosphorylation events on S6 (S235/S236) were durably altered in a time-dependent manner following TKI treatment (**figure 1c**).

Although the BCR-ABL activation loop phosphorylation site Y393, which is essential for kinase activity, was only transiently dephosphorylated following HDP dasatinib treatment, phosphoproteomic and western immunoblot analyses revealed substantial variation in phosphorylation changes of BCR-ABL tyrosine residues (**figure 1d**). Similar phosphorylation changes were observed in K562 and KU812 cells treated with a HDP of the BCR-ABL TKI imatinib (**supplemental figure 1a**), arguing that the observed signaling changes are likely a consequence of BCR-ABL inhibition, and not the result of unintended off-target kinase inhibition. Collectively, our phosphoproteomic and immunoblot analyses, coupled with previous studies suggest a requirement for the maintenance of at least two of the three canonical BCR-ABL activated pathways (JAK/STAT, RAS/MEK/ERK, and PI3K) for CML cell survival in vitro (14), strongly suggest that persistent activation of pathways downstream of GF-R signaling is critical for BCR-ABL-mediated oncogene addiction.

BCR-ABL Confers a State of Oncogene Addiction in Human Myeloid Cells *In Vitro*.

To investigate whether BCR-ABL appropriates GF-R signaling pathways to establish oncogene addiction, we sought to model oncogene addiction *in vitro* by establishing an isogenic cell line model system. Human-derived erythroleukemia TF1 cells require hGM-CSF or hIL-3 for proliferation and survival *in vitro*, but can be transformed to growth factor independence by BCR-ABL (15). We established pools of TF1/puro and TF1/BCR-ABL cells through retroviral transduction and puromycin selection. Western immunoblot analysis of BCR-ABL Y245 phosphorylation in cell lysates generated under cytokine and serum-starve conditions confirmed the expression of active BCR-ABL protein in TF1/BCR-ABL cells as well as increased phosphorylation of downstream targets CRKL (Y207), STAT5A/B (Y694/Y699), ERK1/2 (T202/Y204) and S6 (S235/S236) relative to TF1/puro cells (**supplemental figure 2a, 2b**).

To determine if TF1/BCR-ABL cells have acquired reliance upon BCR-ABL activity for survival, and thereby truly represent a model of oncogene addiction, we measured the amount of apoptosis induced in response to simultaneous growth factor deprivation and dasatinib treatment. hGM-CSF-deprivation alone led to decreased viability in TF1/puro cells, and as expected, dasatinib had no additional impact on the extent of apoptosis induced. In sharp contrast, TF1/BCR-ABL cells underwent a much larger and statistically significant increase in apoptosis when treated with dasatinib (**figure 2a**). Moreover, while continuous co-treatment with hGM-CSF and dasatinib fully rescued TF1/puro cells from apoptosis, TF1/BCR-ABL cells were only partially rescued from dasatinib-mediated apoptosis by hGM-CSF. Similar results were obtained with imatinib (**supplemental table 3**). These observations demonstrate that BCR-ABL expression generates a state of

oncogene addiction in TF1 cells, which is associated with functionally altered GM-CSF receptor (GM-CSFR) signaling. More broadly, these findings implicate rewiring of GF-R signaling pathways in the establishment of the BCR-ABL-addicted state.

BCR-ABL Kinase Activity Attenuates GM-CSF Receptor Signal Transduction in TF1 Cells.

To further characterize the GM-CSFR signaling axis and to investigate the molecular mechanisms through which BCR-ABL may subvert GF-R signaling, we cultured TF1/puro and TF1/BCR-ABL cells under serum and growth factor-deprived conditions and then stimulated the cells with hGM-CSF, which activates the JAK2/STAT5, RAS/MAPK, and PI3K/AKT signaling pathways (16). While robust activation of JAK2 was observed in both cell lines, GTP loading of RAS was only observed in hGM-CSF-stimulated TF1/puro cells (**figure 2b**; lanes 3 versus lanes 7 and **supplemental figure 2c, 2d**). We also assessed the effect of a one-hour dasatinib pretreatment prior to stimulation with hGM-CSF. Again, increased RAS-GTP loading was only observed in TF1/puro cells (**figure 2b**; lane 4 versus lane 8 and **supplemental figure 2d**). Moreover, STAT5, ERK, and AKT activation by hGM-CSF was substantially attenuated in TF1/BCR-ABL cells relative to TF1/puro cells (**figure 2b**). Collectively, these data demonstrate that BCR-ABL kinase activity negatively regulates GM-CSFR signaling, and this regulation persists for more than one hour after BCR-ABL kinase activity is inhibited.

To determine if GF-R signaling in BCR-ABL-expressing cells can be fully restored within 2-4 hours after kinase inhibition, as has been observed with vemurafenib-treated BRAFV600E melanoma cells stimulated with HGF, EGF, or NRG1 (7, 9, 10), TF1/puro and

TF1/BCR-ABL cells were treated with BCR-ABL TKI or vehicle for up to eight hours prior to hGM-CSF stimulation. While a gradual increase in the hGM-CSF-mediated activation of STAT5, ERK, and AKT was observed with more prolonged BCR-ABL inhibition (**figure 2c**; lanes 9, 10, 11, 12; imatinib data not shown), the magnitude of pathway reactivation in TF1/BCR-ABL cells after eight hours of BCR-ABL kinase inhibition was substantially less than that observed in TF1/puro cells (**figure 2c**; lanes 3, 4, 5, 6). Additionally, despite moderate hGM-CSF-mediated rephosphorylation of ERK in TF1/BCR-ABL cells, RAS activation appeared to be minimal after eight hours of BCR-ABL inhibition (**figure 2c**). Importantly, dasatinib sufficiently inhibited BCR-ABL kinase activity, as monitored by BCR-ABL activation loop phosphorylation at residue Y393, throughout the duration and all treatment conditions of the experiment (**figure 2c**).

We next assessed whether more prolonged BCR-ABL inhibition is required to enable a near complete restoration of GM-CSFR signaling. Indeed, treatment of TF1/puro and TF1/BCR-ABL cells with dasatinib for 24 hours prior to hGM-CSF stimulation was associated with more complete RAS activation in TF1/BCR-ABL cells (**figure 2d**). Similarly, activation of STAT5, ERK, and AKT was restored to levels comparable to those observed in TF1/puro cells (**figure 2e**). However, as demonstrated earlier, despite this delayed restoration of growth factor signaling, hGM-CSF failed to fully rescue TF1/BCR-ABL cells from TKI-mediated apoptosis (**figure 2a**). These results demonstrate an important biologic consequence of GF-R signaling rewiring by BCR-ABL: a substantial proportion of cells commit to apoptosis despite the eventual reestablishment of prosurvival growth factor signaling.

BCR-ABL Kinase Activity Attenuates Erythropoietin Receptor Signal Transduction in CML Patient-derived Cells.

To extend our findings to a CML patient-derived cell line, we evaluated whether BCR-ABL rewires GF-R signaling in K562 cells, which express a functional erythropoietin receptor (EPO-R) (17). Relative to HEL erythroleukemia cells harboring the activating JAK2/V617F allele, K562 cells exhibit nearly undetectable levels of JAK2 Y1007 phosphorylation in the absence of erythropoietin (hEPO) (**supplemental figure 3a**). Stimulation of K562 cells with hEPO led to a modest increase in JAK2 activation; brief (one-hour) pretreatment with a BCR-ABL TKI prior to hEPO stimulation did not appreciably impact the degree of JAK2 activation (**figure 3a**).

We next assessed the effect of more prolonged BCR-ABL inhibition (2-24 hours) on hEPO-mediated activation of JAK2 and downstream pathways in K562 cells. We observed a time-dependent increase in hEPO-mediated STAT5, ERK and AKT activation with either dasatinib or imatinib pre-treatment (**figure 3b** and **supplemental figure 3b**). A statistically significant increase in the degree of hEPO-mediated activation of JAK2 (**figure 3c** and **supplemental figure 3c**) and a substantial increase in RAS activity (**figure 3d**) were observed following 24 hours of prior BCR-ABL TKI treatment.

JAK2 Activity Becomes Critical for EPO-R Signaling and K562 Cell Survival After Prolonged BCR-ABL Inhibition.

To determine if the observed restoration of EPO-R signaling following prolonged BCR-ABL inhibition is mediated through the canonical EPO-R/JAK2 axis, we utilized the selective JAK2 inhibitor TG101348. Combined 24-hour pre-treatment of K562 cells with

TG101348 and a BCR-ABL TKI completely prevented hEPO-mediated JAK2 activation and re-phosphorylation of STAT5, ERK, and AKT (**figure 3e** and **figure 3f, lanes 8,9, 11 and 12**). Similar to the partial rescue from apoptosis hGM-CSF provides TKI-treated TF1/BCR-ABL cells (**figure 2a**), hEPO partially rescues K562 cells from imatinib-mediated apoptosis [(18) and **supplemental table 4]**. This partial rescue from imatinib (or dasatinib)-mediated apoptosis was completely reversible by co-administration of TG101348. In the setting of active BCR-ABL, TG101348 had no pro-apoptotic effect on K562 cells (**supplemental table 4**). These observations suggest that JAK2 kinase is minimally active in the presence of BCR-ABL kinase activity, but can become critical for growth-factor-mediated CML cell rescue after prolonged BCR-ABL inhibition.

BCR-ABL Inhibition Down-Regulates Modulators of Negative Feedback and Upregulates the Erythropoietin Receptor.

To better understand the mechanism(s) responsible for the inability of GF-Rs to effectively transduce signal in BCR-ABL-expressing cells, K562 cells were treated with dasatinib and assessed for time-dependent changes in global gene expression by microarray analysis. In total, 1903 genes were significantly differentially expressed at either 4, 8, or 24 hours of dasatinib treatment (**supplemental table 5**). As negative regulators of RAS/MAPK signaling were previously shown to be down-regulated early after MAPK inhibition in BRAFV600E cells (6), we reasoned that key negative regulators of EPO-R signaling in K562 cells would be enriched among those genes significantly down-regulated after 4 hours of dasatinib treatment. In total, 162 genes followed this pattern (FDR<1%) including several well-characterized members of the JAK/STAT and RAS/MAPK

negative feedback machinery: *SOCS1*, *SOCS2*, *CISH*, *SPRY2*, *SPRY4*, *SPRED1*, *SPRED2*, and *PIM1*, but notably excluded were others such as *DUSP4* and *DUSP6* (**figure 4a**). Other genes among these 162 potently down-regulated after 4 hours of treatment were downstream effectors of MEK/ERK signaling, such as cyclin D1 (*CCND1*) as well as genes that traditionally comprise ERK-mediated transcriptional output including transcription factors associated with transformation (*ETV5* and *MYC*) among other ERK targets (*IER3* and *EGR1*).

We explored the 1048 unique probes whose expression increased following the initiation of dasatinib treatment to identify genes that become de-repressed following prolonged BCR-ABL inhibition, as might be expected of positive effectors of GF-R signaling, like JAK2 or the SRC family kinases. Several non-canonical dual-specificity phosphatases (DUSPs) not traditionally involved in negative feedback regulation of the RAS pathway were among this group of genes (i.e. DUSP1, DUSP13, DUSP21, DUSP28). Interestingly, EPO-R expression increased significantly in a time-dependent manner in dasatinib-treated K562 cells (**figure 4a**). The observed changes in a subset of these genes were subsequently validated by quantitative PCR (qPCR) in dasatinib and imatinib treated K562 cells (**figure 4b**). Similar changes in gene expression were observed in K562 cells treated with the allosteric MEK inhibitor PD0325901, suggesting that the RAS/MAPK pathway is primarily responsible for establishing the negative feedback network and subsequent transcriptional output associated with attenuation of myeloid GF-R signaling.

MEK/ERK-Dependent Negative Feedback Attenuates EPO-R Signaling in K562 Cells.

To assess the functional importance of MEK-dependent negative feedback toward GF-R signaling attenuation in CML cells, we treated K562 cells with PD0325901 for 24 hours. MEK inhibition alone (in the absence of hEPO stimulation) produced robust GTP-loading of RAS (**figure 5a**; lane 3), whereas co-treatment with dasatinib/PD0325901 prevented RAS GTP-loading, demonstrating that RAS activation upon MEK inhibition in CML cells is mediated by BCR-ABL and is not the result of exogenous or autocrine growth factors (**figure 5a**; lane 3 and 4) as has been recently documented to occur in acute myeloid leukemia, where HGF secretion by leukemic cells can foster survival in the setting of kinase inhibitor treatment (19). hEPO stimulation of PD0325901 pre-treated cells resulted in further RAS activation, suggesting that efficient EPO-R signaling in K562 cells can be restored by MEK inhibition alone (**figure 5a**; lane 3 and lane 7 and **supplemental figure 4a**).

To investigate whether MEK-dependent negative feedback dampens EPO-R signaling at the level of JAK2, we assessed JAK2 phosphorylation in response to hEPO after a 24-hour pretreatment with PD0325901. Under these conditions, hEPO-mediated JAK2 activation comparable to that observed with a 24-hour dasatinib pretreatment (**figure 5b**; **supplemental figure 4b**), suggesting that MEK-dependent negative feedback acts at the level of EPO-R/JAK2 in K562 cells. No further increase in hEPO-mediated JAK2 activation was detected when cells were pretreated with the combination of dasatinib and MEK inhibitor for 24 hours prior to hEPO stimulation (**figure 5b**; lanes 6, 7 versus lane 8). In the absence of hEPO stimulation, MEK inhibition did not result in a detectable increase in JAK2 phosphorylation (**figure 5b**; lane 3).

To determine if BCR-ABL is itself subjected to MEK-dependent negative feedback, we evaluated the effect of MEK inhibition upon the phosphorylation status of multiple BCR-ABL tyrosine residues, including the activation loop tyrosine (Y393). Across all BCR-ABL phosphotyrosines interrogated, little to no change in phosphorylation was observed (**figure 5c**), suggesting that similar to BRAFV600E and in sharp contrast to RTKs (6), BCR-ABL both establishes and evades a high level of MEK-dependent negative feedback regulation.

K562 Cells Can Commit to Apoptosis Prior to Full Restoration of EPO-R Signaling.

The long delay observed in the restoration of EPO-mediated pathway activation in K562 cells sharply contrasts with the rapid (~2-4 hours) and full reactivation of the MEK/ERK pathway in EGF-stimulated BRAFV600E cells following pre-treatment with BRAF vemurafenib (10). This finding, coupled with the inability of hEPO to fully rescue K562 cells from dasatinib-mediated apoptosis, suggests that TKI-treated CML cells face competing fates: survival mediated by growth factor signaling versus commitment to apoptosis prior to complete restoration of GF-R signaling. To formally test this, we initially assessed the kinetics of apoptosis induction in TKI-treated K562 cells by western immunoblot. While substantial caspase-3 cleavage was detected after 24 hours of dasatinib treatment, we observed very little evidence of apoptosis following 12 hours of treatment (**figure 6a**). To detect caspase-3 activity with a higher degree of sensitivity, we next employed a plasmonic nanosensor technique capable of detecting single molecule caspase-3 cleavage events through a change in light scattering intensity of a gold nanoshell pair (**figure 6b**; **6c**) (20). This assay reliably detected caspase-3 activity following only

eight hours of dasatinib treatment (**figure 6d**), demonstrating that a commitment to apoptosis can precede full restoration of GF-R signaling in CML patient-derived BCR-ABL-addicted cells.

Discussion

The efficacy of BCR-ABL TKI therapy for CML surpasses that of all other FDA-approved targeted kinase inhibitors and thereby provides the most compelling clinical example of oncogene addiction. Our poor understanding of the molecular basis of this phenomenon has been due, in part, to the lack of effective models. Here, we have exposed CML cells transiently to dasatinib and identified durable changes in effectors of GF-R signaling in CML cells treated transiently with dasatinib, which likely explain the cytotoxic effects of BCR-ABL inhibition. We then established and validated an isogenic system of BCR-ABL-mediated oncogene addiction and investigated its molecular features. We found that BCR-ABL-mediated oncogene addiction is the result of physiologic negative feedback inhibition that functionally and persistently dampens GF-R signaling at multiple nodes, including, in the case of EPO-R, at the level of growth factor receptor transcription. Relief from this largely MEK-dependent negative feedback network is required to enable full restoration of GF-R signaling and only occurs after prolonged BCR-ABL kinase inhibition. As with BRAFV600E in melanoma cells, BCR-ABL establishes a high level of MEK-dependent negative feedback. Importantly, negative feedback dampens GF-R signaling substantially longer in CML cells than in BRAFV600E-expressing melanoma cells. As a consequence, GF-R signaling is insufficient to fully rescue cells from the competing fate of apoptosis, which for the first time, we document to be initiated in CML cells as early as eight hours following TKI treatment. As a result of this interplay between a commitment to apoptosis on one hand, and the decay of negative feedback that facilitates restoration of prosurvival growth factor signaling on the other, CML cells demonstrate a profound reliance upon BCR-ABL kinase activity for survival (**figure 7a**; **7b**).

Both experimental and clinical evidence suggest that the effectiveness of BRAFV600E inhibition in melanoma contrasts sharply to BCR-ABL inhibition in CML. *In vitro*, BRAFV600E melanoma cell lines largely fail to undergo apoptosis when treated with BRAF inhibitors such as vemurafenib; only a minor degree of apoptosis is observed even in the presence of high concentrations of BRAF kinase inhibitors (21-24). Although the majority of melanoma patients treated with vemurafinib respond to some degree, most fail to achieve deep remissions (4). A number of BRAFV600E-expressing melanoma and colorectal cancer cell lines can be rescued from BRAF inhibitor treatment by the addition of RTK ligands *in vitro*, leading to subsequent reactivation of MAPK and AKT signaling as soon as 1 hour after BRAF inhibitor treatment (7-10). In contrast, the corresponding time frame we observed in BCR-ABL-expressing cells is markedly different: only partial restoration of GF-R signaling occurs after 8 hours of TKI treatment, at which time a competing commitment to apoptosis has already been initiated in a substantial proportion of cells.

Despite the clinical differences observed with inhibitors of BRAFV600E and BCR-ABL, these two oncoproteins share some similar biological properties. Both are pathologically activated cytosolic kinases that establish and evade a high-degree of MEK-dependent negative feedback (6). Also, a substantial core component of the ERK transcriptional output is similarly diminished when these two oncoproteins are inhibited, including ERK pathway effectors, negative feedback regulators, and downstream transcription factors. For instance, both kinases appear to induce the expression of members of the Sprouty gene family, which typically target the ERK pathway for negative feedback inhibition at the level of RAF, RAS and upstream RTKs.

There are, however, notable differences in the negative feedback networks generated by BCR-ABL and BRAFV600E, particularly with respect to where the feedback is operable. At the GF-R level we found that BCR-ABL kinase activity down-regulates EPO-R expression in K562 cells, largely through MEK/ERK signaling, which may further contribute to the delay in restoring pro-survival GF-R-mediated signaling following BCR-ABL inhibition. In contrast, experimental evidence suggests that there is sufficient RTK expression in BRAFV600E cells such that pro-survival signaling can be restored in timely manner (7-10). Additional differences exist in downstream components of negative feedback, particularly at the level of ERK phosphatases, which target either nuclear or cytosolic ERK for regulation downstream of the oncogenic insult. In sharp contrast to the effect of BRAFV600E inhibition in melanoma cells where downregulation of the dual specificity phosphatase DUSP6 is apparent at multiple levels (6, 10), we failed to detect DUSP6 at the protein level in CML cells (data not shown) and, in agreement with this observation, BCR-ABL inhibition failed to down-regulate the expression levels of *DUSP6*.

Collectively, these differences demonstrate that MEK-dependent negative feedback is oncogene-specific. In BCR-ABL-expressing CML cells, activation of the dual specificity phosphatases *DUSP4/6* is not critical, however, there is a simultaneous need to activate feedback effectors of the parallel JAK/STAT pathway (via *SOCS1* and *SOCS2*). Activation of JAK/STAT feedback effectors is absent in BRAFV600E melanoma cells and instead there is a need for a multifaceted and tiered negative feedback regulation of the RAS/MAPK pathway. Together, these results reaffirm that the networks mediating negative feedback inhibition of oncogenic signaling are multifaceted, pleiotropic, and context-dependent. Further study is required to dissect the importance of the observed qualitative and

quantitative differences in negative feedback elicited by these kinases. To that end, the TF1 model system of oncogene addiction described here may prove particularly useful.

Our work provides important insight into the role of JAK2 in the molecular pathogenesis of CML, which has been a subject of considerable controversy. It is known that CML stem cells persist for at least several years in most, if not all, CML patients. It has been speculated that successful inhibition of BCR-ABL kinase activity in CML stem cells may be insufficient to elicit apoptosis in these cells due to their residence in a cytokine-rich bone marrow microenvironment that maintains the viability of these cells despite BCR-ABL TKI treatment (25). One group provided evidence that combined BCR-ABL and JAK2 inhibition achieves more complete eradication of CML cells in conditioned media *in vitro* (26), while another group recently demonstrated that JAK2 is completely dispensable for nearly all aspects of BCR-ABL-mediated myeloid disease initiation and maintenance (27). Although these studies offer conflicting views on the importance of JAK2 activity for CML pathogenesis, our experimental results and proposed model of BCR-ABL-dependent attenuation of GF-R signaling resolves this apparent paradox. When BCR-ABL is active, JAK2 plays little or no role in signal transduction due to MEK-dependent negative feedback-mediated attenuation of GF-R signaling. However, after prolonged BCR-ABL inhibition, negative feedback is relieved and JAK2 may become critically important as a mediator of STAT5 phosphorylation in the setting of external growth factors. Our data provide mechanistic support for clinical efforts to combine BCR-ABL TKIs with potent JAK2 TKIs, which are predicted to have no activity alone, but would be expected to demonstrate a synthetic lethal interaction with BCR-ABL TKIs in the setting of exogenous growth factors, specifically as a consequence of the negative feedback we describe here. If JAK2 serves a

redundant function in facilitating prosurvival GF-R mediated signaling in the bone marrow microenvironment, alternative approaches will be required.

The oncogenic shock model of oncogene addiction (3) was proposed with limited supporting data, and the molecular mediators of oncogene addiction have remained elusive. Our data strongly implicate persistent negative feedback in the promotion of apoptosis following kinase inactivation, and thus provide valuable molecular mechanistic insights into the basis of both oncogene addiction and the oncogenic shock model. The recent understanding of how rapidly negative feedback decays in BRAFV600E-expressing systems, and thereby facilitates prosurvival signal transduction by growth factor receptors, has led to treatment approaches that combine vemurafenib with multikinase inhibitors. However, given the growing number of signaling molecules that have been found to become activated following inhibition of BRAFV600E, safely and effectively inhibiting all relevant GF-Rs may prove difficult. Our studies of BCR-ABL-mediated oncogene addiction suggest an alternative approach aimed at potentiating negative feedback in the setting of inhibition of pathologically-activated kinases, which is predicted to enhance oncogene addiction and increase sensitivity to targeted therapy. In addition to possibly facilitating deeper clinical responses, this strategy may be applicable to a broad range of malignancies associated with activating mutations in actionable signaling molecules. Efforts to further dissect and modulate molecular mechanisms of negative feedback in relevant tissue contexts are required to formally test this prediction.

Experimental Methods

Cell Line Propagation and Isogenic Cell Line Generation

All cell lines were propagated in RPMI 1640 medium supplemented with 10% fetal bovine serum (FBS; Omega Scientific), L-glutamine, and penicillin/streptomycin (Invitrogen). To generate isogenic TF1 cell lines, parental TF1 cells were engineered to express the ecotropic-receptor (Eco-R) through retroviral transduction (pMOWS-EcoR plasmid). Eco-R expressing TF1 cells underwent a second round of retroviral transduction with pMSCV-puro, pMSCV-BCR-ABL, and pools of each cell line were selected for as described previously (28). TF1-puro cells were supplemented with 2ng/mL hGM-CSF (Peprotech) under normal growth conditions.

Kinase Inhibitors and Drug Treatments

DMSO stock solutions of imatinib and dasatinib were generated at UCSF. The JAK2 inhibitor TG101348, the MEK inhibitor PD0325901, were purchased from Selleckchem. All drug exposures were performed at a cell density of 5×10^6 cells/mL. For cytokine stimulation experiments, cells were starved in reduced serum (0.1% FBS-RPMI) for the indicated amount of time and were subsequently stimulated with either 1U/mL human erythropoietin (hEPO) (R&D Systems) or 10ng/mL of hGM-CSF. Dasatinib HDP and LDC drug exposures were performed as described previously (11).

Quantitative Phosphoproteomics and DAVID Functional Analysis

K562 cells were grown for six days in customized RPMI 1640 medium (Invitrogen) supplemented with heavy (Cambridge Isotope Laboratories; CLM-2265 and CLM-2247) or light (Sigma-Aldrich) 30mg/L Arginine, 40mg/L Lysine, and 10% dialyzed FBS (Invitrogen) prior to drug treatment. The PY100 Phosphoscan Kit (Cell Signaling Technology) was used for the enrichment of phosphotyrosine containing tryptic peptides. To reduce sample complexity prior to MS/MS analysis, phosphotyrosine peptides were fractionated step-wise under alkaline conditions (20mM ammonium formiate, pH 10.3) with increasing amounts of acetonitrile (5% ACN, 10% ACN, 15% ACN, 20% ACN, 90% ACN). Peptides were separated and analyzed using a nano-LC column coupled to a LTQ OrbiTrap XL (Thermo Scientific) at the UCSF Mass Spectrometry Core Facility. An in house software analysis program was used to extract quantitative information for all identified peptides from each nano-LC analysis for all time points. Heat map representation of the phosphoproteomic data was generated using GENE-E (http://www.broadinstitute.org/cancer/software/GENE-E/). We functionally characterized phosphosites durably altered by high-dose pulse dasatinib treatment relative to all identified phosphoproteins (background) using the DAVID tool with default parameters (29, 30)

Cell Lysis and Protein Immunoprecipitation

Cells were lysed in JAK2 IP buffer (50mM Tris pH 7.6, 100mM NaCl, 1mM EDTA, 1mM EGTA, 0.5% NP40, 0.1% Triton) or RAS IP buffer (50mM Tris pH 7.5, 125mM NaCl, 6.5mM $MgCl_2$, 5% glycerol, 0.2% NP40) supplemented with 1% protease and 1% phosphatase

inhibitors (Calbiochem). For JAK2 immunoprecipitations, normalized cell lysates were tumbled overnight at 4°C with anti-total JAK2 antibody (1:100) (Cell Signaling Technology, cat. #3230). Immunoprecipitated JAK2 was collected the following day with protein A Dynabeads (Invitrogen). For RAS GTP-pulldown assays, normalized cell lysates were tumbled for 1hr at 4°C with 20μL of RAS Assay Reagent (Millipore; #14-278).

Antibodies, Western Immunoblot, and Phospho-Flow Cytometry

Cell lysates were resolved by SDS-PAGE and transferred to nitrocellulose as described previously (11). Phospho-specific and total antibodies for STAT5A/B (phospho-Y695/Y699) (cat. 9351 and 9363), ERK1/2(phospho-T202/Y204)(cat. 4370 and 9107), AKT (phospho-S473) (cat. 4060 and 9272), S6 (phospho-S235/S236) (cat. 2211 and 2317), CRKL (phospho-Y207) (cat. 3181), JAK2 (phospho-Y1007) (cat. 3776 and 3230), BCR (phospho-Y177) (cat. 3901), cABL (phospho-Y245 and phospho-Y204) (cat. 2861 and 3009), and cleaved CASP3 (cat. 9664) were purchased from Cell Signaling Technology. Antibodies against total cABL (cat. OP20) and total RAS (cat. 05-516) were purchased from Millipore. Antibodies for cABL (phospho-Y134) (cat. AP3011a) and cABL (phospho-Y251) (cat. AP3014a) were purchased from Abgent. Total GAPDH (cat. sc-25778) was purchased from Santa Cruz. Odyssey imaging technology and software was used for western immunoblot visualization and quantitation (Licor). Cleaved caspase-3 was measured by flow cytometry using FITC-conjugated anti-active caspase-3 antibody purchased from BD (cat. #550480). Analysis of CRKL phosphorylation by flow cytometry was performed as previously reported (11).

Gene Expression Analysis and Quantitative PCR

The Qiagen RNeasy kit was used to extract total cellular RNA for both the Illumina gene expression analysis and the corresponding confirmatory quantitative PCR (qPCR) experiments. For Illumina gene expression analysis, RNA integrity was assessed on a Bioanalyzer using the Agilent RNA 6000 Nano Kit (5067-1511), and cRNA was generated using the Ambion Illumina TotalPrep RNA Amplification kit (AMIL1791). SuperScriptII (Invitrogen) was used to generate cDNA from 2μg of extracted total cellular RNA. Samples were hybridized to the Illumina HT-12 platform by the UCSF Genomics Core and both raw control and sample probe intensities were converted to expression estimates after adjusting for array background, variance stabilization, and normalization, all with the lumi pipeline (PMID: 18467348) Differential gene expression was assessed as a time course with a two-step regression strategy (combining least-squares and stepwise regression) to identify genes with significant temporal expression changes between experimental groups (dasatinib treatment and control) (PMID: 16481333). Genes were considered significantly differentially expressed over the time course if they arose at a false discovery rate less than 1% (q-value < 0.01). Confirmatory qPCR analysis was performed for the following genes using TaqMan probes and TaqMan Universal Master Mix II (Invitrogen): GAPDH (Hs02758991_g1), SOCS1 (Hs00705164_s1), GRB10 (Hs01065498_m1), SPRY4 (Hs01935412_s1), EPOR (Hs00959427_m1).

Single Molecule Imaging of Caspase-3 Activation Using Dimeric Au Nanoshells

Techniques were adapted from (20) and modified in unpublished methods (C. Tajon, Y. Jun, and C. S. Craik). Briefly, a pair of magnetoplasmonic $Zn_{0.4}Fe_{2.6}O_4$@SiO_2@ gold (Au)

nanoshells (50 nm) linked by a pegylated-peptide bearing a selective caspase-3 cleavage site were synthesized. Lysates were prepared from K562 cells pretreated for eight hours with vehicle (DMSO) or dasatinib, and introduced to nanosensors immobilized on a glass flow chamber. As a control 100 uM zDEVD-cmk was added for three hours. Imaging was performed on an inverted microscope (Nikon Ti-E) outfitted with a darkfield dry condenser and recorded at a temporal resolution of 10 Hz using an EMCCD detector (Andor iXon; 512x512 pixel chip). Intensity trajectories of each nanoparticle pair (n= 75) were analyzed by ImageJ. Total cleavage events observed 90 minutes following lysate introduction were counted, normalized against control, and plotted.

References

1. Gorre ME, Mohammed M, Ellwood K, Hsu N, Paquette R, Rao PN*, et al.* Clinical resistance to STI-571 cancer therapy caused by BCR-ABL gene mutation or amplification. *Science* 2001 Aug 3; **293**(5531)**:** 876-880.

2. Druker BJ, Sawyers CL, Kantarjian H, Resta DJ, Reese SF, Ford JM*, et al.* Activity of a specific inhibitor of the BCR-ABL tyrosine kinase in the blast crisis of chronic myeloid leukemia and acute lymphoblastic leukemia with the Philadelphia chromosome. *N Engl J Med* 2001 Apr 5; **344**(14)**:** 1038-1042.

3. Sharma SV, Gajowniczek P, Way IP, Lee DY, Jiang J, Yuza Y*, et al.* A common signaling cascade may underlie "addiction" to the Src, BCR-ABL, and EGF receptor oncogenes. *Cancer Cell* 2006 Nov; **10**(5)**:** 425-435.

4. Flaherty KT, Puzanov I, Kim KB, Ribas A, McArthur GA, Sosman JA*, et al.* Inhibition of mutated, activated BRAF in metastatic melanoma. *N Engl J Med* Aug 26; **363**(9)**:** 809-819.

5. Solit DB, Garraway LA, Pratilas CA, Sawai A, Getz G, Basso A*, et al.* BRAF mutation predicts sensitivity to MEK inhibition. *Nature* 2006 Jan 19; **439**(7074)**:** 358-362.

6. Pratilas CA, Taylor BS, Ye Q, Viale A, Sander C, Solit DB*, et al.* (V600E)BRAF is associated with disabled feedback inhibition of RAF-MEK signaling and elevated transcriptional output of the pathway. *Proc Natl Acad Sci U S A* 2009 Mar 17; **106**(11)**:** 4519-4524.

7. Straussman R, Morikawa T, Shee K, Barzily-Rokni M, Qian ZR, Du J*, et al.* Tumour micro-environment elicits innate resistance to RAF inhibitors through HGF secretion. *Nature* Jul 26; **487**(7408)**:** 500-504.

8. Prahallad A, Sun C, Huang S, Di Nicolantonio F, Salazar R, Zecchin D*, et al.* Unresponsiveness of colon cancer to BRAF(V600E) inhibition through feedback activation of EGFR. *Nature* Mar 1; **483**(7387)**:** 100-103.

9. Wilson TR, Fridlyand J, Yan Y, Penuel E, Burton L, Chan E*, et al.* Widespread potential for growth-factor-driven resistance to anticancer kinase inhibitors. *Nature* Jul 26; **487**(7408)**:** 505-509.

10. Lito P, Pratilas CA, Joseph EW, Tadi M, Halilovic E, Zubrowski M*, et al.* Relief of profound feedback inhibition of mitogenic signaling by RAF inhibitors attenuates their activity in BRAFV600E melanomas. *Cancer Cell* Nov 13; **22**(5)**:** 668-682.

11. Shah NP, Kasap C, Weier C, Balbas M, Nicoll JM, Bleickardt E*, et al.* Transient potent BCR-ABL inhibition is sufficient to commit chronic myeloid leukemia cells irreversibly to apoptosis. *Cancer Cell* 2008 Dec 9; **14**(6)**:** 485-493.

12. Hiwase DK, White DL, Powell JA, Saunders VA, Zrim SA, Frede AK*, et al.* Blocking cytokine signaling along with intense Bcr-Abl kinase inhibition induces apoptosis in primary CML progenitors. *Leukemia* Apr; **24**(4)**:** 771-778.

13. Snead JL, O'Hare T, Adrian LT, Eide CA, Lange T, Druker BJ*, et al.* Acute dasatinib exposure commits Bcr-Abl-dependent cells to apoptosis. *Blood* 2009 Oct 15; **114**(16)**:** 3459-3463.

14. Sonoyama J, Matsumura I, Ezoe S, Satoh Y, Zhang X, Kataoka Y*, et al.* Functional cooperation among Ras, STAT5, and phosphatidylinositol 3-kinase is required for full oncogenic activities of BCR/ABL in K562 cells. *J Biol Chem* 2002 Mar 8; **277**(10)**:** 8076-8082.

15. Kitamura T, Tange T, Terasawa T, Chiba S, Kuwaki T, Miyagawa K*, et al.* Establishment and characterization of a unique human cell line that proliferates dependently on GM-CSF, IL-3, or erythropoietin. *J Cell Physiol* 1989 Aug; **140**(2)**:** 323-334.

16. Guthridge MA, Stomski FC, Thomas D, Woodcock JM, Bagley CJ, Berndt MC*, et al.* Mechanism of activation of the GM-CSF, IL-3, and IL-5 family of receptors. *Stem Cells* 1998; **16**(5)**:** 301-313.

17. Fraser JK, Lin FK, Berridge MV. Expression and modulation of specific, high affinity binding sites for erythropoietin on the human erythroleukemic cell line K562. *Blood* 1988 Jan; **71**(1)**:** 104-109.

18. Kirschner KM, Baltensperger K. Erythropoietin promotes resistance against the Abl tyrosine kinase inhibitor imatinib (STI571) in K562 human leukemia cells. *Mol Cancer Res* 2003 Nov; **1**(13)**:** 970-980.

19. Kentsis A, Reed C, Rice KL, Sanda T, Rodig SJ, Tholouli E*, et al.* Autocrine activation of the MET receptor tyrosine kinase in acute myeloid leukemia. *Nat Med* Jul; **18**(7)**:** 1118-1122.

20. Jun YW, Sheikholeslami S, Hostetter DR, Tajon C, Craik CS, Alivisatos AP. Continuous imaging of plasmon rulers in live cells reveals early-stage caspase-3 activation at the single-molecule level. *Proc Natl Acad Sci U S A* 2009 Oct 20; **106**(42)**:** 17735-17740.

21. Tsai J, Lee JT, Wang W, Zhang J, Cho H, Mamo S*, et al.* Discovery of a selective inhibitor of oncogenic B-Raf kinase with potent antimelanoma activity. *Proc Natl Acad Sci U S A* 2008 Feb 26; **105**(8)**:** 3041-3046.

22. Sondergaard JN, Nazarian R, Wang Q, Guo D, Hsueh T, Mok S*, et al.* Differential sensitivity of melanoma cell lines with BRAFV600E mutation to the specific Raf inhibitor PLX4032. *J Transl Med*; **8:** 39.

23. Sala E, Mologni L, Truffa S, Gaetano C, Bollag GE, Gambacorti-Passerini C. BRAF silencing by short hairpin RNA or chemical blockade by PLX4032 leads to different responses in melanoma and thyroid carcinoma cells. *Mol Cancer Res* 2008 May; **6**(5)**:** 751-759.

24. Joseph EW, Pratilas CA, Poulikakos PI, Tadi M, Wang W, Taylor BS*, et al.* The RAF inhibitor PLX4032 inhibits ERK signaling and tumor cell proliferation in a V600E BRAF-selective manner. *Proc Natl Acad Sci U S A* 2010 Aug 17; **107**(33)**:** 14903-14908.

25. Corbin AS, Agarwal A, Loriaux M, Cortes J, Deininger MW, Druker BJ. Human chronic myeloid leukemia stem cells are insensitive to imatinib despite inhibition of BCR-ABL activity. *J Clin Invest* Jan; **121**(1)**:** 396-409.

26. Traer E, MacKenzie R, Snead J, Agarwal A, Eiring AM, O'Hare T*, et al.* Blockade of JAK2-mediated extrinsic survival signals restores sensitivity of CML cells to ABL inhibitors. *Leukemia* May; **26**(5)**:** 1140-1143.

27. Hantschel O, Warsch W, Eckelhart E, Kaupe I, Grebien F, Wagner KU*, et al.* BCR-ABL uncouples canonical JAK2-STAT5 signaling in chronic myeloid leukemia. *Nat Chem Biol* Mar; **8**(3)**:** 285-293.

28. Smith CC, Wang Q, Chin CS, Salerno S, Damon LE, Levis MJ*, et al.* Validation of ITD mutations in FLT3 as a therapeutic target in human acute myeloid leukaemia. *Nature* May 10; **485**(7397)**:** 260-263.

29. Huang da W, Sherman BT, Lempicki RA. Systematic and integrative analysis of large gene lists using DAVID bioinformatics resources. *Nat Protoc* 2009; **4**(1)**:** 44-57.

30. Huang da W, Sherman BT, Lempicki RA. Bioinformatics enrichment tools: paths toward the comprehensive functional analysis of large gene lists. *Nucleic Acids Res* 2009 Jan; **37**(1)**:** 1-13.

31. Sonnichsen C, Reinhard BM, Liphardt J, Alivisatos AP. A molecular ruler based on plasmon coupling of single gold and silver nanoparticles. *Nat Biotechnol* 2005 Jun; **23**(6)**:** 741-745.

32. Reinhard BM, Siu M, Agarwal H, Alivisatos AP, Liphardt J. Calibration of dynamic molecular rulers based on plasmon coupling between gold nanoparticles. *Nano Lett* 2005 Nov; **5**(11)**:** 2246-2252.

Figure 1. Transient Exposure of CML Cell Lines to Dasatinib Results in Durable Dephosphorylation of Select Tyrosines in Myeloid Growth-Factor Receptor Signaling Pathways.

A. Schematic of SILAC-based quantitative phosphoproteomic analysis of global phosphotyrosine signaling in K562 cells before and after a high-dose pulse (HDP) of dasatinib. K562 cells grown in "light" (non-isotope-containing) RPMI were treated with a 100nM dasatinib for 20 minutes, and cell lysates were generated before HDP (PRE), at the time of drug washout (EOE), and 3hr and 6hrs post-HDP (HDP3, HDP6). Equivalent lysates were generated from K562 cells grown in "heavy" (isotope-containing) RPMI. Light and heavy K562 cell lysates were mixed at a 1:1 ratio prior to phosphotyrosine peptide (PY100) enrichment, peptide fractionation, and MS/MS analysis.

B. Heat map representation of persistent phosphorylation changes in myeloid growth factor receptor signaling pathways identified by bioinformatic functional analysis. Change in phosphorylation at each HDP time point was normalized to the "PRE" condition and are represented on a $\log_2$ - transformed scale. Gray areas designate "no data".

C. Western immunoblot analysis of select myeloid growth factor receptor signaling pathways in K562 and KU812 cells before and after a 100nM HDP of dasatinib.

D. Heat map representation of BCR-ABL phosphorylation identified by phosphoproteomic analysis and western immunoblot analysis in K562 cells before and after a 100nM HDP of dasatinib. (ABL1a numbering).

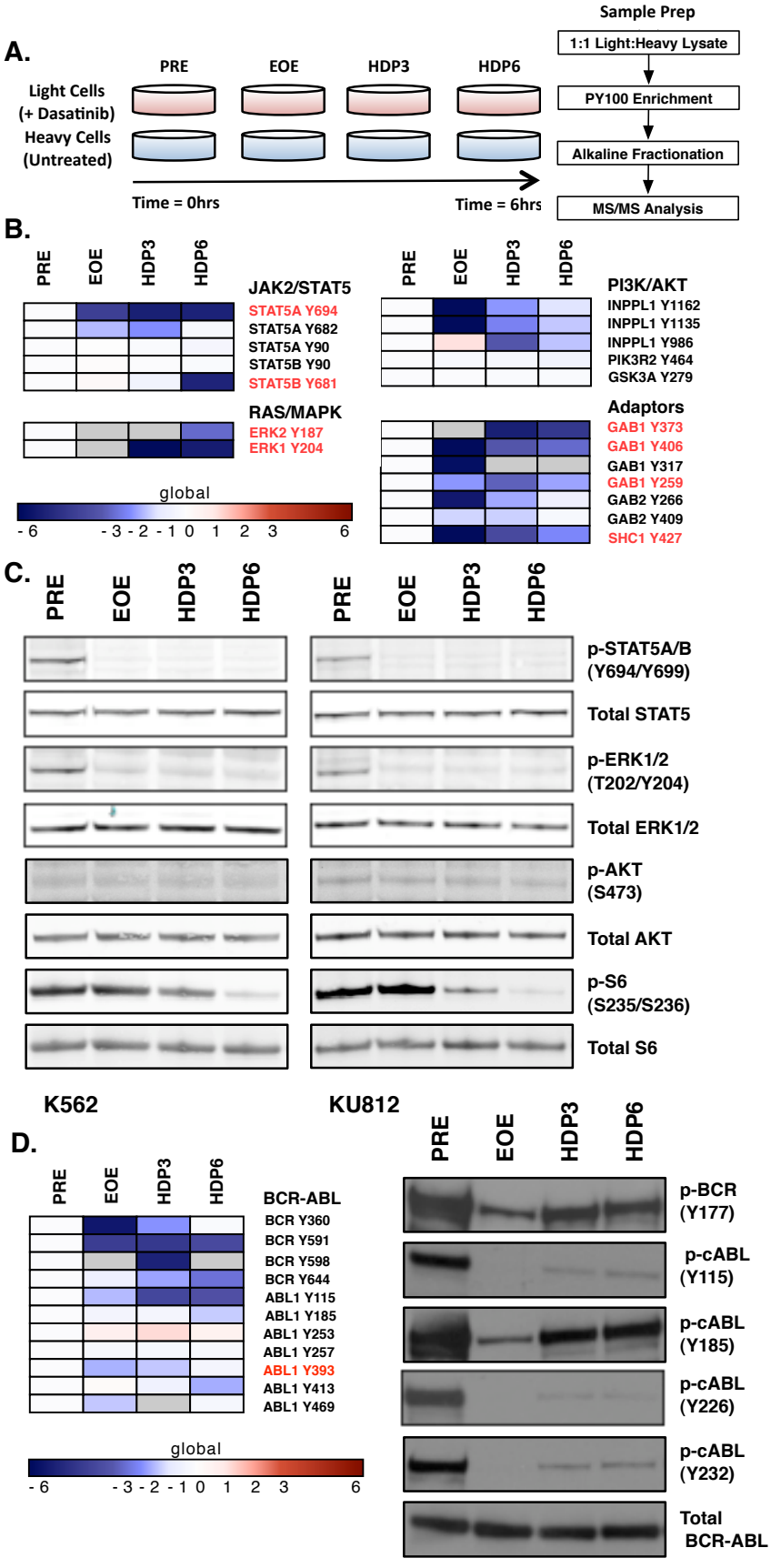
A.
PRE
EOE
HDP3
HDP6
Light Cells
(+ Dasatinib)
Heavy Cells
(Untreated)
Time = 0hrs
Time = 6hrs
Sample Prep
1:1 Light:Heavy Lysate
PY100 Enrichment
Alkaline Fractionation
MS/MS Analysis
B.
JAK2/STAT5
STAT5A Y694
STAT5A Y682
STAT5A Y90
STAT5B Y90
STAT5B Y681
RAS/MAPK
ERK2 Y187
ERK1 Y204
global
- 6 - 3 - 2 - 1 0 1 2 3 6
PI3K/AKT
INPPL1 Y1162
INPPL1 Y1135
INPPL1 Y986
PIK3R2 Y464
GSK3A Y279
Adaptors
GAB1 Y373
GAB1 Y406
GAB1 Y317
GAB1 Y259
GAB2 Y266
GAB2 Y409
SHC1 Y427
C.
p-STAT5A/B
(Y694/Y699)
Total STAT5
p-ERK1/2
(T202/Y204)
Total ERK1/2
p-AKT
(S473)
Total AKT
p-S6
(S235/S236)
Total S6
K562
KU812
D.
BCR-ABL
BCR Y360
BCR Y591
BCR Y598
BCR Y644
ABL1 Y115
ABL1 Y185
ABL1 Y253
ABL1 Y257
ABL1 Y393
ABL1 Y413
ABL1 Y469
p-BCR
(Y177)
p-cABL
(Y115)
p-cABL
(Y185)
p-cABL
(Y226)
p-cABL
(Y232)
Total
BCR-ABL

Figure 2. BCR-ABL Kinase Activity Rewires GM-CSF Receptor Signaling and Confers Oncogene Addiction in TF1 Cells.

A. Fraction cleaved caspase-3 negative population (live cells) of TF1/puro and TF1/BCR-ABL cells following 48 hours of treatment with 100nM dasatinib, 0.2% DMSO, or 100nM dasatinib supplemented with 2ng/mL of hGM-CSF. Active caspase-3 was measured by flow cytometry. Data represent average ± SD (n=3; ***p ≤ 0.001, Two-way ANOVA with Bonferroni post-tests).

B. Upper: Line diagram representation of duration of serum starve, kinase inhibitor treatment, and growth-factor stimulation. Lower: Western immunoblot analysis of hGM-CSF-mediated (10' stimulation) JAK2 activation, RAS-GTP loading, and activation of downstream effectors from whole cell lysates in TF1/puro and TF1/BCR-ABL cells treated for 1 hour with 100nM dasatinib. The activation status of JAK2 was determined by immunoprecipitation and activation loop phosphorylation (Y1007). RAS activation was monitored using a RAS-GTP pull-down assay.

C. Upper: Line diagram representation of duration of serum starve, kinase inhibitor treatment, and growth-factor stimulation. Lower: Western immunoblot analysis of hGM-CSF-mediated (10' stimulation) RAS-GTP loading and activation of downstream effectors in TF1/puro and TF1/BCR-ABL cells after short-term and extended dasatinib treatment (100nM: 1hr, 2hrs, 4hrs, 8hrs). RAS activity was monitored as in (B).

D. Normalized RAS-GTP loading ± SD (n=3; **p ≤ 0.01, Two-way ANOVA with Bonferroni post-tests) in hGM-CSF-stimulated (10') TF1/puro and TF1/BCR-ABL cells after prolonged dasatinib treatment (100nM, 24hrs). RAS activity was monitored as in (B). RAS-GTP

loading was normalized to the level observed in the "TF1/puro - DMSO+hGM-CSF" condition for each experimental replicate.

E. Upper: Line diagram representation of duration of serum starve, kinase inhibitor treatment, and growth-factor stimulation. Lower: Western immunoblot analysis of whole cell lysates from TF1/puro and TF1/BCR-ABL cells after prolonged dasatinib treatment (100nM, 24hrs) and hGM-CSF stimulation (10').

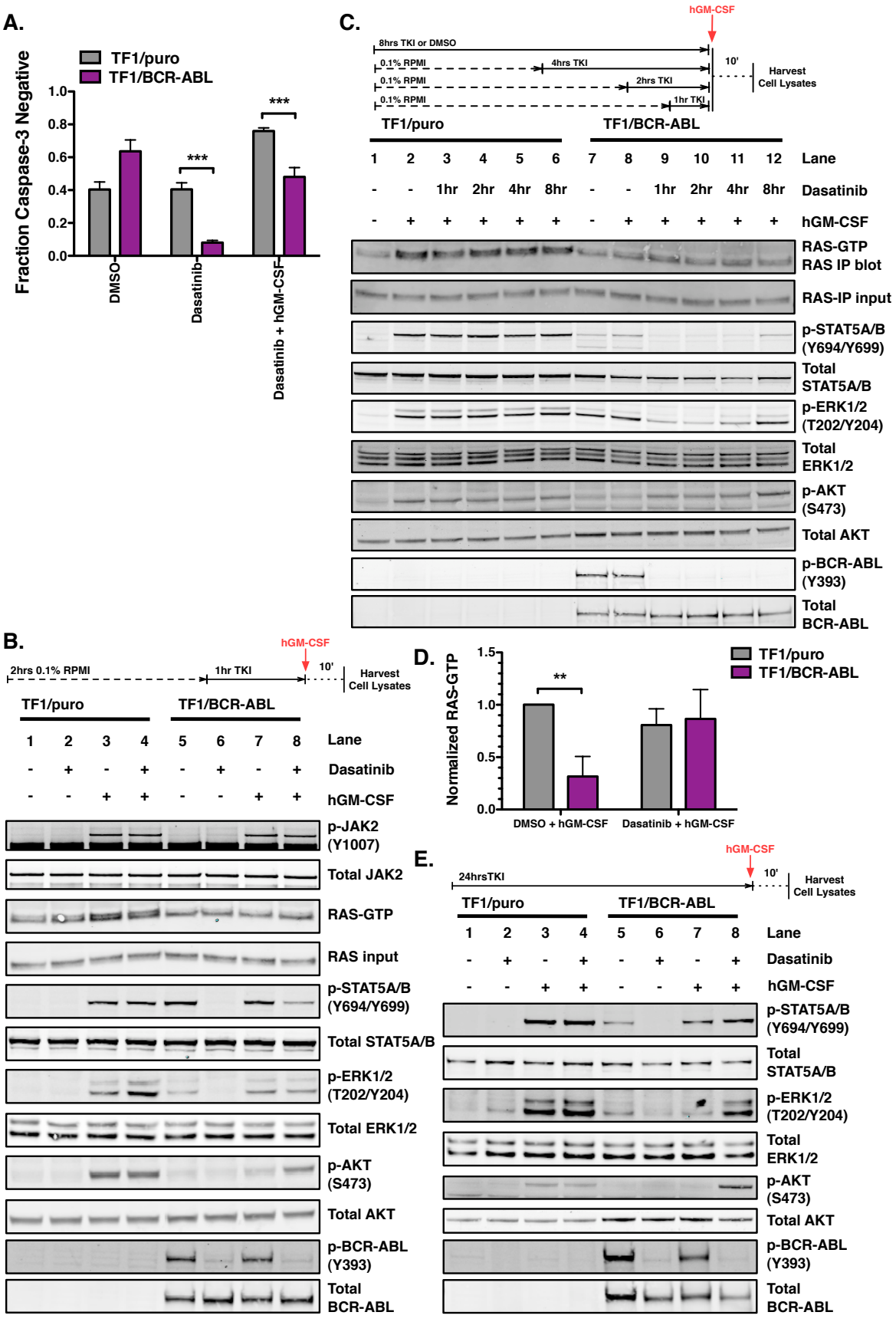
A.
TF1/puro
TF1/BCR-ABL
Fraction Caspase-3 Negative
1.0
0.8
0.6
0.4
0.2
0.0
***
***
DMSO
Dasatinib
Dasatinib + hGM-CSF
C.
hGM-CSF
8hrs TKI or DMSO
0.1% RPMI
4hrs TKI
2hrs TKI
1hr TKI
10'
Harvest Cell Lysates
TF1/puro
TF1/BCR-ABL
1 2 3 4 5 6 7 8 9 10 11 12 Lane
- - 1hr 2hr 4hr 8hr - - 1hr 2hr 4hr 8hr Dasatinib
- + + + + + - + + + + + hGM-CSF
RAS-GTP
RAS IP blot
RAS-IP input
p-STAT5A/B (Y694/Y699)
Total STAT5A/B
p-ERK1/2 (T202/Y204)
Total ERK1/2
p-AKT (S473)
Total AKT
p-BCR-ABL (Y393)
Total BCR-ABL
B.
hGM-CSF
2hrs 0.1% RPMI
1hr TKI
10'
Harvest Cell Lysates
TF1/puro
TF1/BCR-ABL
1 2 3 4 5 6 7 8 Lane
- + - + - + - + Dasatinib
- - + + - - + + hGM-CSF
p-JAK2 (Y1007)
Total JAK2
RAS-GTP
RAS input
p-STAT5A/B (Y694/Y699)
Total STAT5A/B
p-ERK1/2 (T202/Y204)
Total ERK1/2
p-AKT (S473)
Total AKT
p-BCR-ABL (Y393)
Total BCR-ABL
D.
TF1/puro
TF1/BCR-ABL
Normalized RAS-GTP
1.5
1.0
0.5
0.0
**
DMSO + hGM-CSF
Dasatinib + hGM-CSF
E.
hGM-CSF
24hrsTKI
10'
Harvest Cell Lysates
TF1/puro
TF1/BCR-ABL
1 2 3 4 5 6 7 8 Lane
- + - + - + - + Dasatinib
- - + + - - + + hGM-CSF
p-STAT5A/B (Y694/Y699)
Total STAT5A/B
p-ERK1/2 (T202/Y204)
Total ERK1/2
p-AKT (S473)
Total AKT
p-BCR-ABL (Y393)
Total BCR-ABL

Figure 3. Erythropoietin Receptor-Mediated Activation of the JAK2/STAT5, RAS/MAPK, and PI3K/AKT Signaling Pathways is Attenuated by BCR-ABL Kinase Activity in K562 Cells.

A. Normalized hEPO-mediated (10' stimulation) JAK2 activation in K562 cells treated for 1hr with either 100nM dasatinib or 1μM imatinib. Data represents the average ± SD (n=3). JAK2 activation was monitored by immunoprecipitation and activation loop (Y1007) phosphorylation. JAK2 activation was normalized to the level of phospho-Y1007 observed in the "DMSO" condition for each experimental replicate.

B. Upper: Line diagram representation of duration of serum starve, kinase inhibitor treatment, and growth-factor stimulation. Lower: Western immunoblot analysis of whole cell lysates from K562 cells after short-term and prolonged BCR-ABL inhibition (100nM dasatinib: 2hrs, 4hrs, 8hrs, 24hrs; 0.2% DMSO, 24hrs) followed by hEPO stimulation (10').

C. Normalized hEPO-mediated JAK2 activation in K562 cells after short-term (1hr) and prolonged (24hrs) 100nM dasatinib treatment followed hEPO stimulation (10'). Data is representative of triplicate experimental analysis. JAK2 activation and normalization was performed as in (A).

D. Normalized RAS-GTP loading in K562 cells after short-term (1hr) and prolonged (24hrs) 100nM dasatinib treatment followed by hEPO stimulation (10'). Data is representative of triplicate experimental analysis. RAS activation was monitored using a RAS-GTP pulldown assay and RAS-GTP levels were normalized to the "DMSO" condition.

E. Normalized hEPO-mediated (10' stimulation) JAK2 activation in K562 cells pretreated for 24hrs with 0.2% DMSO, 100nM dasatinib, 1μM imatinib, 500nM TG101348,

dasatinib/TG101348, or imatinib/TG101348. JAK2 activation was monitored and normalized as in (A).

F. Upper: Line diagram representation of duration of serum starve, kinase inhibitor treatment, and growth-factor stimulation. Lower: Western immunoblot analysis of whole cell lysates in K562 cells pretreated for 24hrs with 0.2% DMSO, 100nM dasatinib, 1μM imatinib, 500nM TG101348, dasatinib/TG101348, or imatinib/TG101348 followed by hEPO stimulation (10').

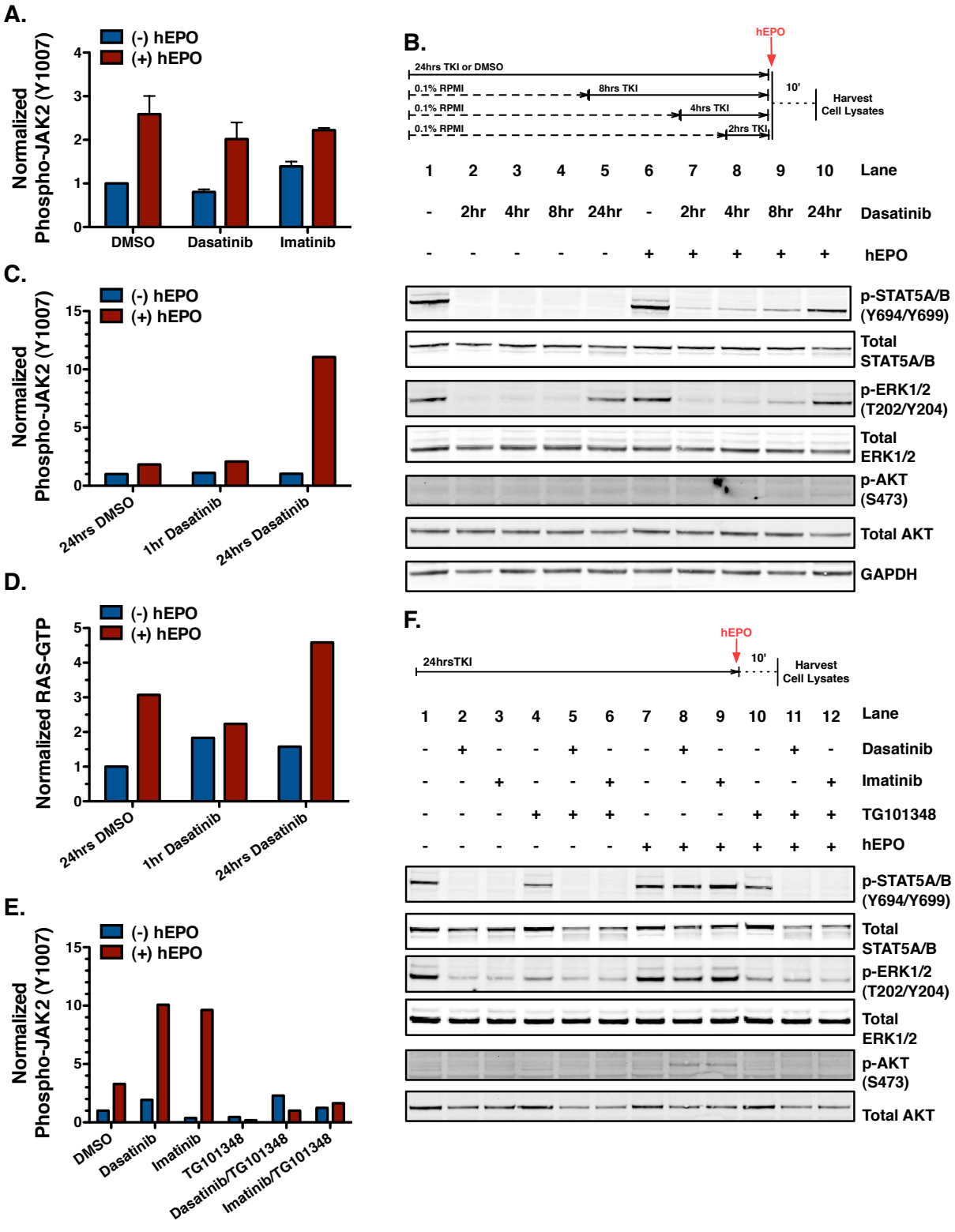
A.
(-) hEPO
(+) hEPO
Normalized Phospho-JAK2 (Y1007)
DMSO
Dasatinib
Imatinib
B.
hEPO
24hrs TKI or DMSO
0.1% RPMI
8hrs TKI
4hrs TKI
2hrs TKI
10'
Harvest Cell Lysates
Lane
Dasatinib
hEPO
p-STAT5A/B (Y694/Y699)
Total STAT5A/B
p-ERK1/2 (T202/Y204)
Total ERK1/2
p-AKT (S473)
Total AKT
GAPDH
C.
24hrs DMSO
1hr Dasatinib
24hrs Dasatinib
D.
Normalized RAS-GTP
E.
DMSO
Dasatinib
Imatinib
TG101348
Dasatinib/TG101348
Imatinib/TG101348
F.
24hrsTKI

Figure 4. Global Gene Expression Analysis of Dasatinib Treated K562 Cells Identifies Candidate Mediators Responsible for the Attenuation of Myeloid GF-R Signaling in CML Cells.

A. Heat map representation of the 162 genes significantly down-regulated after 4, 8, and 24 hours of dasatinib treatment in K562 cells. Heat map inset to the right highlights genes within this group that are associated with negative feedback of the RAS/MAPK and JAK/STAT signaling pathways, as well as the transcriptional output of ERK. The column to the left denotes genes previously reported to be involved in the negative feedback network of BRAFV600E expressing cells (6, 24). The heat map at the bottom highlights a few of the genes with increased expression following dasatinib treatment in K562 cells.

B. Quantitative PCR (qPCR) analysis of potential negative feedback genes in K562 cells treated with dasatinib (100nM), imatinib (1μM), or PD0325901 (500nM). The average fold expression change ($2^{(-\Delta\Delta Ct)}$) and standard deviation ($SD_{fold\text{-}change}$) for each gene is represented (n=3).

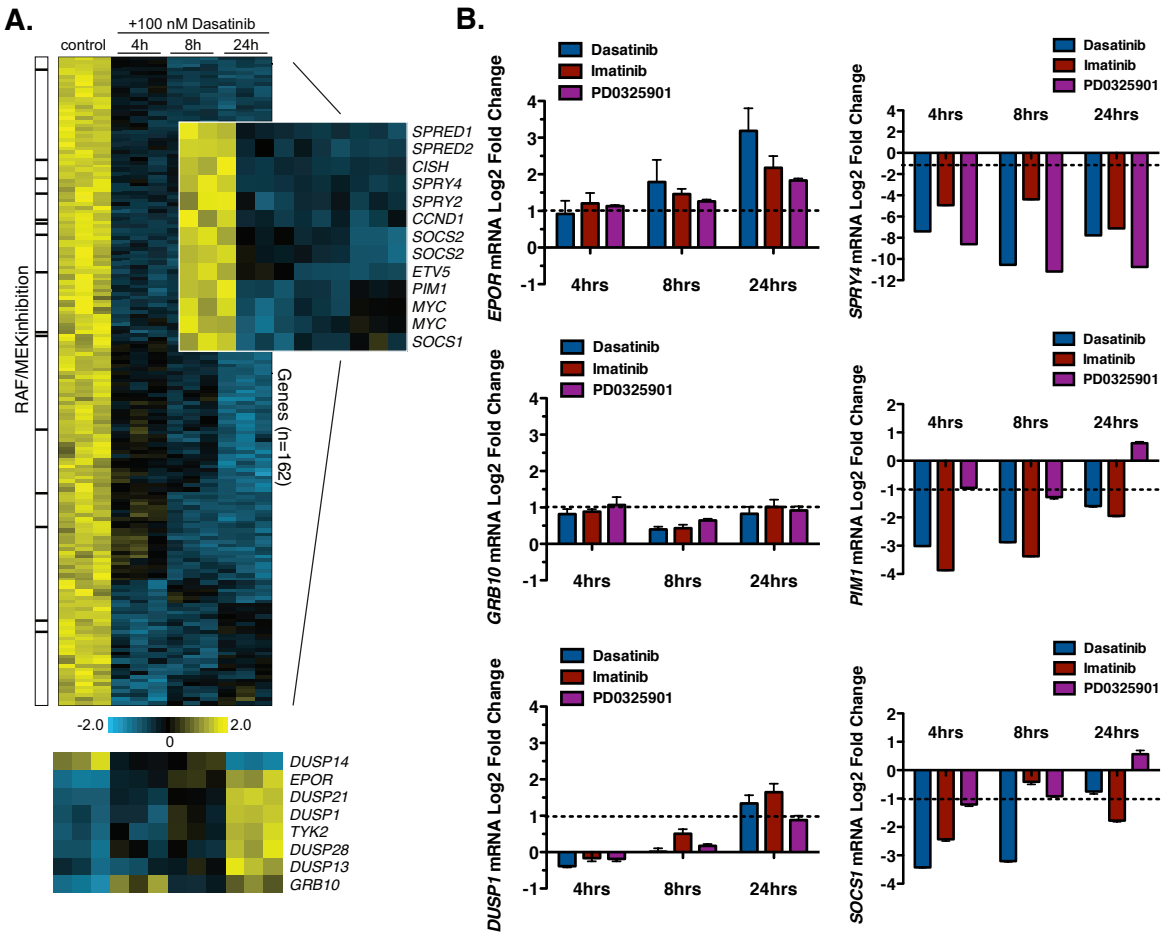
A.
+100 nM Dasatinib
control
4h
8h
24h
RAF/MEKinhibition
Genes (n=162)
SPRED1
SPRED2
CISH
SPRY4
SPRY2
CCND1
SOCS2
SOCS2
ETV5
PIM1
MYC
MYC
SOCS1
-2.0
0
2.0
DUSP14
EPOR
DUSP21
DUSP1
TYK2
DUSP28
DUSP13
GRB10
B.
Dasatinib
Imatinib
PD0325901
EPOR mRNA Log2 Fold Change
SPRY4 mRNA Log2 Fold Change
GRB10 mRNA Log2 Fold Change
PIM1 mRNA Log2 Fold Change
DUSP1 mRNA Log2 Fold Change
SOCS1 mRNA Log2 Fold Change
4hrs
8hrs
24hrs

Figure 5. MEK-Dependent Negative Feedback Attenuates hEPO-Mediated Activation of RAS and JAK2 in K562 Cells But Does Not Directly Impact BCR-ABL Tyrosine Phosphorylation.

A. Upper: Line diagram representation of duration of serum starve, kinase inhibitor treatment, and growth-factor stimulation. Lower: Western immunoblot analysis of RAS and ERK activity before and after hEPO-stimulation (10') in K562 cells pretreated for 24hrs with 0.2% DMSO, 100nM dasatinib, 500nM PD0325901, or dasatinib/PD0325901. RAS activity was monitored using a RAS-GTP pulldown assay.

B. Upper: Line diagram representation of duration of serum starve, kinase inhibitor treatment, and growth-factor stimulation. Lower: Western immunoblot analysis of JAK2 and STAT5 activity before and after hEPO-stimulation in K562 cells treated under the same experimental conditions as (A). JAK2 activation was determined by immunoprecipitation and activation loop (Y1007) phosphorylation.

C. Western immunoblot analysis of the phosphorylation status of tyrosine residues across BCR-ABL following 24 hours of treatment with 100nM dasatinib or 500nM PD0325901.

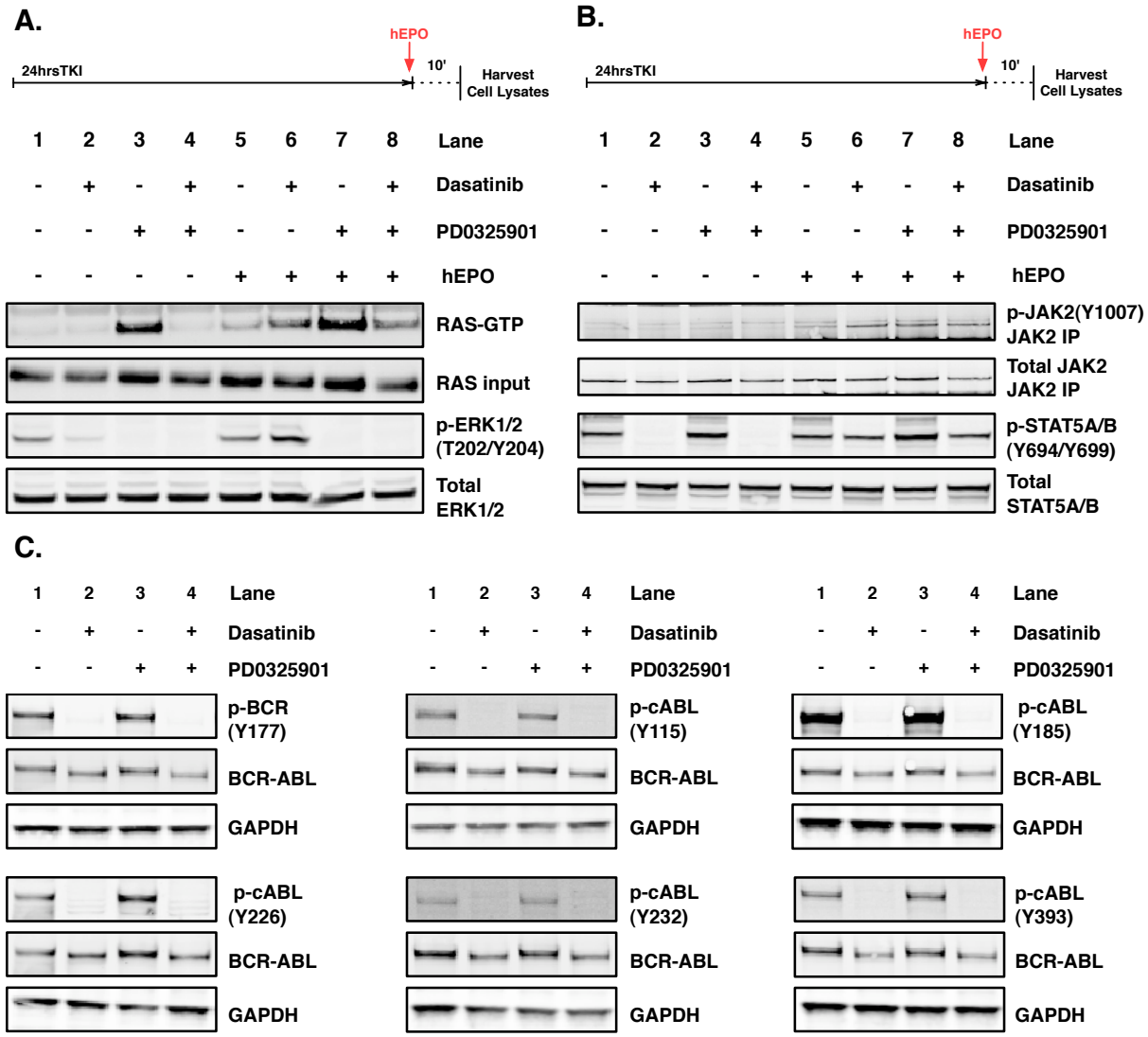
A.
hEPO
24hrsTKI
10'
Harvest Cell Lysates
1 2 3 4 5 6 7 8 Lane
- + - + - + - + Dasatinib
- - + + - - + + PD0325901
- - - - + + + + hEPO
RAS-GTP
RAS input
p-ERK1/2 (T202/Y204)
Total ERK1/2
B.
hEPO
24hrsTKI
10'
Harvest Cell Lysates
1 2 3 4 5 6 7 8 Lane
- + - + - + - + Dasatinib
- - + + - - + + PD0325901
- - - - + + + + hEPO
p-JAK2(Y1007) JAK2 IP
Total JAK2 JAK2 IP
p-STAT5A/B (Y694/Y699)
Total STAT5A/B
C.
1 2 3 4 Lane
- + - + Dasatinib
- - + + PD0325901
p-BCR (Y177)
BCR-ABL
GAPDH
p-cABL (Y226)
BCR-ABL
GAPDH
1 2 3 4 Lane
- + - + Dasatinib
- - + + PD0325901
p-cABL (Y115)
BCR-ABL
GAPDH
p-cABL (Y232)
BCR-ABL
GAPDH
1 2 3 4 Lane
- + - + Dasatinib
- - + + PD0325901
p-cABL (Y185)
BCR-ABL
GAPDH
p-cABL (Y393)
BCR-ABL
GAPDH

Figure 6. Caspase-3 Activity is Detected in Dasatinib Treated K562 Cells Prior to Complete Relief of Negative Feedback.

A. Western immunoblot assessment of cleaved caspase-3 in whole cell lysates from K562 cells treated with 100nM dasatinib for 4hrs, 8hrs, 12hrs, and 24hrs.

B. Representation of a single gold nanosensor intensity trace as a function of time. Intact nanosensor yields a high scattering intensity, while cutting event mediated by caspase-3 is observed as an intensity drop due to loss in plasmon coupling (20, 31, 32).

C. Representative darkfield images of nanosensors before and after exposure to cell lystates from K562 cells treated with vehicle (DMSO) or 100nM dasatinib.

D. Total normalized nanosensor cutting events observed in K562 cell lysates treated with vehicle (DMSO) and 100 nM dasatinib. Treatment of lysates with the caspase-3 inhibitor z-DEVD-cmk is shown as a control.

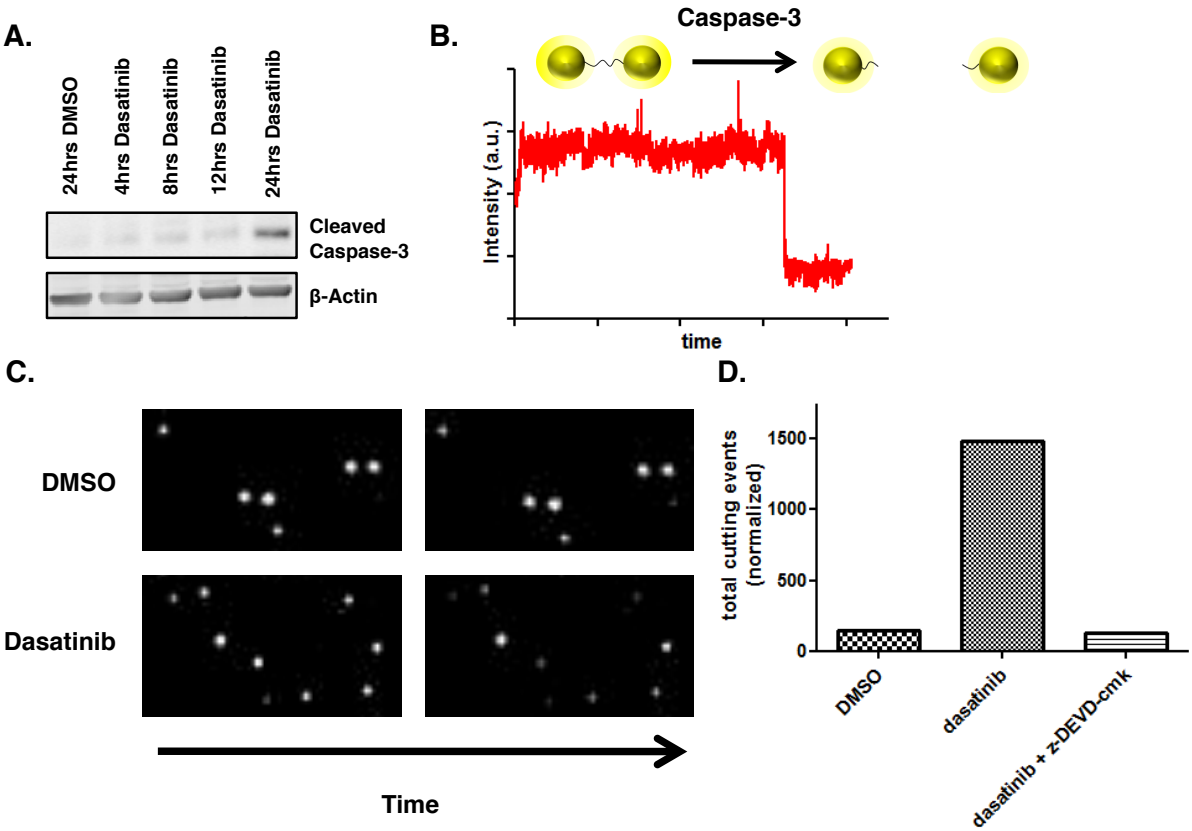
A.
24hrs DMSO
4hrs Dasatinib
8hrs Dasatinib
12hrs Dasatinib
24hrs Dasatinib
Cleaved Caspase-3
β-Actin
B.
Caspase-3
Intensity (a.u.)
time
C.
DMSO
Dasatinib
Time
D.
total cutting events (normalized)
1500
1000
500
0
DMSO
dasatinib
dasatinib + z-DEVD-cmk

Figure 7. Model of BCR-ABL-Mediated Oncogene Addiction.

A. Schematic representation of BCR-ABL-mediated oncogene addiction. BCR-ABL expressing cells initiate and commit to apoptosis prior to the complete relief of MEK-dependent negative feedback at the level of GF-R signaling.

B. Schematic comparison of the kinetics of apoptosis induction (red dashed line) and loss of negative feedback in BRAF-V600E-expressing melanoma cells (cyan solid line) and BCR-ABL-expressing CML cells (blue solid line).

A.

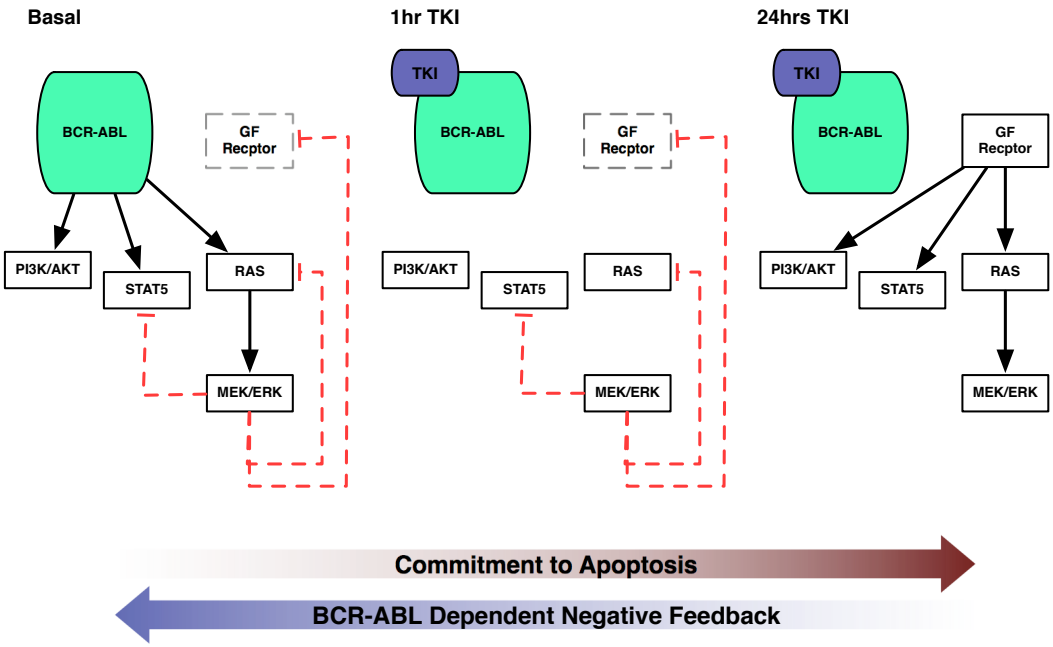
Basal
1hr TKI
24hrs TKI
TKI
BCR-ABL
GF Recptor
PI3K/AKT
STAT5
RAS
MEK/ERK
Commitment to Apoptosis
BCR-ABL Dependent Negative Feedback

B.

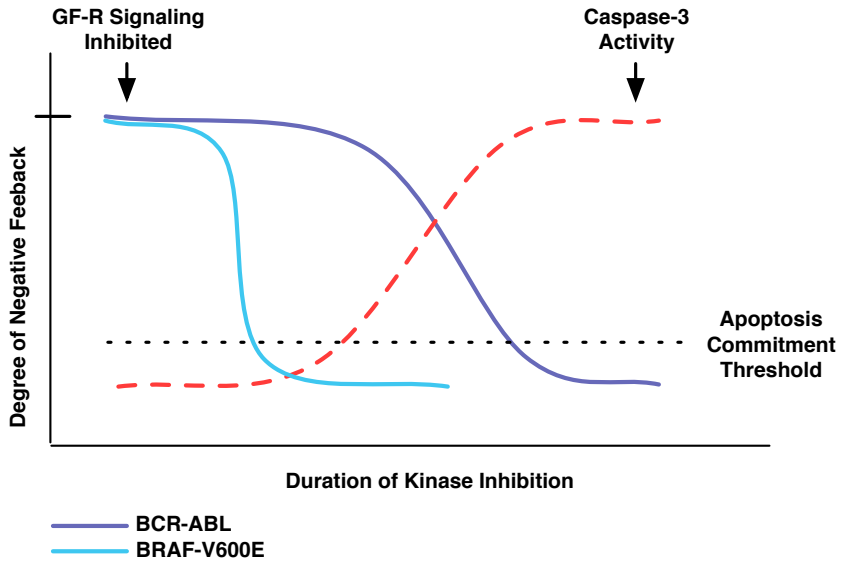
GF-R Signaling Inhibited
Caspase-3 Activity
Degree of Negative Feeback
Apoptosis Commitment Threshold
Duration of Kinase Inhibition
BCR-ABL
BRAF-V600E

Figure S1. Myeloid GF-R Signaling Pathways are Durably Altered Following Transient Imatinib Treatment.

A**.** Western immunoblot analysis of K562 and KU812 whole cell lysates following a HDP of imatinib (32.5μM).

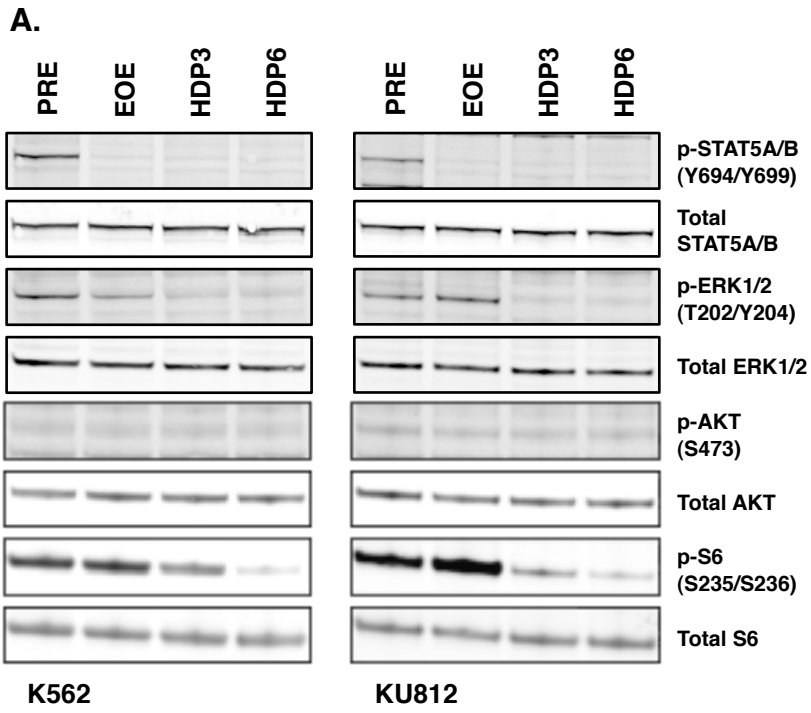
A.
PRE
EOE
HDP3
HDP6
PRE
EOE
HDP3
HDP6
p-STAT5A/B (Y694/Y699)
Total STAT5A/B
p-ERK1/2 (T202/Y204)
Total ERK1/2
p-AKT (S473)
Total AKT
p-S6 (S235/S236)
Total S6
K562
KU812

Figure S2. TF1/BCR-ABL Cells Exhibit Persistent Activation of GM-CSFR Pathway Effectors and Elevated Levels of Phospho-CRKL (Y207).

A. Western immunoblot analysis of TF1/puro and TF1/BCR-ABL whole cell lysates from two independently derived isogenic cell lines. Cells were serum and cytokine starved for 6 hours prior to lysate generation.

B. Flow cytometry assessment of phospho-CRKL (Y207) in TF1/puro and TF1/BCR-ABL cell lines.

C. Normalized phospho-JAK2 mediated by hGM-CSF stimulation (10') in TF1/puro and TF1/BCR-ABL cells following a one-hour treatment with 0.2% DMSO or 100nM dasatinib. Data represents the average ± standard deviation (SD) (n=3; ns – not significant, Two-way ANOVA). Phospho-JAK2 was monitored by immunoprecipitation and activation loop (Y1007) phosphorylation.

D. Normalized RAS-GTP loading mediated by hGM-CSF stimulation (10') in TF1/puro and TF1/BCR-ABL cells following a one-hour treatment with 0.2% DMSO or 100nM dasatinib. Data represents the average ± SD (n=3; **p ≤ 0.01, Two-way ANOVA with Bonferroni post-tests). RAS activity was monitored using a RAS-GTP pulldown assay.

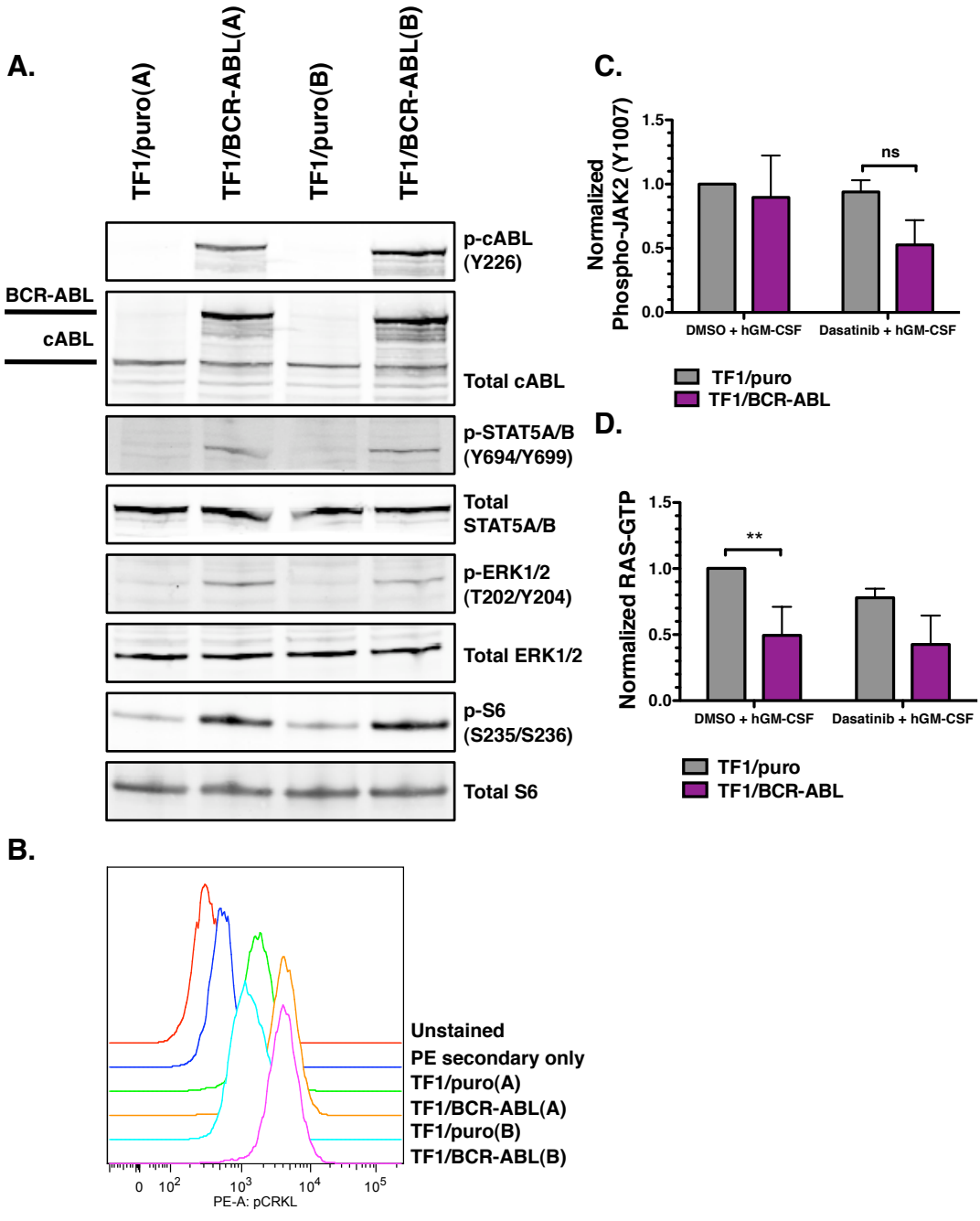
A.
TF1/puro(A)
TF1/BCR-ABL(A)
TF1/puro(B)
TF1/BCR-ABL(B)
BCR-ABL
cABL
p-cABL (Y226)
Total cABL
p-STAT5A/B (Y694/Y699)
Total STAT5A/B
p-ERK1/2 (T202/Y204)
Total ERK1/2
p-S6 (S235/S236)
Total S6
B.
Unstained
PE secondary only
TF1/puro(A)
TF1/BCR-ABL(A)
TF1/puro(B)
TF1/BCR-ABL(B)
0
10^2
10^3
10^4
10^5
PE-A: pCRKL
C.
Normalized Phospho-JAK2 (Y1007)
1.5
1.0
0.5
0.0
ns
DMSO + hGM-CSF
Dasatinib + hGM-CSF
TF1/puro
TF1/BCR-ABL
D.
Normalized RAS-GTP
1.5
1.0
0.5
0.0
**
DMSO + hGM-CSF
Dasatinib + hGM-CSF
TF1/puro
TF1/BCR-ABL

Figure S3. Prolonged BCR-ABL Inhibition is Necessary to Restore EPO-R Signaling in K562 Cells.

A. Western immunoblot analysis of phospho-JAK2 (Y1007) in untreated K562 cells relative to untreated HEL cells, an erythroleukemia cell line harboring an activated allele of JAK2 (V617F). Lysates from K562 and HEL cells treated with XL019, a selective JAK2 inhibitor, served as experimental controls. JAK2 was immunoprecipitated from the cell lysate and probed for activation loop (Y1007) phosphorylation.

B. Western immunoblot analysis of K562 whole cell lysates following prolonged BCR-ABL inhibition (1μM imatinib: 2hrs, 4hrs, 8hrs, 24hrs; 0.2% DMSO, 24 hours) and hEPO stimulation (10').

C. Normalized phospho-JAK2 mediated by hEPO-stimulation (10') in K562 cells following a 24-hour treatment with 0.2% DMSO or 100nM dasatinib. Data represents the average ± SD (n=3; ***$p \leq 0.001$, Two-way ANOVA with Bonferroni post-tests). Phospho-JAK2 was monitored by immunoprecipitation and activation loop (Y1007) phosphorylation.

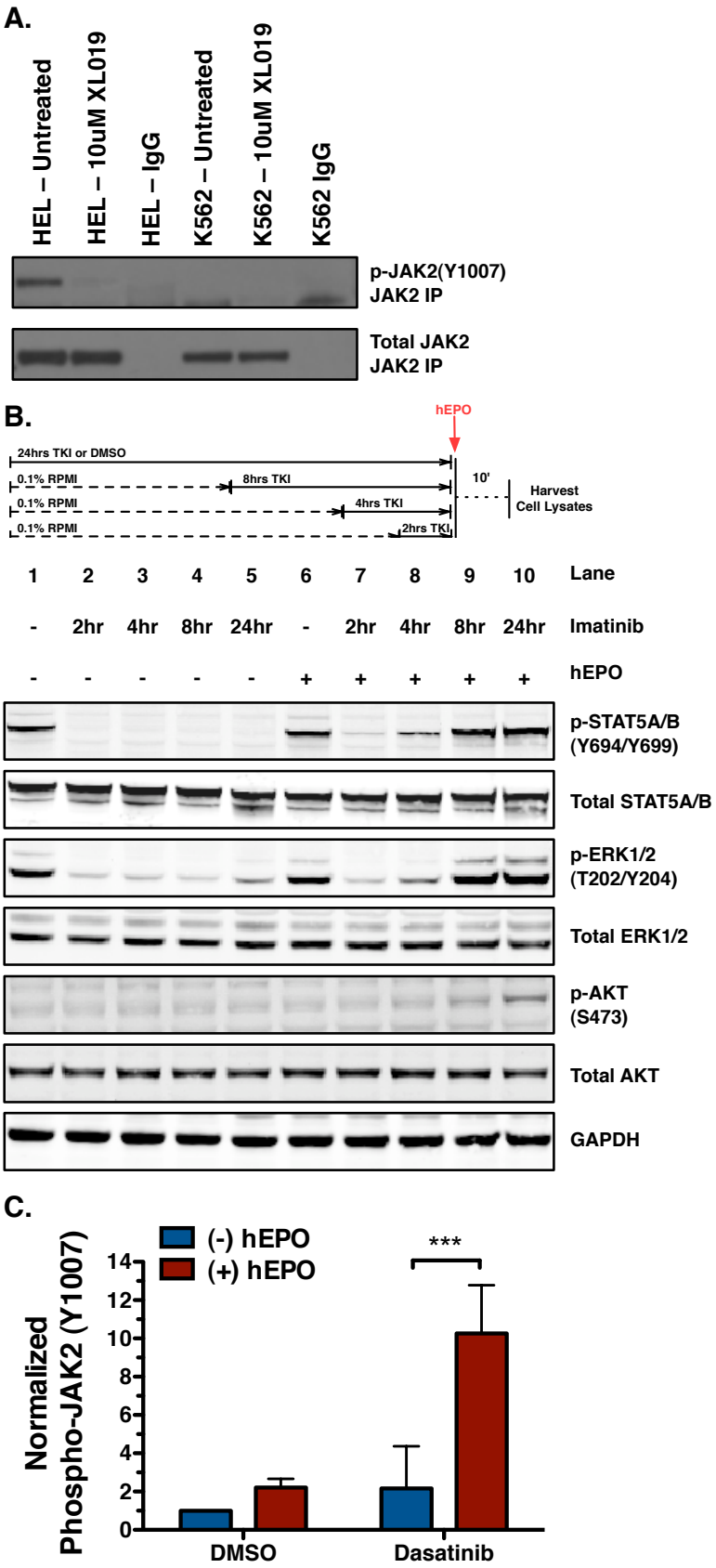
A.
HEL – Untreated
HEL – 10uM XL019
HEL – IgG
K562 – Untreated
K562 – 10uM XL019
K562 IgG
p-JAK2(Y1007)
JAK2 IP
Total JAK2
JAK2 IP
B.
hEPO
24hrs TKI or DMSO
0.1% RPMI
8hrs TKI
10'
Harvest
Cell Lysates
0.1% RPMI
4hrs TKI
0.1% RPMI
2hrs TKI
1 2 3 4 5 6 7 8 9 10
Lane
- 2hr 4hr 8hr 24hr - 2hr 4hr 8hr 24hr
Imatinib
- - - - - + + + + +
hEPO
p-STAT5A/B
(Y694/Y699)
Total STAT5A/B
p-ERK1/2
(T202/Y204)
Total ERK1/2
p-AKT
(S473)
Total AKT
GAPDH
C.
(-) hEPO
(+) hEPO
***
Normalized
Phospho-JAK2 (Y1007)
0
2
4
6
8
10
12
14
DMSO
Dasatinib

Figure S4. Relief of MEK-Dependent Negative Feedback is Associated with Robust RAS-GTP Loading and Increased hEPO-Mediated JAK2 Activation in K562 Cells.

A. Normalized RAS-GTP loading in hEPO-stimulated (10') and non-stimulated K562 cells following a 24-hour treatment with 0.2% DMSO, 100nM dasatinib, 500nM PD0325901, or dasatinib/PD0325901. RAS-GTP activity was monitored using a RAS-GTP pulldown assay.

B. Normalized phospho-JAK2 in K562 cells treated under the same experimental conditions as (A). Phospho-JAK2 was monitored by immunoprecipitation and activation loop (Y1007) phosphorylation.

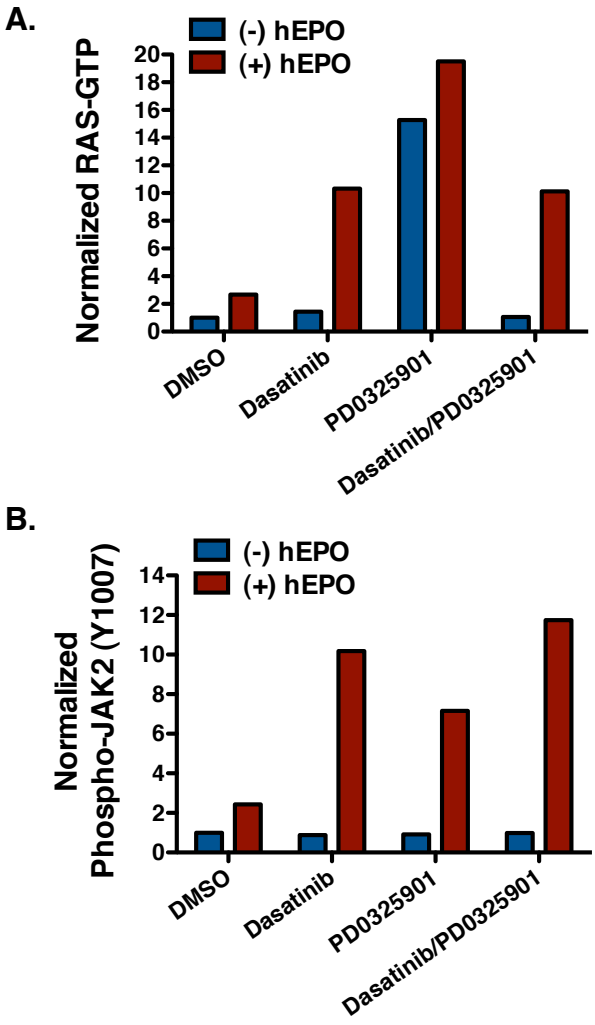
A.
(-) hEPO
(+) hEPO
Normalized RAS-GTP
0
2
4
6
8
10
12
14
16
18
20
DMSO
Dasatinib
PD0325901
Dasatinib/PD0325901
B.
(-) hEPO
(+) hEPO
Normalized Phospho-JAK2 (Y1007)
0
2
4
6
8
10
12
14
DMSO
Dasatinib
PD0325901
Dasatinib/PD0325901

Table S1. Identity and Grouping of Phosphotyrosine Peptides Identified in the SILAC Analysis of K562 Cells.

Identity and grouping of peptides by how each epitope responded to transient dasatinib treatment in the SILAC analysis of K562 cells. Peptides were grouped in the following manner: persistent responders, transient responders, durable responders, hyperphosphorylated responders, and nonresponders. See table for grouping criteria.

Table S2. DAVID Bioinformatic Analysis of Persistently Dephosphorylated Phosphotyrosine Peptides Identified in the SILAC Analysis of K562 Cells.

Top three annotation clusters from the DAVID bioinformatic analysis of persistently dephosphorylated peptides identified in the SILAC analysis of K562 cells.

Table S3. hGM-CSF Partially Rescues TF1/BCR-ABL Cells from Dasatinib and Imatinib Mediated Apoptosis.

Table S3. Percent caspase-3 negative population (live cells) of TF1/puro and TF1/BCR-ABL cell lines after a 48-hour treatment with 0.2% DMSO, 100nM dasatinib, or 1μM imatinib with and without hGM-CSF (2ng/mL). (AVG - average, SD - standard deviation)

	Average Percent Caspase-3 Negative Population (Live Cells)			
	TF1/puro		TF1/BCR-ABL	
	AVG	SD	AVG	SD
DMSO+hGM-CSF	0.730	0.049	0.682	0.036
DMSO	0.404	0.045	0.636	0.070
Dasatinib+hGM-CSF	0.760	0.019	0.481	0.057
Dasatinib	0.404	0.040	0.081	0.013
Imatinib+hGM-CSF	0.734	0.030	0.553	0.066
Imatinib	0.528	0.043	0.297	0.065

Table S4. hEPO-Mediated Rescue from Apoptosis is Dependent on JAK2 Kinase Activity.

Table S4. Percent caspase-3 negative population (live cells) of K562 cells after a 24 or 48-hour treatment with 0.2% DMSO, 100nM dasatinib, 1μM imatinib, 500nM TG101348, dasatinib/TG101348, and imatinib/TG101348 with and without hEPO (1U/mL). (AVG - average, SD - standard deviation)

	Average Percent Caspase-3 Negative Population (Live Cells)			
	24 hours		48 hours	
	AVG	SD	AVG	SD
DMSO	0.879	0.020	0.910	0.015
DMSO+hEPO	0.883	0.022	0.911	0.018
TG101348	0.880	0.016	0.923	0.014
TG101348+hEPO	0.882	0.020	0.927	0.017
Dasatinib	0.213	0.006	0.072	0.008
Dasatinib+hEPO	0.331	0.041	0.115	0.037
Imatinib	0.290	0.016	0.085	0.024
Imatinib+hEPO	0.580	0.029	0.308	0.018
Dasatinib/TG101348	0.194	0.009	0.027	0.008
Dasatinib/TG101348+hEPO	0.176	0.005	0.028	0.008
Imatinib/TG101348	0.187	0.011	0.033	0.007
Imatinib/TG101348+hEPO	0.275	0.040	0.044	0.015

Table S5. Identity of Probes Significantly Altered in K562 Cells Following Dasatinib Treatment.

Identity of the 1903 genes whose expression was significantly altered in K562 cells following dasatinib treatment (100nM; 4hrs, 8hrs, 24hrs).

Chapter 3

High Dose Pulse-Mediated Apoptosis of CML Cells Results from the Intracellular Accumulation and Retention of BCR-ABL Kinase Inhibitors

Introduction

The biological half-life of a small molecule tyrosine kinase inhibitor has been regarded as a critical pharmacokinetic property. To achieve extended target inhibition, a prolonged half-life has typically been desired. Indeed, most clinically active small molecule inhibitors exhibit long half-lives *in vivo.* This includes imatinib (18 hours), nilotinib (20 hours), erlotinib (36 hours) and quizartinib (36 hours) (1-4). In contrast, the half-life of the BCR-ABL inhibitor dasatinib is only three to five hours and in a randomized phase III clinical trail where chronic myeloid leukemia (CML) patients were treated with either once-daily or twice-daily dasatinib, both treatment groups exhibited similar progression free survival rates and time to remission (5, 6). Furthermore, the phosphorylation status of the adaptor protein CRKL in CML patient samples, a pharmacodynamic marker of BCR-ABL kinase inhibition, is transiently altered and subsequently restored within eight hours of dasatinib treatment (7). These clinical observations suggested that continuous BCR-ABL kinase inhibition was not necessarily a prerequisite for clinical efficacy in CML.

It was subsequently documented that transient BCR-ABL tyrosine kinase inhibitor (TKI) treatment inhibits CML cell viability, colony formation, and induces apoptosis *in vitro*, although the mechanism responsible for this effect was not identified (7-9). Each of these investigations used the phosphorylation status of CRKL to argue that BCR-ABL kinase activity is fully restored following drug washout as CRKL is nearly exclusively phosphorylated by BCR-ABL in CML cells (10). However, the phosphorylation status of STAT5A/B tracks more closely with viability when CML cells are treated continuously with low concentrations of imatinib or dasatinib, arguing that phospho-STAT5A/B is a more sensitive readout of BCR-ABL inhibition (7). Prolonged inhibition of phospho-STAT5A/B

following transient imatinib or dasatinib treatment would suggest that residual BCR-ABL kinase inhibition persists despite removal of inhibitor from the culture medium.

A similar response to transient kinase inhibitor therapy *in vitro* has been documented for erlotinib in EGFR-dependent non-small cell lung cancer (NSCLC) and quizartinib in FLT3-dependent acute myeloid leukemia (AML) (7, 11). These findings suggest that cytotoxicity elicited by transient kinase inhibition may be a broader phenomenon. Identification of the mechanism responsible for the inhibition of CML cell viability following transient BCR-ABL inhibition is an important biological question. From a pharmacologic perspective, optimizing the duration of drug exposure to the minimum time of target inhibition necessary for cytotoxicity of malignant cells might minimize undesirable, non-specific drug side effects.

We previously documented that CML cells treated with either a low-dose continuous (LDC) cytotoxic concentration or a transient high-dose pulse (HDP) of dasatinib exhibited nearly identical kinetics of apoptosis induction as measured by annexin-V, cleaved caspase-3 and BIM dephosphorylation (7). From these observations, it was concluded that LDC and HDP dasatinib treatment elicit a very similar or nearly identical mechanism of apoptosis. Here, we sought to determine the effects of HDP treatment on BCR-ABL kinase activity as assessed by more sensitive measures (e.g. STAT5A/B phosphorylation). We found that in contrast to CRKL, STAT5A/B is durably dephosphorylated following HDP treatment, and that this prolonged BCR-ABL inhibition is a consequence of intracellular drug accumulation and retention.

Results

High-Dose Pulse and Low-Dose Continuous TKI Treatment Elicit Similar Signaling Changes in CML Cell Lines.

It was previously shown that HDP and LDC TKI treatment elicit nearly identical kinetics of apoptosis in CML cells (7). To determine if HDP and LDC TKI treatment also elicit similar changes in phospho-STAT5A/B, a more sensitive marker of BCR-ABL kinase inhibition, the CML cell lines K562 and KU812 were treated with either a HDP or LDC exposure of dasatinib or imatinib. In contrast to previous results observed with CRKL, similar kinetics, duration, and magnitude of STAT5A/B de-phosphorylation was observed following HDP or LDC TKI treatment in both cell lines (**figure 1a, 1b**). The phosphorylation status of other BCR-ABL canonical signaling pathways was also interrogated across the same experimental conditions. The kinetics and magnitude of ERK1/2 and S6 de-phosphorylation were similar in both treatment conditions (**figure 1a, 1b**). HDP and LDC TKI treatment also elicited similar changes in BCR-ABL tyrosine phosphorylation (**figure 1c**). These observations suggest that a low level of BCR-ABL kinase inhibition persists following HDP treatment, despite extensive efforts to remove inhibitor from the culture medium.

An Additional Delayed Media Wash Rescues CML Cells from HDP-Mediated Apoptosis.

Identical changes in STAT5A/B, ERK1/2, S6, and BCR-ABL tyrosine phosphorylation suggest that HDP and LDC inhibitor treatment elicit apoptosis in CML cells through a

shared mechanism of action. Although cells are washed with three full-volume medium washes following transient inhibitor treatment, HDP-mediated intracellular drug retention and residual BCR-ABL kinase inhibition is potentially responsible for the observed similarities. To address the possibility that residual BCR-ABL kinase inhibition is responsible for HDP-mediated apoptosis of CML cells, HDP treated K562 cells were given one additional delayed, full-volume medium wash either one-hour or five-hours following drug washout (see **figure 2a** for experimental design). This type of HDP treatment, a traditional HDP followed by a delayed medium wash, will subsequently be referred to as a non-standard HDP (NS-HDP). One additional delayed medium wash at one-hour or five-hours post drug washout was sufficient to rescue K562 cells from either imatinib or dasatinib HDP-mediated apoptosis and partially restored cell viability (**figure 2b, 2c**). These observations suggest that residual BCR-ABL kinase inhibition could be responsible for HDP-mediated apoptosis of CML cells.

BCR-ABL-Expressing Ba/F3 Cells are Sensitive to HDP Extracellular Medium.

To address the possibility that the delayed medium wash of a NS-HDP removed a cytotoxic agent other than extracellular imatinib or dasatinib, murine Ba/F3 cells expressing the native TKI-sensitive allele (p210-Ba/F3) or the TKI-resistant T315I allele of BCR-ABL (T315I-Ba/F3) were re-suspended in the extracellular medium collected following a HDP treatment of K562 cells and cell viability was monitored (see **figure 2a** for experimental design). Ba/F3-expressing BCR-ABL cells are reliant on BCR-ABL kinase activity for survival and are sensitive to BCR-ABL inhibition (12). The viability of p210-Ba/F3 cells was selectively inhibited following re-suspension in extracellular medium

collected from a dasatinib or imatinib HDP of K562 cells, while T315I-Ba/F3 cell viability was unaffected (**figure 3a**). The selective inhibition of TKI-sensitive p210-Ba/F3 cells suggests that removal of extracellular inhibitor in the medium is responsible for the rescue of apoptosis associated with NS-HDP treatment.

To determine if the intracellular retention of imatinib and dasatinib following HDP treatment is unique to BCR-ABL-expressing cells, the human acute myeloid leukemia cell line MV4;11 was treated with a HDP of imatinib and BCR-ABL-expressing Ba/F3 cells were re-suspended in the extracellular medium collected five-hours post drug washout (same experimental design depicted in **figure 2a**). MV4;11-HDP extracellular medium selectively inhibited the viability of p210-Ba/F3 cells, but not T315I-Ba/F3 cells (**figure 3b**). This observation suggests that the intracellular retention of imatinib and dasatinib during a HDP is not unique to BCR-ABL expressing cells, but is rather a more general cellular phenomenon of these inhibitors.

HDP-Mediated Intracellular Drug Retention Generates a "LDC-like" State Following Drug Washout.

To document the presence of residual TKI in the medium of CML cells following HDP treatment, K562 cells were treated with a HDP of imatinib and LC-MS/MS was used to monitor concentrations of inhibitor in the extracellular medium over time following drug washout (see **figure 4a** for experimental design). Imatinib was chosen for this analysis since its effect on CML cell survival occurs within the LC-MS/MS limit of detection (13). A time-dependent increase in the concentration of extracellular imatinib was detected following HDP treatment (**figure 4b**). Interestingly, the measured concentration of

imatinib in the extracellular medium was above the reported IC50 value for K562 cells (**figure 4b**, dashed line) (13). To determine if the increase in extracellular imatinib was associated with a corresponding decrease in intracellular inhibitor, the intracellular concentration of imatinib in K562 cells was also monitored. LC-MS/MS analysis revealed an opposing time-dependent decrease in the concentration of intracellular imatinib following drug washout (**figure 4c**). Together, these observations suggest that during a HDP of imatinib, intracellular accumulation of inhibitor is sufficient to establish a "LDC-like" state in the surrounding medium following drug washout.

NS-HDP treatment restores cell viability and effectively rescues K562 cells from imatinib or dasatinib HDP mediated apoptosis (**figure 2b, 2c**). To determine if the rescue from apoptosis observed following a NS-HDP is associated with the removal of cytotoxic concentrations of extracellular inhibitor, the concentration of imatinib in the extracellular medium was measured by LC-MS/MS before and after the additional delayed medium wash of NS-HDP treated K562 cells. The concentration of imatinib in the extracellular medium following the additional delayed media wash was lower than the reported IC50 of imatinib in K562 cells (**figure 4d**, dashed line). These results suggest that removal of imatinib in the extracellular media following HDP treatment is sufficient to rescue CML cells from HDP-mediated apoptosis.

An Additional Delayed Media Wash Rescues BCR-ABL Tyrosine Phosphorylation and Canonical BCR-ABL Pathway Activation.

To determine if BCR-ABL canonical pathway signaling and BCR-ABL tyrosine phosphorylation is restored following a NS-HDP, the phosphorylation status of STAT5A/B,

ERK1/2, S6, and BCR-ABL in K562 cells was assessed following a standard HDP and NS-HDP of dasatinib. Re-phosphorylation of BCR-ABL, STAT5A/B, ERK1/2, and S6 was observed following a NS-HDP at 24-hours post drug washout (**figure 5a, 5b**). Re-phosphorylation of these residues was not observed at any point in time following standard HDP treatment. These observations suggest that re-phosphorylation of STAT5A/B, ERK1/2, S6 and BCR-ABL is critical for the rescue from apoptosis associated with NS-HDP treatment.

Discussion

In this study, we have documented that HDP-mediated apoptosis of CML cells *in vitro* is the result of intracellular drug retention. Our experimental findings suggest that during HDP treatment, CML cells accumulate a substantial amount of inhibitor, sufficient to establish a low, but cytotoxic level of inhibitor in a large volume of extracellular medium upon delayed efflux from the cells following drug washout. Removal of extracellular inhibitor by an additional medium wash at either one or five-hours following drug washout effectively rescued K562 cells from HDP-mediated apoptosis. Furthermore, extracellular medium collected from K562 cells following a HDP treatment of imatinib or dasatinib inhibits the proliferation of native BCR-ABL expressing-Ba/F3 cells, but not drug-resistant T315I-expressing Ba/F3 cells. This experimental observation is important, as it documents the selective biologic activity of the post-HDP extracellular medium. Finally, the measured concentrations of intracellular and extracellular imatinib following a HDP treatment of K562 cells were inversely related, suggesting that intracellular drug is rapidly effluxed into the extracellular medium following drug washout.

Previous observations suggested that a shared mechanism might be responsible for HDP- and LDC-mediated apoptosis. We previously documented that the kinetics of BIM dephosphorylation and caspase-3 activation were similar in CML cells following dasatinib HDP or LDC treatment (7). From these observations, we sought to determine if HDP and LDC-mediated inhibition of canonical BCR-ABL signaling pathways was also similar. We found that the kinetics, duration, and magnitude of STAT5A/B, ERK1/2 and S6 dephosphorylation were similar in both treatment conditions while interrogation of BCR-ABL tyrosine phosphorylation revealed additional similarities. Finally, these epitopes were

re-phosphorylated in the NS-HDP treatment condition. Together, these results provided further evidence for a shared mechanism of apoptosis and also validated the importance of these signaling pathways in CML cell survival.

Our experimental investigation revealed a time-dependent increase in the concentration of extracellular inhibitor following HDP drug washout. Measured concentrations of extracellular drug were similar to the amount of drug present in the LDC condition, providing an explanation for the observed similarities of HDP and LDC inhibitor treatment. Although the mechanism responsible for the HDP-mediated intracellular retention of these inhibitors is unknown, we propose the following scenarios as potential hypotheses. The first scenario involves non-specific inhibitor-protein binding, either with other kinases or non-kinase proteins in the cell. Efforts to identify the cellular binding profile of imatinib and dasatinib have generated a list of kinase and non-kinase protein targets that associate with these small molecule inhibitors in various cell types (14-17). Although the reported kinase profiles for imatinib and dasatinib differ, both inhibitors have been documented to bind a number of proteins with ATP or other nucleotide-binding affinity (15, 17). Importantly, this mechanism is supported by our experimental observations. The extracellular medium collected from HDP imatinib treated K562 or MV4;11 cells was equally effective in selectively inhibiting the viability of p210-Ba/F3 cells, suggesting that intracellular accumulation of imatinib is not unique to BCR-ABL expressing cells. Despite evidence supporting this hypothesis, defining the specific cellular proteins or kinases involved will be difficult to address experimentally as this effect may be a collective result of non-specific protein binding to many different cellular entities. Preliminary mechanistic experiments could involve pre-treating CML cells with a non-selective kinase

inhibitor like staurosporine prior to imatinib or dasatinib treatment to determine if pre-incubation with a general kinase inhibitor precludes the intracellular accumulation and retention of BCR-ABL inhibitors.

"Ion trapping" is a second potential hypothesis and explanation for the observed intracellular accumulation of imatinib and dasatinib during HDP treatment. This phenomenon involves the sequestration of amine-containing small molecules into acidic cellular compartments, like the lysosomes, endosomes, and Golgi apparatus (reviewed in (18, 19)). Small molecules exhibiting this property are referred to as lysosomotropic agents (18). Briefly, uncharged amine-containing small molecules enter the cell via passive diffusion, but become protonated and charged upon entry into an acidic intracellular compartment (20). Once protonated, these small molecules can no longer diffuse back into the cytoplasm and become trapped at high concentrations in the acidic intracellular compartments (19). Ion trapping has been documented to be dependent on the activity of vacuolar proton ATPase transporters, as treatment with bafilomycin A or other proton pump inhibitors prevents the cellular accumulation of lysosomotropic agents. Ion trapping is a documented characteristic of a number of amine containing small molecules, including imatinib, dasatinib, and several other tyrosine kinase inhibitors (21). Pretreatment of CML cells with bafilomycin A prior to a HDP of dasatinib or imatinib could be used to determine if ion trapping is necessary for HDP-mediated apoptosis. Future work will focus on determining if ion trapping is responsible for the intracellular accumulation and retention of imatinib and dasatinib during HDP treatment.

Prolonged kinase inhibitor residence time is a third potential hypothesis and explanation for the HDP-mediated intracellular accumulation and retention of BCR-ABL

kinase inhibitors. An inhibitor's kinase residence time refers to the length of time a particular inhibitor remains associated with its target kinase before dissociation occurs. The prediction is that kinase inhibitors capable of inducing HDP-mediated apoptosis of CML cells will also exhibit a prolonged residence time on BCR-ABL. Indeed, in a recent publication O'hare et al used a FRET-based assay to document that dasatinib exhibits a more prolonged residence time on BCR-ABL relative to imatinib (24). This observation has important implications for future drug development efforts as kinase inhibitors with shorter $t_{1/2}$, but extended kinase residence periods, may still exhibit clinical efficacy with less non-specific, cytotoxicities.

The significance of STAT5A/B, RAS/MAPK, and PI3K/AKT pathway activation in CML cell survival has been documented previously and this work further validates their importance (22). Interestingly, the kinetics of pathway re-activation following a NS-HDP is delayed relative to the removal of drug in the extracellular medium. Partial re-phosphorylation of critical epitopes was detected at the 24-hour time point in the NS-HDP treatment condition. However, canonical pathway and BCR-ABL re-phosphorylation is absent at the six-hour time point in a NS-HDP, an hour after the delayed medium wash (**figure 5a, 5b**). An extensive time-course of analysis of epitope re-phosphorylation in the NS-HDP treatment condition has not yet be performed, so the initial time of detectable re-phosphorylation is currently unknown.

During our experimental investigation of intracellular drug retention in CML cells following HDP inhibitor treatment, Lipka and colleagues published a manuscript describing the same phenomenon (23). The NS-HDP used by Lipka et al differs slightly from the one described here, but the outcome on cell viability and apoptosis is identical in both

situations. Lipka et al also documented a time-dependent release of inhibitor into the extracellular medium that was associated with a corresponding decrease in intracellular inhibitor concentrations. A second more recent publication also documents that intracellular drug retention is responsible for HDP-mediated apoptosis of CML cells (24).

Our interrogation of the mechanism responsible for HDP-mediated cytotoxicity in CML cells has provided valuable pharmacokinetic information for the development of new small molecule inhibitors. Small molecules exhibiting an affinity for intracellular accumulation and retention may not necessarily need to possess a long half-life *in vivo* for clinical efficacy. Optimizing these properties may allow for the development of compounds with a reduced number of non-specific side effects while allowing for better drug safety profiles and patient tolerability.

Experimental Methods

LC-MS Instrument, Analytical Methods, and Sample Preparation

All LC-MS/MS analyses were performed on a Shimadzu LC-20AD (Kyoto, Japan) HPLC system coupled to an Applied Biosystem/MDS Sciex API (Framingham, MA) 4000 triple quadrupole mass spectrometer outfitted with a Turbo V ion source LC-MS/MS. LC-MS/MS analyses for the detection of imatinib and carbamazepine (internal standard) were accomplished using a reverse phase column, BDS Hpersil C18 (50 x 4.6 mm, 5.0 µm) (Waltham, MA) with an elution gradient of 30% 5 mM aqueous ammonium acetate, 0.1 % formic acid (pH 3.2) to 98% methanol over 4.5 mins at a flow rate of 0.5 ml/min. For LC-MS/MS analyses, 20µl aliquot of sample were injected onto the column and mass spectral analyses were performed using positive ionization mode multiple reaction monitoring. The mass transitions for each compound were as follows: MH+ m/z 494 to 394 (imatinib) and MH+ m/z 237 to 194 (carbamazepine). The elution times for imatinib and carbamazepine were 3.95 and 4.32 mins, respectively. Samples were prepped for LC-MS analysis in the following manner. Samples were mixed in a 1:1 ratio with acetonitrile containing 1µM of the internal standard carbamazepine. Samples were subsequently pelleted at 14,000 × g for 5 minutes at room temperature. Cleared supernatant (150µL) was transferred to a HPLC vial for LC-MS/MS analysis.

Tissue Culture, Cell Viability, and Drug Exposures

K562, KU812, MV4;11, p210-Ba/F3 and T315I/p210-Ba/F3 cells were propagated in RPMI 1640 medium supplemented with 10% fetal bovine serum (FBS; Omega Scientific), L-

glutamine, and penicillin/streptomycin (Invitrogen). Ba/F3 cells were engineered to express BCR-ABL or T315I/BCR-ABL through retroviral transduction as described previously (25). Cell viability was determined after 48-hours of low-dose continuous (LDC) or high-dose pulse (HDP) treatment by trypan blue exclusion using the Vi-Cell cell viability analyzer. K562 cells were plated at a density of 0.1×10^6 and BCR-ABL-expressing Ba/F3 cells were plated at a density of 0.05×10^6 for viability experiments. HDP and LDC treatments were performed as described previously (7). In a non-standard HDP (NS-HDP), cells were treated with a traditional HDP followed by one additional delayed, full volume medium wash of the cells at either one-hour or five-hours post drug washout.

Tyrosine Kinase Inhibitors, Western Immunobloting, and Antibodies

DMSO stock solutions of dasatinib and imatinib were generated at UCSF. Cell lysates were resolved by SDS-PAGE and transferred to nitrocellulose as described previously (7). Cells were prepped and stained for flow cytometry analysis of cleaved caspase-3 as previously reported (7). The following antibodies were purchased from Cell Signaling Technology: phospho-STAT5A/B (Y695/Y699) (cat. 9351), total STAT5A/B (cat. 9363), phospho-ERK1/2 (T202/Y204) (cat. 4370), total ERK1/2 (cat. 9107), phospho-S6 (S235/S236) (cat. 2211), total S6 (cat. 2317), phospho-BCR (Y177) (cat. 3901), and phospho-cABL (Y185, Y226) (cat. 3009 and 2861). The following antibodies were purchased from Abgent: phospho-cABL (Y115) (cat. AP3011a) and phospho-cABL (Y232) (cat. AP3014a). Total cABL (cat. OP20) was purchased from Millipore and FITC-conjugated anti-active caspase-3 was purchased from BD Biosciences (cat. #550480).

References

1. Cortes J, Foran J, Ghirdaladze D, DeVetten MP, Zodelava M, Holman P*, et al.* AC220, a Potent, Selective, Second Generation FLT3 Receptor Tyrosine Kinase (RTK) Inhibitor, in a First-in-Human (FIH) Phase 1 AML Study. *ASH Annual Meeting Abstracts* 2009 November 20, 2009; **114**(22)**:** 636-.

2. Lu JF, Eppler SM, Wolf J, Hamilton M, Rakhit A, Bruno R*, et al.* Clinical pharmacokinetics of erlotinib in patients with solid tumors and exposure-safety relationship in patients with non-small cell lung cancer. *Clin Pharmacol Ther* 2006 Aug; **80**(2)**:** 136-145.

3. Tanaka C, Yin OQ, Sethuraman V, Smith T, Wang X, Grouss K*, et al.* Clinical pharmacokinetics of the BCR-ABL tyrosine kinase inhibitor nilotinib. *Clin Pharmacol Ther* 2010 Feb; **87**(2)**:** 197-203.

4. le Coutre P, Kreuzer KA, Pursche S, Bonin M, Leopold T, Baskaynak G*, et al.* Pharmacokinetics and cellular uptake of imatinib and its main metabolite CGP74588. *Cancer Chemother Pharmacol* 2004 Apr; **53**(4)**:** 313-323.

5. Shah NP, Kantarjian HM, Kim DW, Rea D, Dorlhiac-Llacer PE, Milone JH*, et al.* Intermittent target inhibition with dasatinib 100 mg once daily preserves efficacy and improves tolerability in imatinib-resistant and -intolerant chronic-phase chronic myeloid leukemia. *J Clin Oncol* 2008 Jul 1; **26**(19)**:** 3204-3212.

6. Steinberg M. Dasatinib: a tyrosine kinase inhibitor for the treatment of chronic myelogenous leukemia and philadelphia chromosome-positive acute lymphoblastic leukemia. *Clin Ther* 2007 Nov; **29**(11)**:** 2289-2308.

7. Shah NP, Kasap C, Weier C, Balbas M, Nicoll JM, Bleickardt E*, et al.* Transient potent BCR-ABL inhibition is sufficient to commit chronic myeloid leukemia cells irreversibly to apoptosis. *Cancer Cell* 2008 Dec 9; **14**(6)**:** 485-493.

8. Hiwase DK, White DL, Powell JA, Saunders VA, Zrim SA, Frede AK*, et al.* Blocking cytokine signaling along with intense Bcr-Abl kinase inhibition induces apoptosis in primary CML progenitors. *Leukemia* Apr; **24**(4)**:** 771-778.

9. Snead JL, O'Hare T, Adrian LT, Eide CA, Lange T, Druker BJ*, et al.* Acute dasatinib exposure commits Bcr-Abl-dependent cells to apoptosis. *Blood* 2009 Oct 15; **114**(16)**:** 3459-3463.

10. Druker BJ, Sawyers CL, Kantarjian H, Resta DJ, Reese SF, Ford JM*, et al.* Activity of a specific inhibitor of the BCR-ABL tyrosine kinase in the blast crisis of chronic myeloid leukemia and acute lymphoblastic leukemia with the Philadelphia chromosome. *N Engl J Med* 2001 Apr 5; **344**(14)**:** 1038-1042.

11. Gunawardane RN, Nepomuceno RR, Rooks AM, Hunt JP, Ricono JM, Belli B*, et al.* Transient exposure to quizartinib mediates sustained inhibition of FLT3 signaling while specifically inducing apoptosis in FLT3-activated leukemia cells. *Mol Cancer Ther* 2013 Apr; **12**(4)**:** 438-447.

12. Daley GQ, Baltimore D. Transformation of an interleukin 3-dependent hematopoietic cell line by the chronic myelogenous leukemia-specific P210bcr/abl protein. *Proc Natl Acad Sci U S A* 1988 Dec; **85**(23)**:** 9312-9316.

13. Deininger MW, Goldman JM, Lydon N, Melo JV. The tyrosine kinase inhibitor CGP57148B selectively inhibits the growth of BCR-ABL-positive cells. *Blood* 1997 Nov 1; **90**(9)**:** 3691-3698.

14. Rix U, Hantschel O, Durnberger G, Remsing Rix LL, Planyavsky M, Fernbach NV*, et al.* Chemical proteomic profiles of the BCR-ABL inhibitors imatinib, nilotinib, and dasatinib reveal novel kinase and nonkinase targets. *Blood* 2007 Dec 1; **110**(12)**:** 4055-4063.

15. Bantscheff M, Eberhard D, Abraham Y, Bastuck S, Boesche M, Hobson S*, et al.* Quantitative chemical proteomics reveals mechanisms of action of clinical ABL kinase inhibitors. *Nat Biotechnol* 2007 Sep; **25**(9)**:** 1035-1044.

16. Fabian MA, Biggs WH, 3rd, Treiber DK, Atteridge CE, Azimioara MD, Benedetti MG*, et al.* A small molecule-kinase interaction map for clinical kinase inhibitors. *Nat Biotechnol* 2005 Mar; **23**(3)**:** 329-336.

17. Fischer JJ, Dalhoff C, Schrey AK, Graebner OY, Michaelis S, Andrich K*, et al.* Dasatinib, imatinib and staurosporine capture compounds - Complementary tools for the profiling of kinases by Capture Compound Mass Spectrometry (CCMS). *J Proteomics* 2011 Dec 10; **75**(1)**:** 160-168.

18. Marceau F, Bawolak MT, Lodge R, Bouthillier J, Gagne-Henley A, Gaudreault RC*, et al.* Cation trapping by cellular acidic compartments: beyond the concept of lysosomotropic drugs. *Toxicol Appl Pharmacol* 2012 Feb 15; **259**(1)**:** 1-12.

19. Aki T, Nara A, Uemura K. Cytoplasmic vacuolization during exposure to drugs and other substances. *Cell Biol Toxicol* 2012 Jun; **28**(3)**:** 125-131.

20. de Duve C, de Barsy T, Poole B, Trouet A, Tulkens P, Van Hoof F. Commentary. Lysosomotropic agents. *Biochem Pharmacol* 1974 Sep 15; **23**(18)**:** 2495-2531.

21. Nadanaciva S, Lu S, Gebhard DF, Jessen BA, Pennie WD, Will Y. A high content screening assay for identifying lysosomotropic compounds. *Toxicol In Vitro* 2011 Apr; **25**(3)**:** 715-723.

22. Sonoyama J, Matsumura I, Ezoe S, Satoh Y, Zhang X, Kataoka Y*, et al.* Functional cooperation among Ras, STAT5, and phosphatidylinositol 3-kinase is required for full oncogenic activities of BCR/ABL in K562 cells. *J Biol Chem* 2002 Mar 8; **277**(10)**:** 8076-8082.

23. Lipka DB, Wagner MC, Dziadosz M, Schnoder T, Heidel F, Schemionek M*, et al.* Intracellular retention of ABL kinase inhibitors determines commitment to apoptosis in CML cells. *PLoS One*; **7**(7)**:** e40853.

24. O'Hare T, Eide CA, Agarwal A, Adrian LT, Zabriskie MS, Mackenzie RJ*, et al.* Threshold levels of ABL tyrosine kinase inhibitors retained in chronic myeloid leukemia cells determine their commitment to apoptosis. *Cancer Res* 2013 Jun 1; **73**(11)**:** 3356-3370.

25. Smith CC, Wang Q, Chin CS, Salerno S, Damon LE, Levis MJ*, et al.* Validation of ITD mutations in FLT3 as a therapeutic target in human acute myeloid leukaemia. *Nature* May 10; **485**(7397)**:** 260-263.

Figure 1. HDP and LDC Treatment of CML Cells Elicit Similar Changes in the Phosphorylation of STAT5A/B, ERK1/2, S6, and BCR-ABL.

A. Western immunoblot analysis of STAT5A/B, ERK1/2, and S6 phosphorylation in the CML cell lines K562 and KU812 before and after high-dose pulse (HDP) or low-dose continuous (LDC) dasatinib treatment. In the HDP treatment condition, CML cells were treated with 100nM dasatinib for 20 minutes prior to drug washout and lysates were collected at the indicated times. In the LDC treatment condition, CML cells were treated with 1nM dasatinib continuously and lysates were collected at the indicated times. (EOE: end of HDP exposure, HDP3hrs/6hrs: 3hrs and 6hrs post-HDP, LDC3hrs/6hrs: 3hrs and 6hrs of 1nM dasatinib treatment).

B. Western immunoblot analysis of STAT5A/B, ERK1/2, and S6 phosphorylation in K562 and KU812 cells before and after HDP (32.5μM) or LDC (1μM) imatinib treatment. Lysates were generated as in (A).

C. Western immunoblot analysis of BCR-ABL tyrosine phosphorylation before and after HDP and LDC dasatinib treatment in K562 cells. Lysates were generated as in (A). (ABL1a numbering).

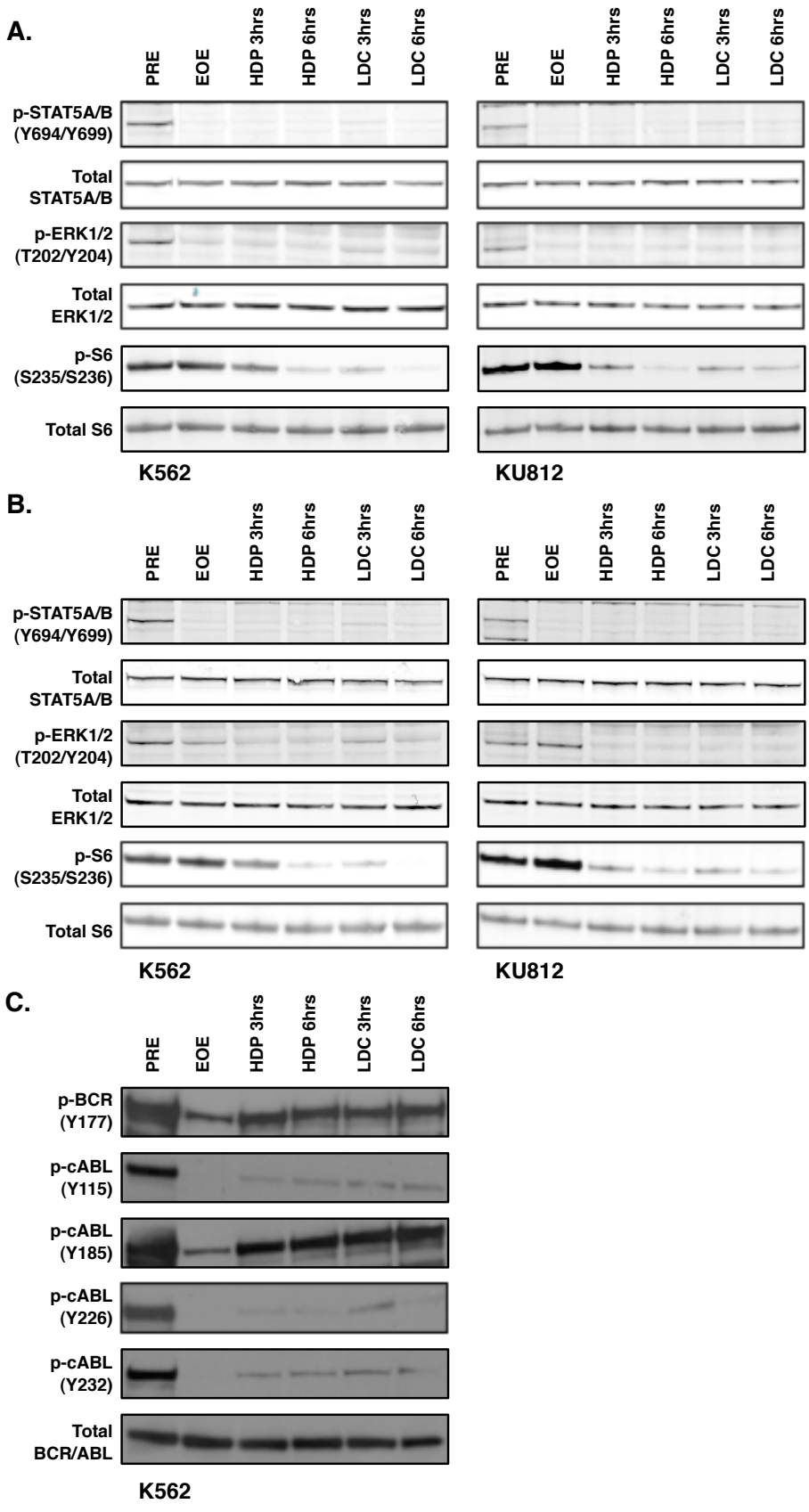
A.
PRE
EOE
HDP 3hrs
HDP 6hrs
LDC 3hrs
LDC 6hrs
p-STAT5A/B (Y694/Y699)
Total STAT5A/B
p-ERK1/2 (T202/Y204)
Total ERK1/2
p-S6 (S235/S236)
Total S6
K562
KU812
B.
C.
p-BCR (Y177)
p-cABL (Y115)
p-cABL (Y185)
p-cABL (Y226)
p-cABL (Y232)
Total BCR/ABL

Figure 2. A Single Delayed Media Wash Rescues CML Cells from HDP-Mediated Apoptosis.

A. Experimental schematic of standard HDP and non-standard HDP (NS-HDP) treatment. The last step depicts the re-suspension of BCR-ABL-expressing Ba/F3 cells in the extracellular medium collected during a NS-HDP treatment of CML cells.

B. Apoptosis in K562 cells 48 hours after standard HDP or NS-HDP treatment (HDP with 5hr medium wash) of either dasatinib or imatinib as measured by cleaved caspase-3. Red histogram: standard HDP treatment, blue histogram: NS-HDP treatment, shaded histogram: untreated cells.

C. K562 cell viability 48 hours after a HDP, NS-HDP, or continuous treatment with either dasatinib (left: 100nM HDP; 10nM LDC) or imatinib (right: 32.5μM HDP; 1μM LDC).

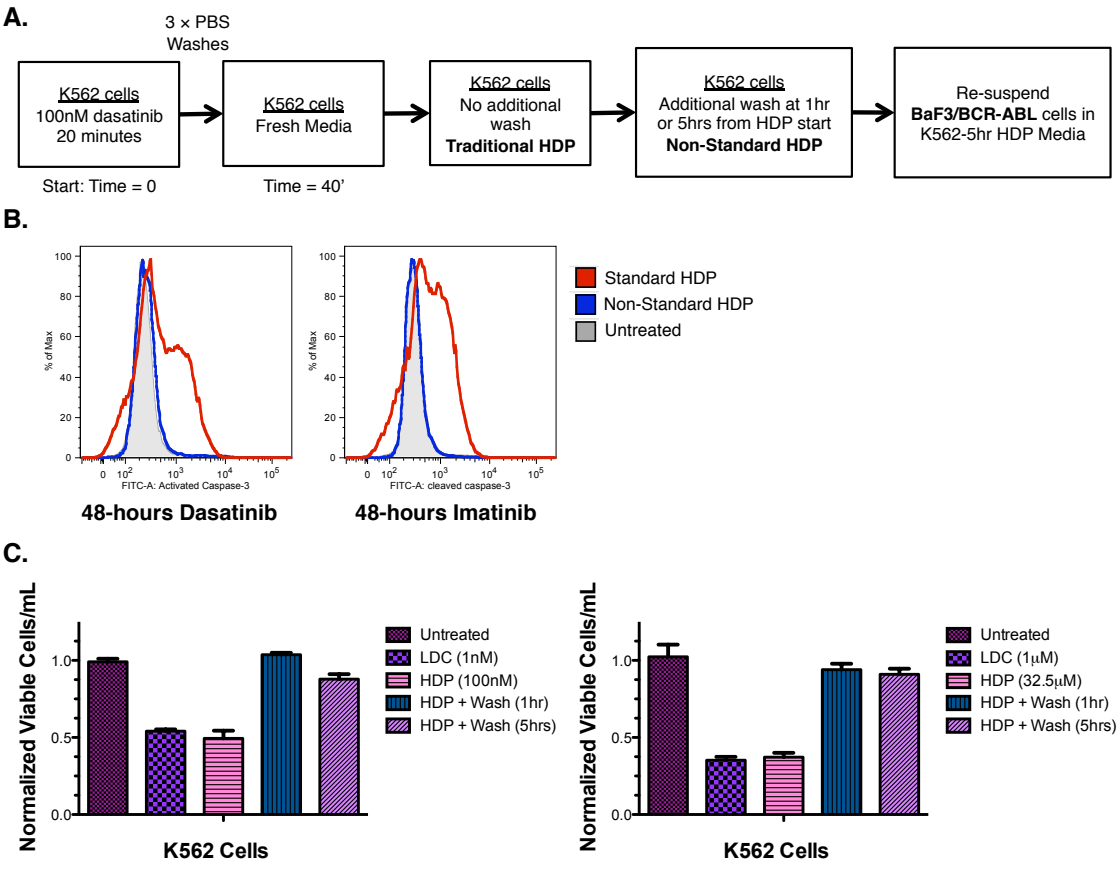
A.
3 × PBS Washes
K562 cells
100nM dasatinib
20 minutes
Start: Time = 0
K562 cells
Fresh Media
Time = 40'
K562 cells
No additional wash
Traditional HDP
K562 cells
Additional wash at 1hr or 5hrs from HDP start
Non-Standard HDP
Re-suspend BaF3/BCR-ABL cells in K562-5hr HDP Media
B.
% of Max
FITC-A: Activated Caspase-3
48-hours Dasatinib
FITC-A: cleaved caspase-3
48-hours Imatinib
Standard HDP
Non-Standard HDP
Untreated
C.
Normalized Viable Cells/mL
K562 Cells
Untreated
LDC (1nM)
HDP (100nM)
HDP + Wash (1hr)
HDP + Wash (5hrs)
Normalized Viable Cells/mL
K562 Cells
Untreated
LDC (1μM)
HDP (32.5μM)
HDP + Wash (1hr)
HDP + Wash (5hrs)

Figure 3. BCR-ABL-Expressing Ba/F3 Cell Viability is Inhibited Following Re-suspension in Post-HDP Extracellular Medium.

A. Native BCR-ABL-expressing Ba/F3 (p210-Ba/F3) and T315I BCR-ABL-expressing Ba/F3 (T315I-Ba/F3) cell viability 48 hours after re-suspension in the extracellular medium collected during a dasatinib (left) or imatinib (right) NS-HDP treatment of K562 cells.

B. p210-Ba/F3 and T315I-Ba/F3 cell viability 48 hours after re-suspension in the extracellular medium collected during a mock NS-HDP and an imatinib NS-HDP of K562 or MV4;11 cells.

A.

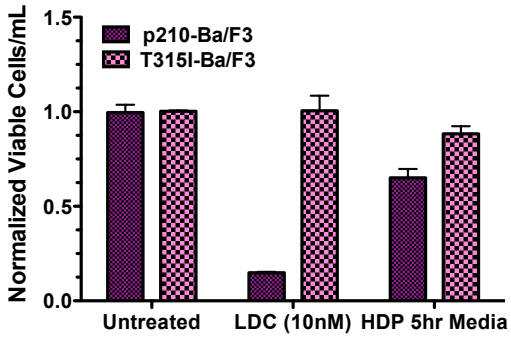
Normalized Viable Cells/mL
1.5
1.0
0.5
0.0
p210-Ba/F3
T315I-Ba/F3
Untreated
LDC (10nM)
HDP 5hr Media

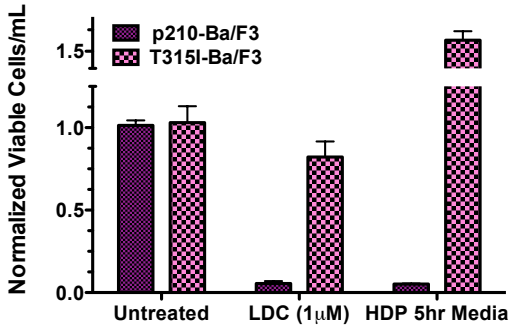
Normalized Viable Cells/mL
1.5
1.0
0.5
0.0
p210-Ba/F3
T315I-Ba/F3
Untreated
LDC (1μM)
HDP 5hr Media

B.

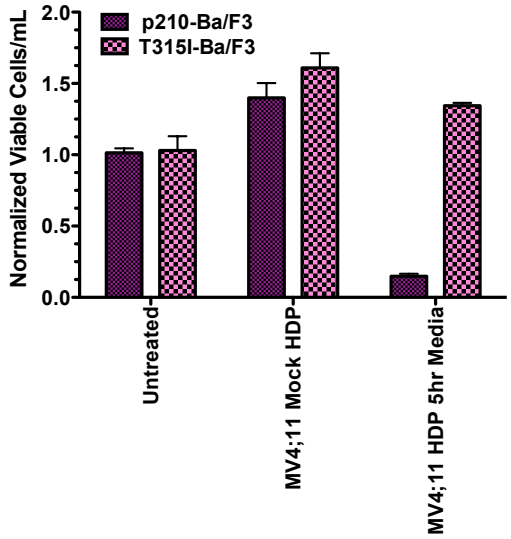
Normalized Viable Cells/mL
2.0
1.5
1.0
0.5
0.0
p210-Ba/F3
T315I-Ba/F3
Untreated
MV4;11 Mock HDP
MV4;11 HDP 5hr Media

Figure 4. The Extracellular Concentration of Imatinib Increases in a Time-Dependent Manner following HDP Treatment.

A. Schematic depicting relationship between experimental time and real time during a HDP treatment of CML cells. (PW0: post-wash zero minutes, PW5: post-wash five minutes, etc.)

B. The concentration of extracellular imatinib measured by LC-MS/MS following a HDP treatment of K562 cells. Data represents the average ± standard deviation (n=4). The dashed line depicts the reported IC50 value for imatinib in K562 cells.

C. The concentration of intracellular imatinib measured by LC-MS/MS following a HDP treatment of K562 cells. Data represents the average ± standard deviation (n=3).

D. The concentration of imatinib in the extracellular medium measured by LC-MS/MS before and after a single delayed medium wash at PW60' or PW120' after imatinib HDP treatment of K562 cells.

A.

Time Point	Real Time
PRE	0’
EOE	20’
PW0’	45’
PW5’	50’
PW10’	55’
PW30’	75’
PW60’	105’
PW255’	300’

B.

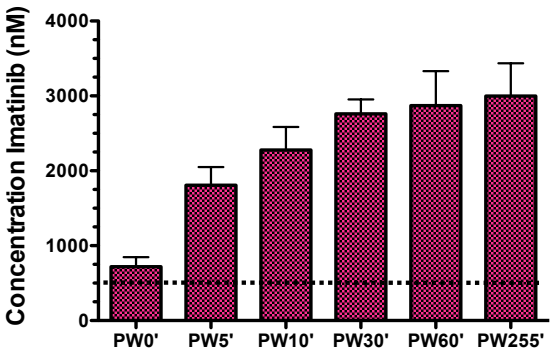

C.

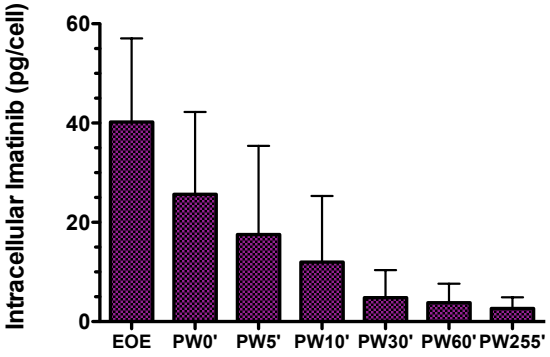

D.

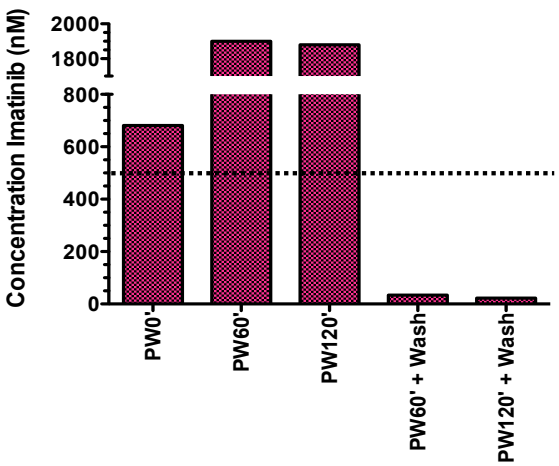

Figure 5. STAT5A/B, ERK1/2, S6, and BCR-ABL Phosphorylation is Restored after NS-HDP Treatment.

A. Western immunoblot analysis of BCR-ABL tyrosine phosphorylation before and after standard HDP and NS-HDP dasatinib treatment in K562 cells. Lysates were generated at the indicated time points.

B. Western immunoblot analysis of STAT5A/B, ERK1/2, and S6 phosphorylation before and after standard HDP and NS-HDP dasatinib treatment in K562 cells. Lysates were generated as in (A).

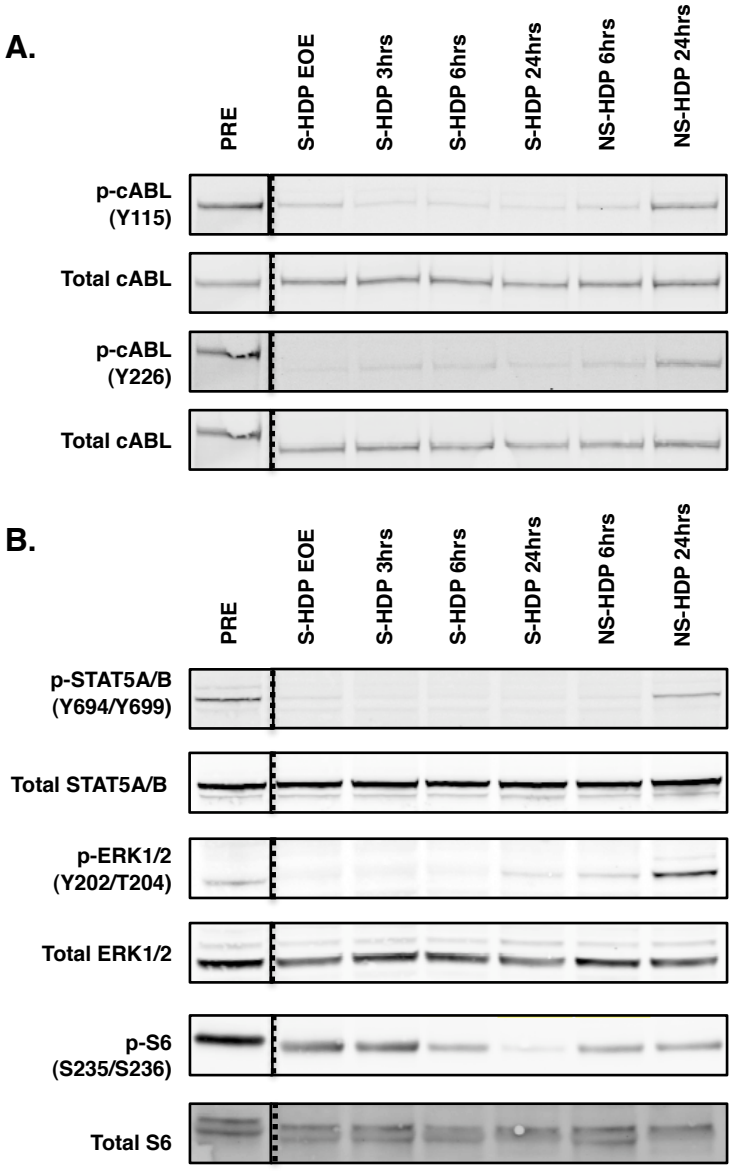
A.
PRE
S-HDP EOE
S-HDP 3hrs
S-HDP 6hrs
S-HDP 24hrs
NS-HDP 6hrs
NS-HDP 24hrs
p-cABL (Y115)
Total cABL
p-cABL (Y226)
Total cABL
B.
PRE
S-HDP EOE
S-HDP 3hrs
S-HDP 6hrs
S-HDP 24hrs
NS-HDP 6hrs
NS-HDP 24hrs
p-STAT5A/B (Y694/Y699)
Total STAT5A/B
p-ERK1/2 (Y202/T204)
Total ERK1/2
p-S6 (S235/S236)
Total S6

Chapter 4

Aurora B is the Critical Kinase Target of Dual ABL/Aurora Inhibitors in Chronic Myeloid Leukemia Cells

Abstract

Second-generation tyrosine kinase inhibitors have successfully targeted the majority of imatinib-resistant alleles of BCR-ABL, the oncogenic fusion kinase responsible for chronic myeloid leukemia (CML). The exception to this is an isoleucine for threonine substitution at the gatekeeper residue in the kinase domain of BCR-ABL (T315I). While ponatinib is a recently approved, third generation tyrosine kinase inhibitor that effectively targets the T315I mutant, patients who are unable to tolerate ponatinib require alternative therapeutic options. The first compounds to exhibit activity against the T315I mutant *in vitro* were dual ABL/Aurora kinase inhibitors, and encouragingly, clinical responses were observed in T315I-positive CML patients in early clinical trials. Since the Aurora kinases are critical for mitosis in all dividing cells, the role of Aurora kinase inhibition to dual ABL/Aurora inhibitor cytotoxicity in CML cells is unclear. Here, we have sought to delineate the contribution and significance of Aurora and BCR-ABL inhibition in BCR-ABL-expressing cells. We first generated a Ba/F3 cell line that is cross-resistant to the clinically active dual ABL/Aurora inhibitors XL228, danusertib, and MK-0457. Characterization of this cell line revealed a tyrosine to asparagine (Y161N) point mutation in Aurora B and persistence of phospho-H3 despite exposure to ABL/Aurora inhibitors. BCR-ABL-expressing Y161N-Ba/F3 cells displayed substantial resistance to all ABL/Aurora inhibitors tested, demonstrating that the mechanism of action of these agents in BCR-ABL-expressing cells is primarily mediated by inhibition of Aurora B.

Introduction

Clinical resistance to targeted therapy has been extensively described in chronic myeloid leukemia (CML) where small molecule tyrosine kinase inhibitors (TKIs) targeting the fusion protein BCR-ABL are used as frontline therapy. The scope of resistance-conferring mutations in the kinase domain of BCR-ABL has been defined *in vitro* for the BCR-ABL TKIs imatinib, nilotinib, dasatinib and ponatinib (1-3). Many mutations identified *in vitro* have been observed clinically in CML patients treated with these inhibitors, documenting the power of resistance-defining screens and validating BCR-ABL as a therapeutic target (4-6).

The scope of resistance-conferring mutations varies for each BCR-ABL inhibitor; however, the clinically relevant threonine to isoleucine (T315I) gatekeeper mutant confers resistance to all first and second-generation ABL kinase inhibitors. The recently approved third generation TKI ponatinib (AP24534) represents the first effective clinical option for T315I-positive CML patients. In early clinical trials, all T315I-positive chronic phase CML patients treated with ponatinib achieved a complete hematologic response, and a majority of patients achieved a complete cytogenetic response (7). However, ponatinib can be associated with serious toxicity, and the US FDA label includes a "black box" warning for thrombotic events, which were observed in 8% of patients, as well as rare fatal liver toxicity. Additionally, many patients experience difficulty tolerating ponatinib due to dermatologic toxicity, abdominal pain, and pancreatitis, among other issues. For T315I-positive patients who cannot tolerate ponatinib, alternative therapies are needed.

Prior to the development of ponatinib, a series of small molecules originally developed as Aurora kinase inhibitors were documented to inhibit T315I-BCR-ABL in

preclinical studies, including danusertib (PHA-739358), MK-0457 (VX-680), and XL228 (8-12). In preclinical studies both danusertib and MK-0457 showed promising, broad antitumor activity (13-15). In clinical trials in which solid tumor patients were treated with danusertib or MK-0457, the best clinical outcome observed has typically been disease stabilization (16, 17). However, the clinical experience with these dual ABL/Aurora kinase inhibitors in CML has been more encouraging, with a subset of patients with TKI refractory or T315I-positive CML patients achieving a complete response to XL228, danusertib, or MK-0457 therapy (18-22).

The Aurora kinases are a family of kinases (Aurora A, Aurora B, and Aurora C) involved in cell division. The individual functions of Aurora A and Aurora B in mitosis are generally well understood. Aurora A localizes to the spindle poles and plays a role in centrosome maturation, while Aurora B is involved in the processes of sister chromatid biorientation, chromosome condensation, cytokinesis, and the spindle-assembly checkpoint (23). While the activity of these kinases is critical for the successful completion of mitosis in all proliferating cells, overexpression of the Aurora kinases in various malignancies has been previously documented, suggesting that a therapeutic window may exist (24-26). In a preclinical study supporting the use of danusertib in T315I-positive CML, inhibition of cell proliferation and colony formation in BCR-ABL-negative cell lines as well as normal primary samples was observed (27). While these observations suggest that a therapeutic window for dual ABL/Aurora kinase inhibitor therapy in CML may be narrow, if present at all, the fact that clinical responses have been observed raises the possibility that effective BCR-ABL inhibition is responsible. Whether the cytotoxic effects and clinical benefits observed with dual ABL/Aurora inhibitors is the result of Aurora

kinase inhibition, ABL kinase inhibition, or both remains an important unanswered question which has implications for future drug development efforts in CML.

We therefore sought to better define the role of Aurora kinase inhibition in BCR-ABL-expressing cells treated with dual ABL/Aurora kinase inhibitors. We generated an ABL/Aurora-resistant Ba/F3 cell line through selection in escalating concentrations of the ABL/Aurora inhibitor XL228 and documented the presence of a drug-resistant allele in Aurora B in these cells. To dissect the contribution of BCR-ABL and Aurora kinase inhibition, these cells were engineered to express BCR-ABL. While sensitivity to BCR-ABL inhibition was retained, these cells were highly resistant to ABL/Aurora inhibitors, suggesting that the anti-proliferative and cytotoxic effects of dual ABL/Aurora kinase inhibitors in BCR-ABL-expressing cells are the result of Aurora kinase inhibition. These findings implicate Aurora B as an adjunctive target in CML.

Results

Dual ABL/Aurora Kinase Inhibitors Exhibit a Narrow Therapeutic Window *In Vitro*.

To determine if dual ABL/Aurora kinase inhibitors selectively inhibit the viability of CML cells *in vitro*, the half maximal inhibitory concentration-50 (IC_{50}) of XL228, danusertib, and MK-0457 was determined for parental Ba/F3 (Par-Ba/F3) and Ba/F3 cells expressing native BCR-ABL (p210-Ba/F3) or the drug-resistant T315I allele of BCR-ABL (T315I-Ba/F3). Murine lymphoid Ba/F3 cells are dependent on murine IL3 (mIL3) for survival and proliferation, but can be transformed to cytokine independence by expression of BCR-ABL (28). If the growth-inhibitory effects of dual ABL/Aurora kinase inhibitor treatment result from selective inhibition of BCR-ABL, then the IC_{50} of p210-Ba/F3 and T315I-Ba/F3 cells would be expected to be significantly lower than the IC_{50} of Par-Ba/F3 cells. When Par-Ba/F3, p210-Ba/F3 or T315I-Ba/F3 were treated with XL228, danusertib or MK-0457, the IC_{50} values we obtained for each cell line were nearly identical, suggesting that little to no therapeutic window exists between BCR-ABL and Aurora inhibition with these compounds (**figure 1a** and **supplemental table 1**).

The phosphophorylation status of the adaptor protein Crkl is typically used as a surrogate for BCR-ABL kinase activity in clinical assays; however, Stat5a/b phosphorylation is a more sensitive marker of BCR-ABL kinase inhibition (29-31). In the patient-derived CML cell line K562, the IC_{50} for achieving dephosphorylation of STAT5A/B is nearly identical to the IC_{50} for cell growth when using the BCR-ABL TKIs dasatinib or imatinib (30). The phosphorylation status of Histone H3 can be used as a biomarker of Aurora kinase B activity (32). To determine if the growth-inhibitory effects of XL228,

danusertib or MK-0457 treatment in BCR-ABL-expressing Ba/F3 cells was associated with inhibition of BCR-ABL, Aurora kinases, or both, the phosphorylation status of Stat5a/b and Histone H3 before and after treatment with increasing concentrations of inhibitors was determined by phospho-flow cytometry. Interestingly, treatment of BCR-ABL-expressing Ba/F3 cells with increasing concentrations of XL228, danusertib, or MK-0457 only modestly inhibited Stat5a/b phosphorylation (phospho-Stat5a/b) in p210-Ba/F3 cells relative to dasatinib treatment, and failed to inhibit phospho-Stat5a/b in T315I-Ba/F3 cells (**figure 1b** and **supplemental figure 1a**). In contrast, a concentration-dependent inhibition of Histone H3 phosphorylation (phospho-H3) was observed in all cell lines treated with ABL/Aurora kinase inhibitors, but as expected, not with the BCR-ABL inhibitor dasatinib (**figure 1c** and **supplemental figure 1b**). The consistent concentration-dependent inhibition of phospho-H3 suggests that the growth-inhibitory effects of ABL/Aurora kinase inhibitor treatment in Parental and BCR-ABL-expressing Ba/F3 cells may be a consequence of Aurora kinase inhibition.

XL228-Resistant Parental Ba/F3 Cells Harbor a Mutation in Aurora Kinase B.

To determine if Aurora kinase inhibition is associated with the growth inhibitory effects of dual ABL/Aurora kinase inhibitor treatment in Ba/F3 cells, we employed N-ethyl-N-nitrosourea (ENU) mutagenesis to generate an XL228-resistant Par-Ba/F3 cell line (see **figure 2a** for experimental design). Following ENU treatment, resistant cells were selected for growth in step-wise, increasing concentrations of XL228 until a population of ENU-mutagenized Par-Ba/F3 cells was successfully proliferating at 750nM XL228. Attempts to increase the cellular resistance above 750nM XL228 were unsuccessful.

While XL228 was pursued clinically as a T315I/BCR-ABL inhibitor, it has also been documented to inhibit Aurora A and Aurora B (8, 9). To determine if XL228-resistant, ENU-mutagenized Par-Ba/F3 cells have acquired a drug-resistant mutation in an allele of the Aurora kinases, individual Aurora A (*Aurka*) and Aurora B (*Aurkb*) cDNA molecules were cloned and sequenced from clonal XL228-resistant populations. No point mutations were identified in *Aurka*; however, a T→A transversion was identified at nucleotide 480 in the coding region of subcloned cDNA molecules of *Aurkb*, resulting in an amino acid substitution at codon 161 in the murine Aurkb protein sequence (tyrosine to asparagine; Y161N). The overall frequency of the Y161N allele (0.42) and the chromatogram sequencing trace of the *Aurkb* cDNA total PCR product suggests that the mutation is heterozygous in these cells (**figure 2b**).

To further characterize the impact of the Y161N allele on resistance to ABL/Aurora inhibitors, we assessed the sensitivity of Par-Ba/F3 and Y161N/Par-Ba/F3 cells (both grown in the presence of mIL3) to increasing concentrations of XL228, danusertib, or MK-0457. Y161N/Par-Ba/F3 cells were cross-resistant to all three ABL/Aurora inhibitors (**figure 2c**). To assess if this resistance is mediated biochemically, we evaluated the phospho-H3 positive proportion of cells before and after inhibitor treatment. Phospho-H3 was inhibited in Par-Ba/F3 cells, but was preserved in the resistant Y161N/Par-Ba/F3 cells following XL228, danusertib, or MK-0457 treatment (**figure 2d** and **supplemental figure 2a**). Collectively, these data suggest that the Y161N mutation in Aurkb confers resistance to Aurora inhibitors at the biochemical level and confers cross-resistance to multiple ABL/Aurora kinase inhibitors.

BCR-ABL Expressing Y161N-Ba/F3 Cells are Resistant to ABL/Aurora Inhibitors but Sensitive to BCR-ABL Inhibitors.

To determine the contribution of BCR-ABL inhibition toward the growth-inhibitory effects of dual ABL/Aurora inhibitors, we transformed Y161N/Par-Ba/F3 cells to mIL3 independence with BCR-ABL (Y161N/p210-Ba/F3 and Y161N/T315I-Ba/F3). Y161N/p210-Ba/F3 cells remain sensitive to dasatinib at concentrations previously reported to be effective in mIL3-independent, BCR-ABL-transformed Ba/F3 cells lacking a Y161N mutation (**figure 3a**), and the IC_{50} of phospho-Stat5a/b in Y161N/p210-Ba/F3 cells was nearly identical to the viability IC_{50}, occurring between 1nM and 10nM of dasatinib treatment (**figure 3b**) (2, 33). In contrast, Y161N/p210-Ba/F3 and Y161N/T315I-Ba/F3 cells were profoundly more resistant to all three ABL/Aurora inhibitors relative to p210-Ba/F3 and T315I-Ba/F3 cells (**figure 4a** and **supplemental table 1**), suggesting that the observed activity of these agents in BCR-ABL-expressing cells is mediated through inhibition of Aurkb, and not BCR-ABL.

Phospho-Stat5a/b and phospho-H3 were also monitored to delineate BCR-ABL-specific and Aurora-specific growth inhibitory effects in the dual ABL/Aurora inhibitor treated Y161N/BCR-ABL cell lines. Following XL228 treatment, a dose-dependent dephosphorylation of Stat5a/b was observed in both the Y161N/Par-Ba/F3 and Y161N/BCR-ABL cell lines (**figure 4b**), suggesting that the growth inhibitory effects of XL228 in Y161N/BCR-ABL cells is unrelated to BCR-ABL kinase inhibition. In contrast to XL228, a dose-dependent dephosphorylation of Stat5a/b was observed in danusertib and MK-0457 treated Y161N/p210-Ba/F3 and Y161N/T315I-Ba/F3 cells, but not in Y161N/Par-Ba/F3 cells (**figure 4b**). The inhibition of phospho-Stat5a/b in Y161N/BCR-

ABL expressing cells suggests that, in contrast to BCR-ABL-expressing parental Ba/F3 cells, the observed response to danusertib and MK-0457 treatment in the Y161N genetic background may be partially mediated by BCR-ABL kinase inhibition. Finally, a dose-dependent dephosphorylation of phospho-H3 was observed in all Y161N Ba/F3 cell lines treated with dual ABL/Aurora inhibitors (**figure 4c**). However, the IC_{50} of phospho-H3 dephosphorylation is at least 50-fold higher in the background of the Y161N Aurora B mutation (**supplemental table 2**), suggesting that the Y161N mutation confers biochemical resistance, but is still a primary target of XL228, danusertib, and MK-0457 in this system. We conclude from these observations that Aurkb is the critical kinase target of dual ABL/Aurora inhibitors in BCR-ABL-expressing Ba/F3 cells *in vitro*, and the mechanism of action of these compounds involves inhibition of Aurkb rather than inhibition of BCR-ABL kinase activity.

Aurora B is the Primary Target of Dual ABL/Aurora Inhibitors in Patient-Derived CML Cells.

To determine if Aurora B is the critical target of dual ABL/Aurora inhibitors in patient-derived CML cells, K562 and KU812 cell lines were treated with increasing concentrations of XL228, danusertib, and MK-0457 and the IC_{50} for each inhibitor and cell line was determined. HL60 cells, a BCR-ABL-negative, promyelocytic leukemia cell line, were used as a control to distinguish BCR-ABL specific from non-specific effects of dual ABL/Aurora inhibitor treatment. Interestingly, the two CML cell lines are more sensitive than HL60 cells to XL228 and danusertib, but not to MK-0457 treatment (**figure 5a** and **supplemental table 3**). A dose-dependent dephosphorylation of STAT5A/B was also

observed across increasing concentrations of dual ABL/Aurora inhibitors in K562 and KU812 cells, suggesting that the effects of dual ABL/Aurora inhibitor treatment are partially mediated by BCR-ABL inhibition in CML patient-derived cell lines, which is in contrast to BCR-ABL-expressing Ba/F3 cells (**figure 5b**). Finally, a dose-dependent dephosphorylation of phospho-H3 was observed following XL228 and MK-0457, but not danusertib treatment (**figure 5c**). From this data we can conclude that the effects of XL228 and MK-0457 treatment are mediated through a combination of BCR-ABL and Aurora kinase inhibition in patient-derived CML cells. However, danusertib more selectively inhibits BCR-ABL in patient-derived CML cells where inhibition of phospho-STAT5A/B, but not inhibition of phospho-H3, correlated with inhibition of cell viability in K562 and KU812 cells (**figure 5a, figure 5b,** and **figure 5c**).

Discussion

Until the recent approval of ponatinib, the dual ABL/Aurora inhibitors XL228, danusertib, and MK0457 were some of the only TKIs with documented preclinical and clinical activity against the T315I mutant of BCR-ABL. However, it remained unclear if Aurora kinase inhibition was critical for the observed clinical efficacy of dual ABL/Aurora kinase inhibitors. To delineate the effects of BCR-ABL and Aurora kinase inhibition, we generated a Par-Ba/F3 cell line harboring and mutation in Aurkb (Y161N), which conferred biochemical resistance to XL228, danusertib, and MK-0457. Expression of BCR-ABL in Y161N/Par-Ba/F3 cells conferred dasatinib sensitivity, documenting that BCR-ABL-dependence can be achieved in Y161N/Par-Ba/F3 cells. BCR-ABL-expressing Y161N-Ba/F3 cells are resistant to XL228, danusertib, and MK-0457 relative to BCR-ABL-expressing Par-Ba/F3 cells, suggesting that Aurkb is the critical kinase target of dual ABL/Aurora inhibitors.

A number of Aurora kinase inhibitors are in clinical development; however, there are few reports of on-target resistance to this family of kinase inhibitors. To the best of our knowledge, saturation mutagenesis of Aurora B has not yet been performed, so it is unclear how many point mutations in Aurora B are capable of conferring drug resistance. Girdler et al described several Aurora B kinase domain mutations (human AURKB residues: G160E/V, Y156H, H250Y) capable of conferring resistance to the selective Aurora B inhibitor ZM447439 *in vitro* (34). Failes et al has also described *in vitro* resistance to ZM447439 through a mutation at G160E in AURKB of human leukemia cells (35). Both reports argue that mutations in AURKB can be used to delineate which Aurora kinase is responsible for the cytotoxic effects of selective and dual Aurora inhibitors and the same

point can be made for dual ABL/Aurora kinase inhibitors in the setting of CML. The degree of XL228, danusertib, and MK-0457 resistance conferred by the Y161N mutation clearly designates Aurora B, and not BCR-ABL, as the critical kinase responsible for the inhibition of cell viability observed in Par-Ba/F3 and BCR-ABL-expressing Ba/F3 cells. Because Ba/F3 cells are extensively utilized to assess the activity of BCR-ABL kinase inhibitors, this work demonstrates how, in the setting of multikinase inhibitors, results observed in this system need to be interpreted with caution.

Y161N/BCR-ABL-expressing Ba/F3 cells are resistant to dual ABL/Aurora inhibitor treatment relative to Par-Ba/F3 BCR-ABL-expressing cells (**supplementary table 1**). However, in the Y161N background there is evidence for some BCR-ABL kinase inhibition at higher concentrations of danusertib and MK-0457 where concentration-dependent inhibition of phospho-Stat5a/b was observed (**figure 4b**). Interestingly, the Y161N/p210-Ba/F3 and Y161N/T315I-Ba/F3 cells are slightly more sensitive to danusertib treatment but are equally sensitive to MK-0457 treatment relative to Y161N/Par-Ba/F3 cells. Future experiments will focus on determining if the increased danusertib sensitivity of Y161N/BCR-ABL expressing cells is due to BCR-ABL kinase inhibition or a "synthetic lethal" interaction between BCR-ABL and Aurkb. Although we have shown that BCR-ABL is not the critical kinase target of dual ABL/Aurora inhibitors, the work presented here suggests that inhibition of Aurora B in CML cells may be beneficial therapeutically. It has been suggested that these inhibitors may be used to manage disease in ponatinib-intolerant T315I-positive CML patients prior to a stem cell transplant procedure (22).

Experimental Methods

Cell Lines, Retroviral Transductions, and Cellular Viabilities

Murine Ba/F3, K562, KU812, HL60, and MV4;11 cells were propagated in RPMI 1640 supplemented with 10% fetal bovine serum (FBS; Omega Scientific), 1% L-glutamine, and 1% penicillin/streptomycin (Invitrogen). Par-Ba/F3 and Y161N-Par Ba/F3 cells were supplemented with 2ng/mL of recombinant murine IL-3 (Invitrogen). Par-Ba/F3 and Y161N-Par Ba/F3 cells were engineered to express BCR-ABL through retroviral transduction as described previously (30). Cellular viabilities were also performed as described previously (36). To obtain the IC_{50} for each inhibitor and cell line, the log of the inhibitor concentration versus the normalized viability response was fitted using nonlinear regression with the following parameters: variable slope with the bottom value constrained at zero.

ENU-Mutagenesis of Parental Ba/F3 Cells

ENU-mutagenesis of parental Ba/F3 cells was adapted from Bradeen et al (3). Briefly, 5-6 million parental Ba/F3 cells per $10cm^2$ dish were exposed to 50μg/mL of ENU for 24 hours. Following removal of ENU, parental Ba/F3 cells were allowed to recover for 24 hours. Recovered ENU-mutagenized Ba/F3 cells were subsequently plated in 250nM XL228. Cell growth was observed at 250nM XL228 approximately two weeks later. The drug selection process was repeated in an increasing, stepwise manner of 250nM XL228 increments until ENU-mutagenized Ba/F3 cells were successfully proliferating in 750nM XL228. A limiting

dilution assay was performed to obtain clonal populations of ENU-mutagenized Ba/F3 cells proliferating at 750nM XL228.

Cloning and Sequencing of Murine Aurora Kinase B

To clone individual AurB mRNA molecules for sequencing, total cellular RNA was extracted using TRIzol Reagent following the manufacturers protocol (Invitrogen). SuperScriptII (Invitrogen) was used to generate cDNA from 1μg of extracted total cellular RNA. AurB mRNA was PCR amplified from cDNA using the following primers: F1 (5'-CAAATCGATGAAAGGGACATGGCTGTTGAGGGCGAGC-3') and R1 (5'-AGACTCGAGCTAAAGGGCAGAGGGAGGCAGAACCC-3'). The forward primer was engineered to contain a ClaI restriction enzyme site and the reverse primer was engineered to contain a XhoI restriction enzyme site for ligation into pBlueScript-KS(+) (Stratagene), transformation into Top10 chemically competent *Escherichia coli* (Invitrogen), and blue/white colony selection. To sequence AurB in pBlueScript the M13 forward primer, the M13 reverse primer, and the following primers were used: F1 (5'-TAATCCTGGAATACGCCCCTCG-3') and R2 (5'- CTCCCTGCAGACCTAACAGC-3').

Phospho-Flow Cytometry, Antibodies, and Tyrosine Kinase Inhibitors

Drug exposures and sample preparation for flow cytometry analysis of phospho-protein modulation was performed as described previously(30). Antibodies for phospho-Crkl (Y207; cat. 3181) and phospho-Histone H3 (S10; cat. 9706) were purchased from Cell Signaling Technology. Anti-phospho-Stat5a/b-Alx647 was purchased from BD Biosciences. DMSO stock solutions of dasatinib, danusertib (PHA-739358), and MK-0457 (VX-680) were

generated at UCSF. The use of XL228 was permitted through a materials transfer agreement (MTA) with Excelixis (South San Francisco).

Calculating the IC_{50} of Phospho-Stat5a/b and Phospho-Histone H3 Dephosphorylation

To determine the IC_{50} of phospho-Stat5a/b dephosphorylation, the median fluorescence intensity (MFI) of phospho-Stat5a/b was used to derive the percent inhibition of phospho-Stat5a/b following dual ABL/Aurora inhibitor treatment relative to the DMSO condition. Maximal Stat5a/b inhibition was determined by dasatinib treatment and the percent of maximal phospho-Stat5a/b inhibition for dual ABL/Aurora inhibitor treatment was determined by normalizing each dual ABL/Aurora inhibitor condition to the dasatinib condition in p210-Ba/F3 or Y161N/p210-Ba/F3 cells. The inverse of the percent maximal phospho-Stat5a/b inhibition for each dual ABL/Aurora kinase inhibitor was then plotted against inhibitor concentration to determine the IC_{50} of phospho-Stat5a/b inhibition. The data was fitted in Prism using the nonlinear regression function with the following parameters: variable slope, bottom constrained to zero, top constrained to one. The same process was repeated to determine the IC_{50} of phospho-Histone H3 dephosphorylation except that the percent maximal inhibition was determined by the amount of dephosphorylation observed at the highest concentration of XL228 for each particular experiment and cell line.

References

1. Azam M, Latek RR, Daley GQ. Mechanisms of autoinhibition and STI-571/imatinib resistance revealed by mutagenesis of BCR-ABL. *Cell* 2003 Mar 21; **112**(6)**:** 831-843.

2. Burgess MR, Skaggs BJ, Shah NP, Lee FY, Sawyers CL. Comparative analysis of two clinically active BCR-ABL kinase inhibitors reveals the role of conformation-specific binding in resistance. *Proc Natl Acad Sci U S A* 2005 Mar 1; **102**(9)**:** 3395-3400.

3. Bradeen HA, Eide CA, O'Hare T, Johnson KJ, Willis SG, Lee FY*, et al.* Comparison of imatinib mesylate, dasatinib (BMS-354825), and nilotinib (AMN107) in an N-ethyl-N-nitrosourea (ENU)-based mutagenesis screen: high efficacy of drug combinations. *Blood* 2006 Oct 1; **108**(7)**:** 2332-2338.

4. Shah NP, Nicoll JM, Nagar B, Gorre ME, Paquette RL, Kuriyan J*, et al.* Multiple BCR-ABL kinase domain mutations confer polyclonal resistance to the tyrosine kinase inhibitor imatinib (STI571) in chronic phase and blast crisis chronic myeloid leukemia. *Cancer Cell* 2002 Aug; **2**(2)**:** 117-125.

5. Gorre ME, Mohammed M, Ellwood K, Hsu N, Paquette R, Rao PN*, et al.* Clinical resistance to STI-571 cancer therapy caused by BCR-ABL gene mutation or amplification. *Science* 2001 Aug 3; **293**(5531)**:** 876-880.

6. Talpaz M, Shah NP, Kantarjian H, Donato N, Nicoll J, Paquette R*, et al.* Dasatinib in imatinib-resistant Philadelphia chromosome-positive leukemias. *N Engl J Med* 2006 Jun 15; **354**(24)**:** 2531-2541.

7. Cortes JE, Kantarjian H, Shah NP, Bixby D, Mauro MJ, Flinn I*, et al.* Ponatinib in refractory Philadelphia chromosome-positive leukemias. *N Engl J Med* 2012 Nov 29; **367**(22)**:** 2075-2088.

8. Shah NP, Kasap C, Paquette R, Cortes J, Pinilla J, Talpaz M*, et al.* Targeting Drug-Resistant CML and Ph+-ALL with the Spectrum Selective Protein Kinase Inhibitor XL228. *ASH Annual Meeting Abstracts* 2007 December 12, 2007; **110**(11)**:** 474.

9. Clary DO, Ollmann MM, Detmer SA, Fitzgerald K, Francis R, Kim EO*, et al.* Abstract C192: Characterization of the target profile of XL228, a multi-targeted protein kinase inhibitor in phase 1 clinical development. *Molecular Cancer Therapeutics* 2009 December 10, 2009; **8**(Supplement 1)**:** C192.

10. Carter TA, Wodicka LM, Shah NP, Velasco AM, Fabian MA, Treiber DK*, et al.* Inhibition of drug-resistant mutants of ABL, KIT, and EGF receptor kinases. *Proc Natl Acad Sci U S A* 2005 Aug 2; **102**(31)**:** 11011-11016.

11. Young MA, Shah NP, Chao LH, Seeliger M, Milanov ZV, Biggs WH, 3rd*, et al.* Structure of the kinase domain of an imatinib-resistant Abl mutant in complex with the Aurora kinase inhibitor VX-680. *Cancer Res* 2006 Jan 15; **66**(2)**:** 1007-1014.

12. Modugno M, Casale E, Soncini C, Rosettani P, Colombo R, Lupi R*, et al.* Crystal structure of the T315I Abl mutant in complex with the aurora kinases inhibitor PHA-739358. *Cancer Res* 2007 Sep 1; **67**(17)**:** 7987-7990.

13. Harrington EA, Bebbington D, Moore J, Rasmussen RK, Ajose-Adeogun AO, Nakayama T*, et al.* VX-680, a potent and selective small-molecule inhibitor of the Aurora kinases, suppresses tumor growth in vivo. *Nat Med* 2004 Mar; **10**(3)**:** 262-267.

14. Carpinelli P, Ceruti R, Giorgini ML, Cappella P, Gianellini L, Croci V*, et al.* PHA-739358, a potent inhibitor of Aurora kinases with a selective target inhibition profile relevant to cancer. *Mol Cancer Ther* 2007 Dec; **6**(12 Pt 1)**:** 3158-3168.

15. Fancelli D, Moll J, Varasi M, Bravo R, Artico R, Berta D*, et al.* 1,4,5,6-tetrahydropyrrolo[3,4-c]pyrazoles: identification of a potent Aurora kinase inhibitor with a favorable antitumor kinase inhibition profile. *J Med Chem* 2006 Nov 30; **49**(24)**:** 7247-7251.

16. Steeghs N, Eskens FA, Gelderblom H, Verweij J, Nortier JW, Ouwerkerk J*, et al.* Phase I pharmacokinetic and pharmacodynamic study of the aurora kinase inhibitor danusertib in patients with advanced or metastatic solid tumors. *J Clin Oncol* 2009 Oct 20; **27**(30)**:** 5094-5101.

17. Rubin EH, Shapiro GI, Stein MN, Watson P, Bergstrom D, Xiao A*, et al.* A phase I clinical and pharmacokinetic (PK) trial of the aurora kinase (AK) inhibitor MK-0457 in cancer patients. *ASCO Meeting Abstracts* 2006 June 16, 2006; **24**(18_suppl)**:** 3009.

18. Cortes J, Paquette R, Talpaz M, Pinilla J, Asatiani E, Wetzler M*, et al.* Preliminary Clinical Activity in a Phase I Trial of the BCR-ABL/IGF- 1R/Aurora Kinase Inhibitor XL228 in Patients with Ph++ Leukemias with Either Failure to Multiple TKI Therapies or with T315I Mutation. *ASH Annual Meeting Abstracts* 2008 December 5, 2008; **112**(11)**:** 3232.

19. Paquette RL, Shah NP, Sawyers CL, Martinelli G, John N, Chalukya M*, et al.* PHA-739358, an Aurora Kinase Inhibitor, Induces Clinical Responses in Chronic Myeloid Leukemia Harboring T315I Mutations of BCR-ABL. *ASH Annual Meeting Abstracts* 2007 November 16, 2007; **110**(11)**:** 1030-.

20. Cortes-Franco J, Dombret H, Schafhausen P, Brummendorf TH, Boissel N, Latini F*, et al.* Danusertib Hydrochloride (PHA-739358), a Multi-Kinase Aurora Inhibitor, Elicits Clinical Benefit in Advanced Chronic Myeloid Leukemia and Philadelphia

Chromosome Positive Acute Lymphoblastic Leukemia. *ASH Annual Meeting Abstracts* 2009 November 20, 2009; **114**(22)**:** 864-.

21. Giles FJ, Cortes J, Jones D, Bergstrom D, Kantarjian H, Freedman SJ. MK-0457, a novel kinase inhibitor, is active in patients with chronic myeloid leukemia or acute lymphocytic leukemia with the T315I BCR-ABL mutation. *Blood* 2007 Jan 15; **109**(2)**:** 500-502.

22. Giles FJ, Swords RT, Nagler A, Hochhaus A, Ottmann OG, Rizzieri DA*, et al.* MK-0457, an Aurora kinase and BCR-ABL inhibitor, is active in patients with BCR-ABL T315I leukemia. *Leukemia* 2013 Jan; **27**(1)**:** 113-117.

23. Carmena M, Earnshaw WC. The cellular geography of aurora kinases. *Nat Rev Mol Cell Biol* 2003 Nov; **4**(11)**:** 842-854.

24. Bischoff JR, Anderson L, Zhu Y, Mossie K, Ng L, Souza B*, et al.* A homologue of Drosophila aurora kinase is oncogenic and amplified in human colorectal cancers. *EMBO J* 1998 Jun 1; **17**(11)**:** 3052-3065.

25. Zhou H, Kuang J, Zhong L, Kuo WL, Gray JW, Sahin A*, et al.* Tumour amplified kinase STK15/BTAK induces centrosome amplification, aneuploidy and transformation. *Nat Genet* 1998 Oct; **20**(2)**:** 189-193.

26. Sen S, Zhou H, White RA. A putative serine/threonine kinase encoding gene BTAK on chromosome 20q13 is amplified and overexpressed in human breast cancer cell lines. *Oncogene* 1997 May 8; **14**(18)**:** 2195-2200.

27. Gontarewicz A, Balabanov S, Keller G, Colombo R, Graziano A, Pesenti E*, et al.* Simultaneous targeting of Aurora kinases and Bcr-Abl kinase by the small molecule inhibitor PHA-739358 is effective against imatinib-resistant BCR-ABL mutations including T315I. *Blood* 2008 Apr 15; **111**(8)**:** 4355-4364.

28. Daley GQ, Baltimore D. Transformation of an interleukin 3-dependent hematopoietic cell line by the chronic myelogenous leukemia-specific P210bcr/abl protein. *Proc Natl Acad Sci U S A* 1988 Dec; **85**(23)**:** 9312-9316.

29. ten Hoeve J, Arlinghaus RB, Guo JQ, Heisterkamp N, Groffen J. Tyrosine phosphorylation of CRKL in Philadelphia+ leukemia. *Blood* 1994 Sep 15; **84**(6)**:** 1731-1736.

30. Shah NP, Kasap C, Weier C, Balbas M, Nicoll JM, Bleickardt E*, et al.* Transient potent BCR-ABL inhibition is sufficient to commit chronic myeloid leukemia cells irreversibly to apoptosis. *Cancer Cell* 2008 Dec 9; **14**(6)**:** 485-493.

31. Lipka DB, Wagner MC, Dziadosz M, Schnoder T, Heidel F, Schemionek M*, et al.* Intracellular retention of ABL kinase inhibitors determines commitment to apoptosis in CML cells. *PLoS One*; **7**(7)**:** e40853.

32. Hsu JY, Sun ZW, Li X, Reuben M, Tatchell K, Bishop DK*, et al.* Mitotic phosphorylation of histone H3 is governed by Ipl1/aurora kinase and Glc7/PP1 phosphatase in budding yeast and nematodes. *Cell* 2000 Aug 4; **102**(3)**:** 279-291.

33. Shah NP, Tran C, Lee FY, Chen P, Norris D, Sawyers CL. Overriding imatinib resistance with a novel ABL kinase inhibitor. *Science* 2004 Jul 16; **305**(5682)**:** 399-401.

34. Girdler F, Sessa F, Patercoli S, Villa F, Musacchio A, Taylor S. Molecular basis of drug resistance in aurora kinases. *Chem Biol* 2008 Jun; **15**(6)**:** 552-562.

35. Failes TW, Mitic G, Abdel-Halim H, Po'uha ST, Liu M, Hibbs DE*, et al.* Evolution of resistance to Aurora kinase B inhibitors in leukaemia cells. *PLoS One* 2012; **7**(2)**:** e30734.

36. Smith CC, Wang Q, Chin CS, Salerno S, Damon LE, Levis MJ*, et al.* Validation of ITD mutations in FLT3 as a therapeutic target in human acute myeloid leukaemia. *Nature* May 10; **485**(7397)**:** 260-263.

Figure 1. Parental and BCR-ABL-Expressing Murine Ba/F3 Cells Respond Similarly to Dual ABL/Aurora Inhibitor Treatment.

A. IC_{50} of Par-Ba/F3, p210-Ba/F3 and T315I-Ba/F3 cells following a 48-hour treatment with increasing concentrations of XL228, danusertib, and MK-0457. Data represents the average ± standard deviation of three biological replicates (n=3).

B. Stat5a/B phosphorylation in Par-Ba/F3, p210-Ba/F3, and T315I-Ba/F3 cells following a 90-minute treatment with increasing concentrations of XL228, danusertib, and MK-0457. The median fluorescence intensity (MFI) Stat5a/b phosphorylation was determined by phospho-flow cytometry, was converted to percent maximal inhibition relative to dasatinib treatment, and is plotted against inhibitor concentration. (See experimental methods.)

C. Histone H3 phosphorylation in Par-Ba/F3, p210-Ba/F3, and T315I-Ba/F3 cells following a 90-minute treatment with increasing concentrations of XL228, danusertib, and MK-0457. Histone H3 phosphorylation was determined by phospho-flow cytometry, was converted to percent maximal inhibition relative to 1μM XL228 treatment, and is plotted against inhibitor concentration as in (B). (See experimental methods.)

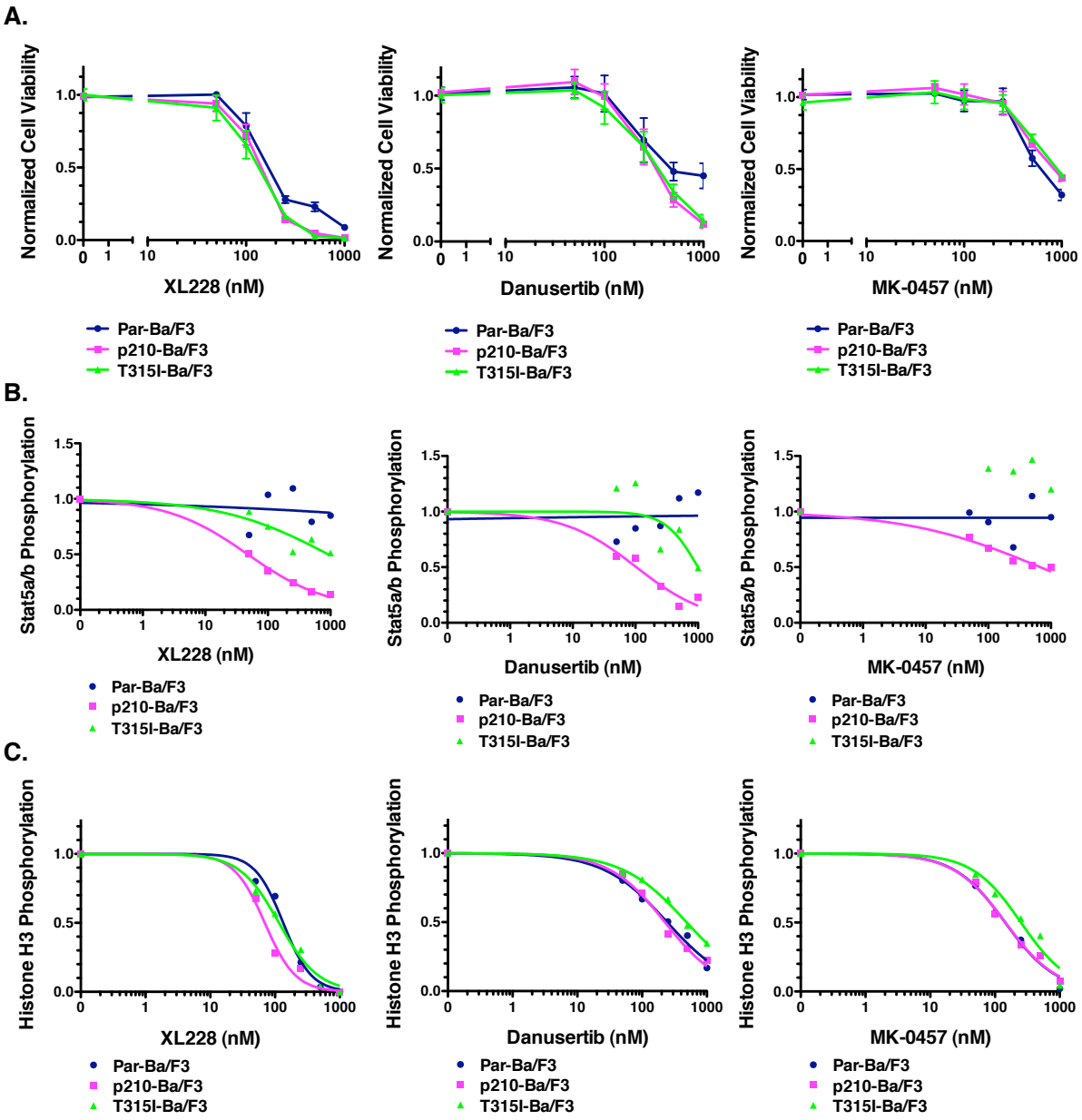
A.
Normalized Cell Viability
1.0
0.5
0.0
0 1 10 100 1000
XL228 (nM)
Danusertib (nM)
MK-0457 (nM)
Par-Ba/F3
p210-Ba/F3
T315I-Ba/F3
B.
Stat5a/b Phosphorylation
1.5
1.0
0.5
0.0
C.
Histone H3 Phosphorylation

Figure 2. Y161N/Par-Ba/F3 Cells Exhibit Biochemical Cross-Resistance to XL228, Danusertib, and MK-0457 Treatment.

A. Experimental design for the ENU-mutagenesis and selection of 750nM XL228-resistant Par-Ba/F3 cells.

B. Sequencing chromatogram of the total PCR product from *AurB* mRNA isolated from Par-Ba/F3 and 750nM XL228-resistant Ba/F3 cells. Arrow designates the T→A transversion at nucleotide 480 in the coding region of *AurB*.

C. IC_{50} of Par-Ba/F3 and Y161N/Par-Ba/F3 cells following a 48-hour treatment with increasing concentrations of XL2228, danusertib, or MK-0457. Data represents the average ± standard deviation of three biological replicates (n=3).

D. Histone H3 phosphorylation in Par-Ba/F3 and Y161N/Par-Ba/F3 cells following a 90-minute treatment with 500nM XL228, 1μM danusertib, or 1μM MK-0457.

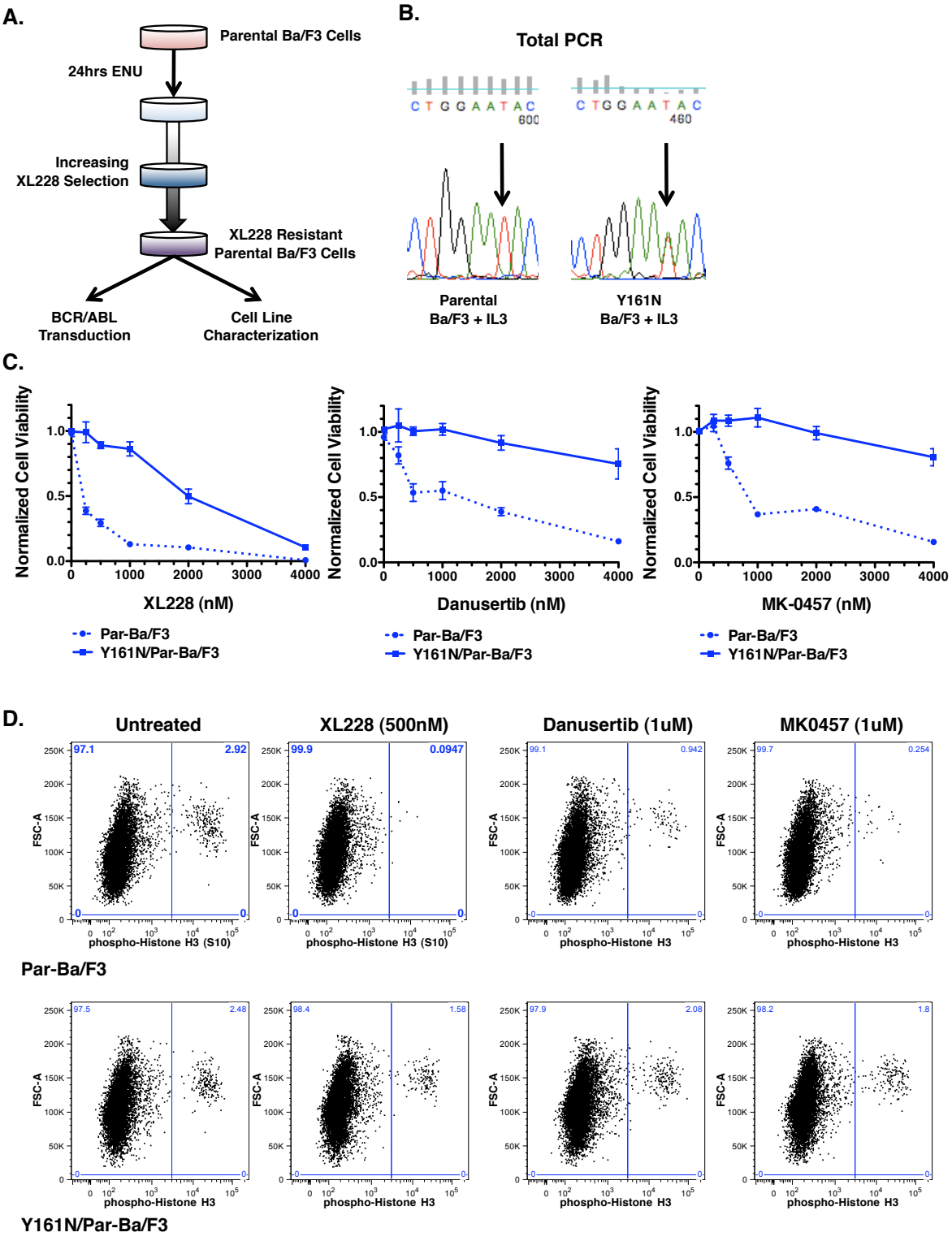
A.
Parental Ba/F3 Cells
24hrs ENU
Increasing
XL228 Selection
XL228 Resistant
Parental Ba/F3 Cells
BCR/ABL
Transduction
Cell Line
Characterization
B.
Total PCR
C T G G A A T A C
600
C T G G A A T A C
460
Parental
Ba/F3 + IL3
Y161N
Ba/F3 + IL3
C.
Normalized Cell Viability
XL228 (nM)
Danusertib (nM)
MK-0457 (nM)
Par-Ba/F3
Y161N/Par-Ba/F3
D.
Untreated
XL228 (500nM)
Danusertib (1uM)
MK0457 (1uM)
FSC-A
phospho-Histone H3 (S10)
phospho-Histone H3
97.1
2.92
99.9
0.0947
99.1
0.942
99.7
0.254
Par-Ba/F3
97.5
2.48
98.4
1.58
97.9
2.08
98.2
1.8
Y161N/Par-Ba/F3

Figure 3. BCR-ABL-Expressing Y161N Ba/F3 Cells Exhibit Dasatinib Sensitivity.

A. IC_{50} of Y161N/Par-Ba/F3, Y161N/p210-Ba/F3, and Y161N/T315I-Ba/F3 cells following a 48-hour treatment with increasing concentrations of dasatinib. Data represents the average ± standard deviation of three biological replicates (n=3).

B. Stat5a/b phosphorylation in Y161N/Par-Ba/F3, Y161N/p210-Ba/F3 and Y161N/T315I-Ba/F3 cells following a 90-minute treatment with increasing concentrations of dasatinib.

A.

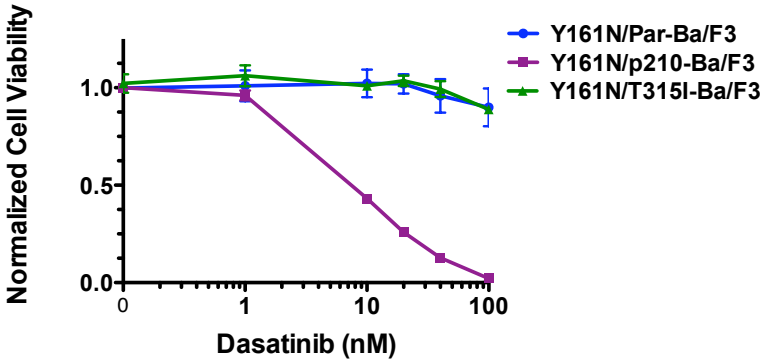
Normalized Cell Viability
1.0
0.5
0.0
0
1
10
100
Dasatinib (nM)
Y161N/Par-Ba/F3
Y161N/p210-Ba/F3
Y161N/T315I-Ba/F3

B.

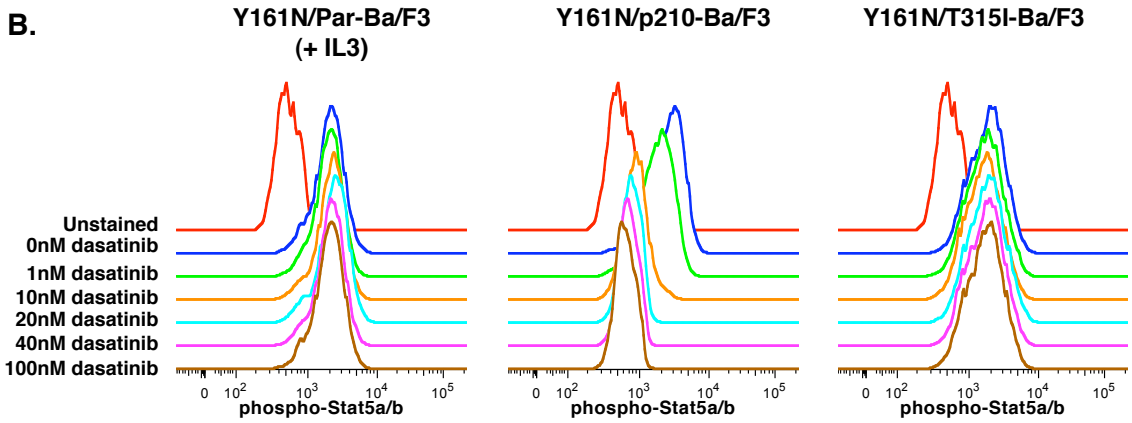
Y161N/Par-Ba/F3
(+ IL3)
Y161N/p210-Ba/F3
Y161N/T315I-Ba/F3
Unstained
0nM dasatinib
1nM dasatinib
10nM dasatinib
20nM dasatinib
40nM dasatinib
100nM dasatinib
0
10^2
10^3
10^4
10^5
phospho-Stat5a/b

Figure 4. Y161N/BCR-ABL Cells are Resistant to Dual ABL/Aurora Kinase Inhibitors.

A. IC_{50} of Y161N/Par-Ba/F3, Y161N/p210-Ba/F3, and Y161N/T315I-Ba/F3 cells following a 48-hour treatment with increasing concentrations of XL228, danusertib, or MK-0457. Data represents the average ± standard deviation of three biological replicates (n=3).

B. Stat5a/b phosphorylation in Y161N/Par-Ba/F3, Y161N/p210-Ba/F3 and Y161N/T315I-Ba/F3 cells following a 90-minute treatment with increasing concentrations of XL228, danusertib, or MK-0457. Data is represented as in figure 1B.

C. Histone H3 phosphorylation in Y161N/Par-Ba/F3, Y161N/p210-Ba/F3 and Y161N/T315I-Ba/F3 cells following a 90-minute treatment with increasing concentrations of XL228, danusertib, or MK-0457. Data is represented as in figure 1C.

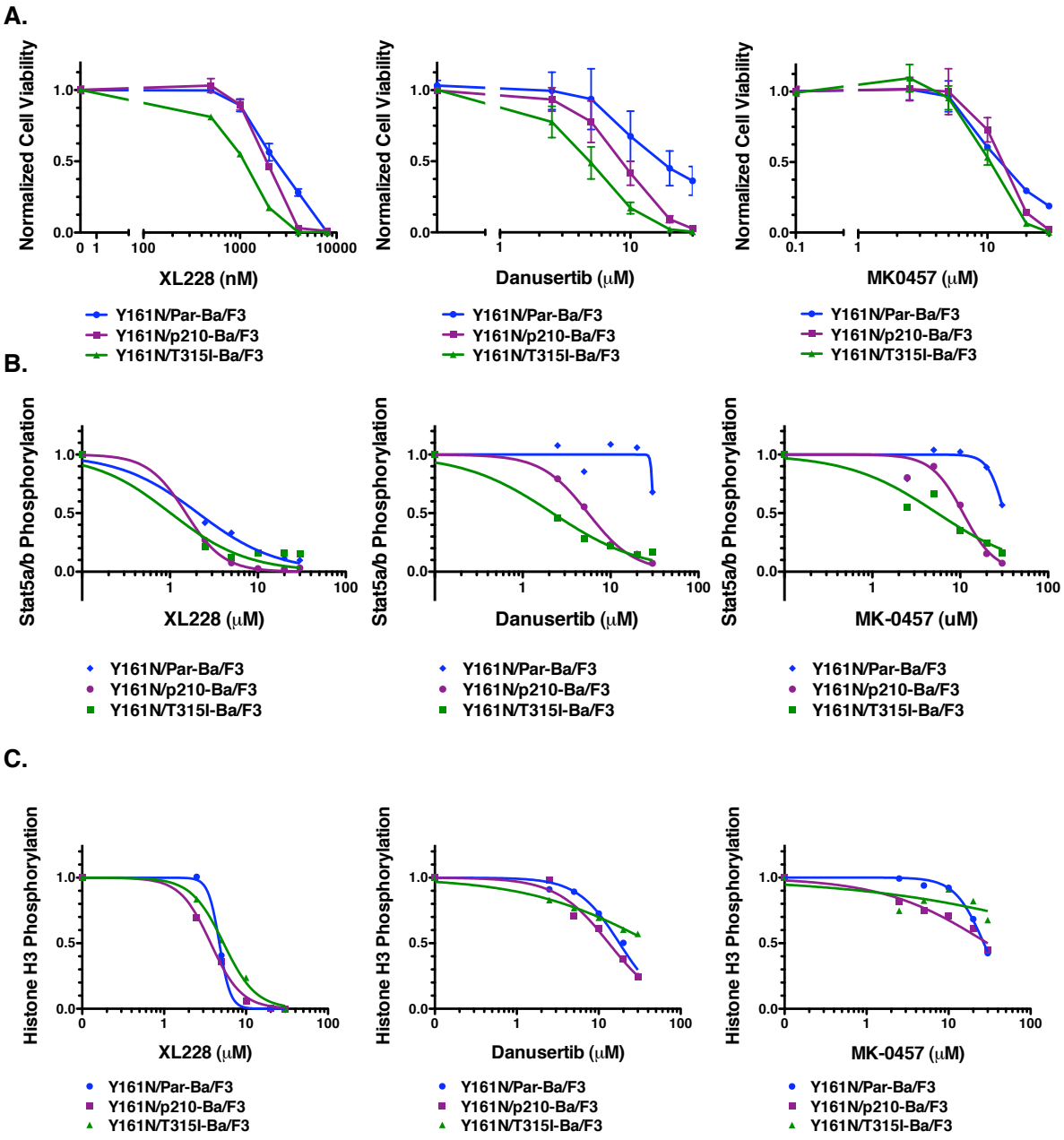
A.
Normalized Cell Viability
XL228 (nM)
Danusertib (μM)
MK0457 (μM)
Y161N/Par-Ba/F3
Y161N/p210-Ba/F3
Y161N/T315I-Ba/F3
B.
Stat5a/b Phosphorylation
XL228 (μM)
Danusertib (μM)
MK-0457 (uM)
Y161N/Par-Ba/F3
Y161N/p210-Ba/F3
Y161N/T315I-Ba/F3
C.
Histone H3 Phosphorylation
XL228 (μM)
Danusertib (μM)
MK-0457 (μM)
Y161N/Par-Ba/F3
Y161N/p210-Ba/F3
Y161N/T315I-Ba/F3

Figure 5. The Effects of Dual ABL/Aurora Inhibitor Treatment are Mediated by Both BCR-ABL and Aurora Kinase Inhibition in CML Patient-Derived Cell Lines.

A. IC_{50} of K562, KU812, and HL60 cells following a 48-hour treatment with increasing concentrations of XL228, danusertib, or MK-0457. Data represents the average ± standard deviation of three biological replicates (n=3).

B. STAT5A/B phosphorylation in K562 and KU812 cells following a 90-minute treatment with increasing concentrations of XL228, danusertib, or MK-0457. Data is represented as in figure 1B.

C. Histone H3 phosphorylation in K562, KU812, and HL60 cells following a 90-minute treatment with increasing concentrations of XL228, danusertib, or MK-0457. Data is represented as in figure 1C.

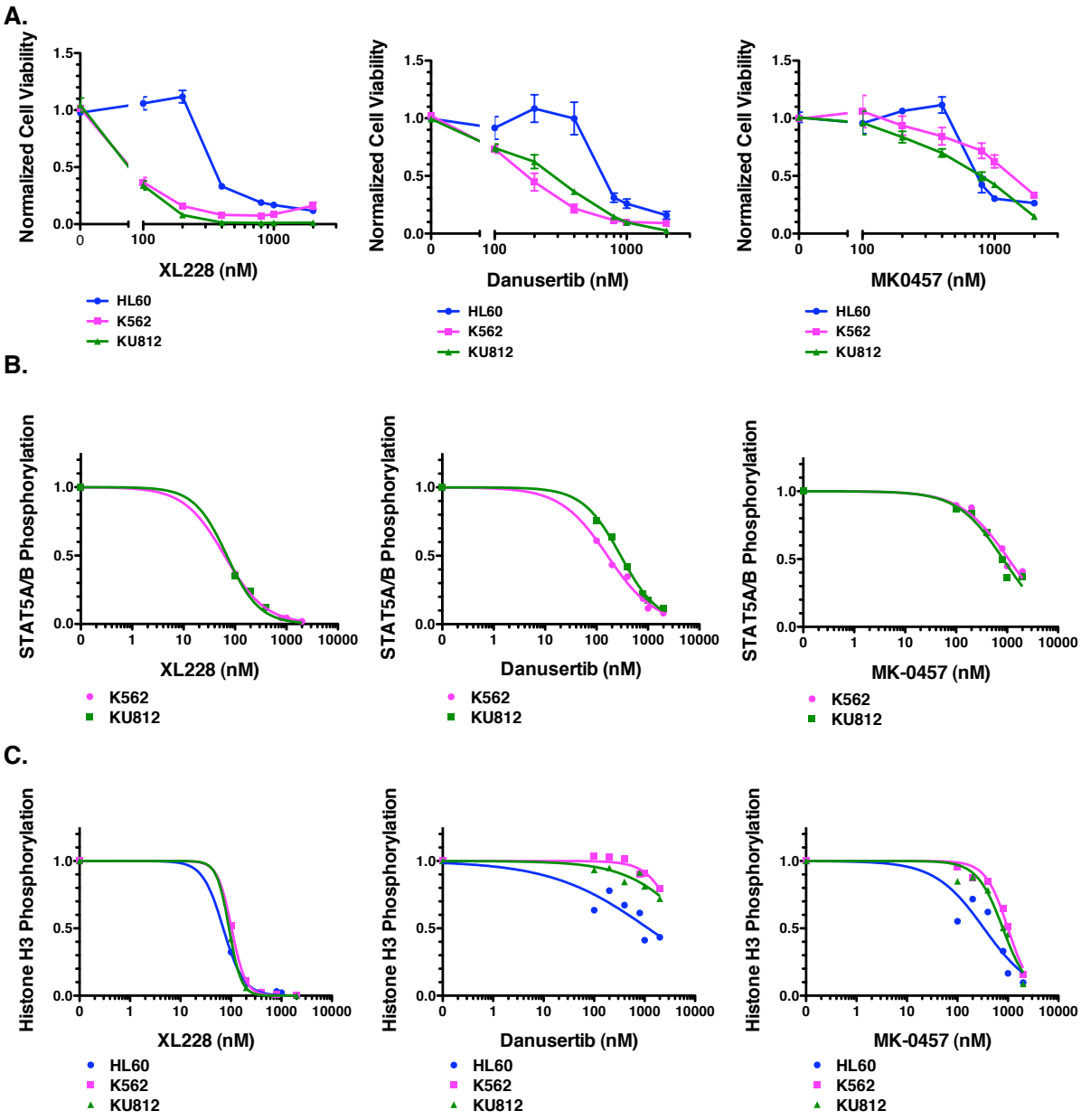
A.
Normalized Cell Viability
XL228 (nM)
Danusertib (nM)
MK0457 (nM)
HL60
K562
KU812
B.
STAT5A/B Phosphorylation
XL228 (nM)
Danusertib (nM)
MK-0457 (nM)
K562
KU812
C.
Histone H3 Phosphorylation
XL228 (nM)
Danusertib (nM)
MK-0457 (nM)
HL60
K562
KU812

Figure S1. **Dual ABL/Aurora Inhibitor Treatment Fails to Effectively Inhibit BCR-ABL Kinase Activity.**

A. Stat5a/B phosphorylation in Par-Ba/F3, p210-Ba/F3, and T315I-Ba/F3 cells following a 90-minute treatment with 0.2% DMSO, 100nM dasatinib, 500nM XL228, 1μM danusertib, and 1μM MK-0457.

B. Histone H3 phosphorylation in Par-Ba/F3, p210-Ba/F3, and T315I-Ba/F3 cells following a 90-minute treatment with 0.2% DMSO or 100nM dasatinib.

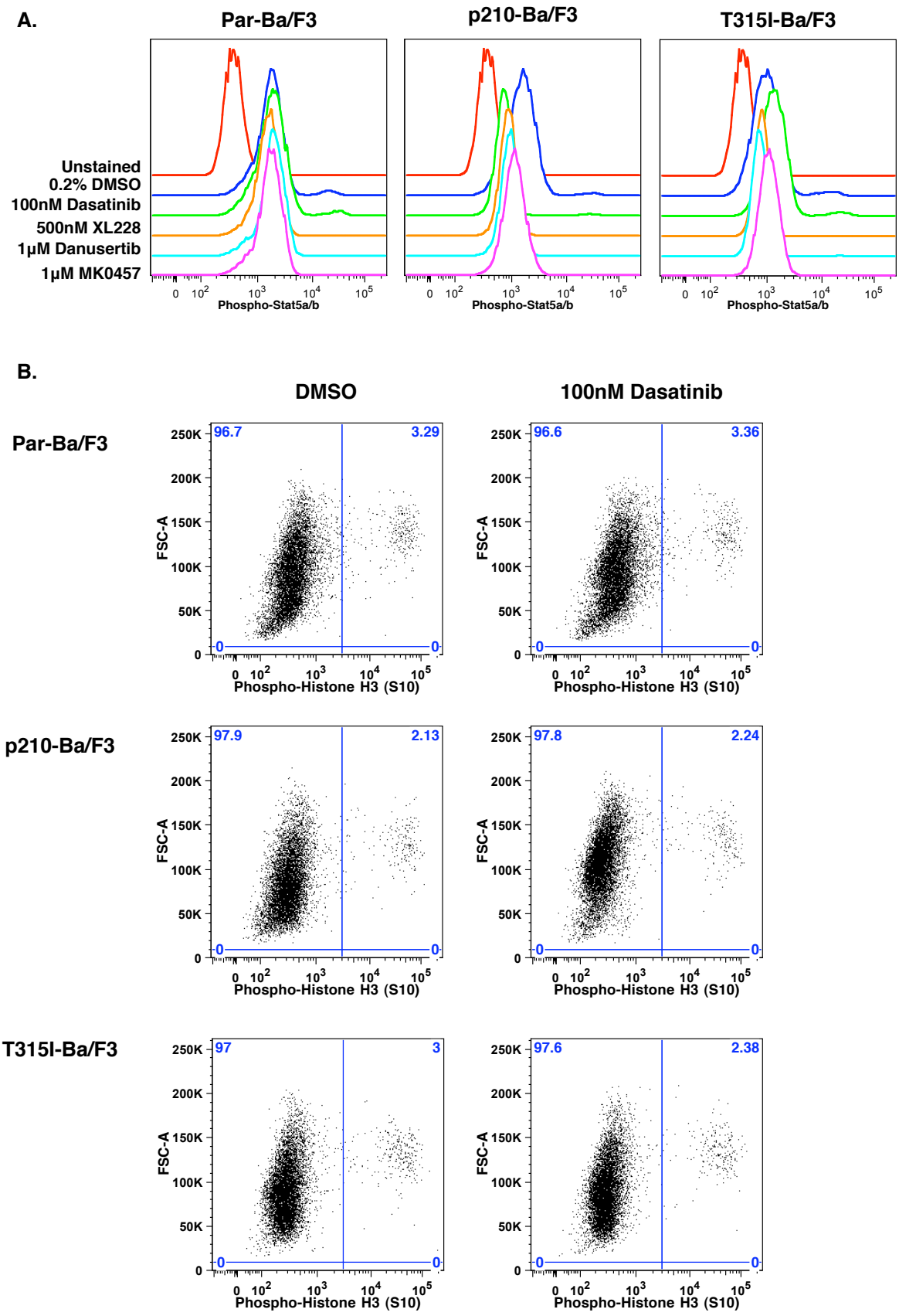
A.
Par-Ba/F3
p210-Ba/F3
T315I-Ba/F3
Unstained
0.2% DMSO
100nM Dasatinib
500nM XL228
1μM Danusertib
1μM MK0457
Phospho-Stat5a/b
B.
DMSO
100nM Dasatinib
Par-Ba/F3
p210-Ba/F3
T315I-Ba/F3
96.7
3.29
96.6
3.36
97.9
2.13
97.8
2.24
97
3
97.6
2.38
FSC-A
Phospho-Histone H3 (S10)

Figure S2. **Y161N/Par-Ba/F3 Cells Exhibit Biochemical Resistance to Dual ABL/Aurora Inhibitor Treatment.**

A. Histone H3 phosphorylation in Par-Ba/F3 and Y161N/Par-Ba/F3 cells following a 90-minute treatment with increasing concentrations of XL228, danusertib, or MK-0457. Phospho-Histone H3 phosphorylation was plotted against increasing concentrations of inhibitor and the data was fitted in Prism. (See Experimental Methods.)

A.

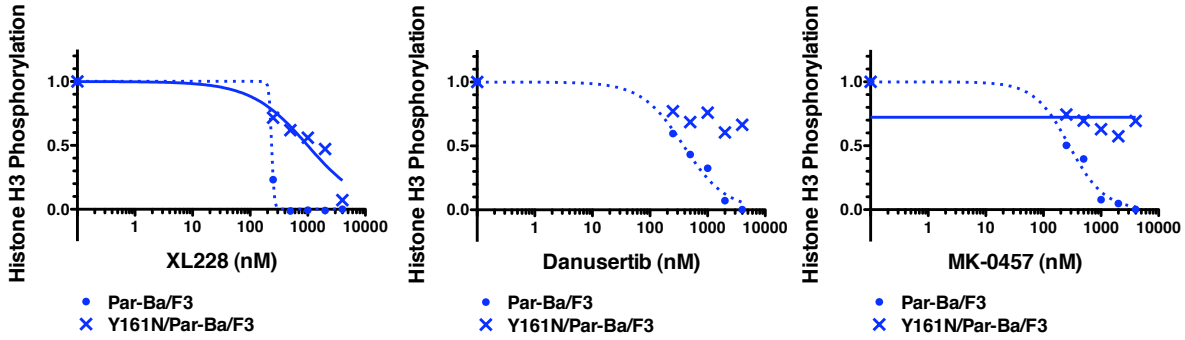
Histone H3 Phosphorylation
1.0
0.5
0.0
1
10
100
1000
10000
XL228 (nM)
Par-Ba/F3
Y161N/Par-Ba/F3
Histone H3 Phosphorylation
Danusertib (nM)
Par-Ba/F3
Y161N/Par-Ba/F3
Histone H3 Phosphorylation
MK-0457 (nM)
Par-Ba/F3
Y161N/Par-Ba/F3

Table S1. Y161N/BCR-ABL Cells are Resistant to Dual ABL/Aurora Inhibitor Treatment.

Average IC_{50} values of Par-Ba/F3 (+IL3), p210-Ba/F3, T315I-Ba/F3, Y161N/Par-Ba/F3 (+IL3), Y161N/p210-Ba/F3, and Y161N/T315I-Ba/F3 cells treated with XL228, Danusertib, or MK-0457. Data represents the average (Avg.) ± standard deviation (SD) of three biological replicates (n=3).

	XL228 (μM)		Danusertib (μM)		MK-0457 (μM)	
	Avg. IC50	SD	Avg. IC50	SD	Avg. IC50	SD
Par-Ba/F3 + IL3	0.179	0.023	0.536	0.144	0.630	0.050
p210-Ba/F3	0.140	0.013	0.312	0.054	0.780	0.026
T315I-Ba/F3	0.130	0.015	0.338	0.050	0.891	0.062
Y161N/Par-Ba/F3 + IL3	2.334	0.214	16.467	5.223	12.807	0.104
Y161N/p210-Ba/F3	1.882	0.059	8.413	1.519	12.627	0.927
Y161N/T315I-Ba/F3	1.059	0.037	4.760	1.132	10.086	0.633

Table S2. Y161N Aurora B Confers Biochemical Resistance to Dual ABL/Aurora Inhibitor treatment in Y161N/Par-Ba/F3 and Y161N/BCR-ABL Cell Lines.

IC_{50} value of phospho-Histone H3 dephosphorylation in Parental Ba/F3, p210-Ba/F3, T315I-Ba/F3, Y161N/Par-Ba/F3, Y161N/p210-Ba/F3, and Y161N/T315I-Ba/F3 cells treated with XL228, Danusertib, or MK-0457.

Phospho-H3 IC_{50}	XL228 (μM)	Danusertib (μM)	MK-0457 (μM)
Par-Ba/F3 + IL3	0.133	0.244	0.144
p210-Ba/F3	0.069	0.225	0.145
T315I-Ba/F3	0.115	0.485	0.252
Y161N/Par-Ba/F3 + IL3	4.726	17.940	26.870
Y161N/p210-Ba/F3	3.707	13.310	29.920
Y161N/T315I-Ba/F3	5.318	> 30	> 30

Table S3. Patient-Derived CML Cell Lines Exhibit Increased Sensitivity to XL228 and Danusertib, but not MK-0457 Treatment.

Average IC_{50} values of HL60, K562 and KU812 cells treated with XL228, Danusertib, or MK0457. Data represents the average (Avg.) ± standard deviation (SD) of three biological replicates (n=3).

	XL228 (nM)		Danusertib (nM)		MK-0457 (nM)	
	Avg. IC50	SD	Avg. IC50	SD	Avg. IC50	SD
HL60	371.8	20.4	706.5	24.3	784.9	50.0
K562	36.3	11.1	176.5	24.8	1315.0	173.9
KU812	74.6	3.0	266.6	19.5	742.4	78.8

Chapter 5

Conclusions

Conclusions

The work presented in this dissertation has focused on identifying and understanding the important aspects of BCR-ABL-mediated oncogene addiction in chronic myeloid leukemia (CML). The success of tyrosine kinase inhibitor (TKI) therapy in the treatment of CML represents the first clinical documentation of oncogene addiction and has paved the way for the development of other clinically active kinase inhibitors. This includes kinase inhibitors targeting EGFR in NSCLC, FLT3 in AML, and BRAF-V600E in malignant melanoma. Each of these kinase inhibitors are active in their respective diseases; however, the number of durable responses are infrequent in number relative to the extent of durable responses achieved in the chronic phase CML patient population. From these observations, we propose that BCR-ABL establishes a unique state of addiction that renders CML cells exquisitely sensitive to inhibition of BCR-ABL kinase activity. We also propose that investigating the mechanism of action of TKI therapy in CML cells will provide further insight into the intricacies of BCR-ABL-mediated oncogene addiction. Here, we provide evidence for BCR-ABL-dependent negative feedback as being the biologic process responsible for this unique state of addiction in CML (chapter 2).

One of the major conclusions from this dissertation is that CML cell survival is dependent on BCR-ABL-mediated activation of the RAS/MAPK, STAT5, and S6 signaling pathways. This conclusion is supported by previous work where it was documented that dominant negative alleles of RAS, STAT5, and PI3K can induce apoptosis in CML cells (1). An unbiased, quantitative phosphoproteomic analysis of phosphotyrosine signaling in CML cells before and after transient dasatinib treatment revealed durable dephosphorylation of tyrosines on MAPK1/2 and STAT5A/B, among others (chapter 2). Western immunoblot

analysis confirmed these durable dephosphorylation events and also revealed durable dephosphorylation of serine residues in S6 following transient dasatinib treatment.

To confirm the importance of these signaling changes, the human erythroleukemia cell line TF1 was engineered to express BCR-ABL. TF1/BCR-ABL cells exhibited dependency on BCR-ABL kinase activity and underwent a large degree of apoptosis following BCR-ABL TKI treatment (chapter 2). Importantly, the increased TKI sensitivity of TF1/BCR-ABL cells relative to TF1/puro cells exemplifies oncogene addiction. TF1/BCR-ABL cells exhibit constitutive activation of the RAS/MAPK, STAT5, and S6 signaling pathways, which suggests that these pathways are critical for BCR-ABL-mediated oncogene addiction. Finally, reactivation of these signaling pathways partially rescued CML cells from TKI mediated apoptosis. This was observed when TF1/BCR-ABL cells were treated with a TKI in the presence of hGM-CSF. This effect was replicated in K562 cells treated with a TKI in the presence of hEPO (chapter 2). Restoration of these signaling pathways and rescue from TKI-mediated apoptosis was also observed in high-dose pulse treated K562 cells following a delayed medium wash (chapter 3). The work presented here validates the importance of these signaling pathways in BCR-ABL-mediated oncogene addiction and CML cell survival.

In investigating the importance of the RAS/MAPK, STAT5, and S6 signaling pathways in CML cells, we have found that BCR-ABL-dependent negative feedback determines growth factor responsiveness as well as the timing of pathway reactivation following BCR-ABL kinase inhibition (chapter 2). We have shown that BCR-ABL-dependent negative feedback persists for an extended period of time following the initiation of dasatinib or imatinib treatment and provide evidence that CML cells commit to apoptosis

prior to the complete restoration of growth factor-receptor (GF-R) signaling (chapter 2). This is in contrast to BRAF-V600E-dependent melanoma, colorectal, and thyroid cancer cell lines and patient samples where negative feedback is rapidly attenuated and GF-R signaling effectively rescues these cells from BRAF inhibitor-mediated apoptosis (2-6). Future work will focus on determining the critical molecular entities responsible for negative feedback in patient-derived CML cell lines *in vitro* and in CML patient samples *ex vivo*.

A portion of this dissertation focused on identifying the mechanism responsible for apoptosis in high dose pulse (HDP) treated CML cells. This work was initiated by the observation that dasatinib exhibits a relatively short-half life *in vivo* as well as the observation that transient dasatinib treatment *in vitro* commits CML cells to apoptosis (7-11). We provide experimental evidence for the intracellular accumulation of TKIs in CML cells during *in vitro* HDP treatment (chapter 3). During HDP treatment, intracellular accumulation of TKIs promotes extended BCR-ABL kinase inhibition following drug washout as monitored by STAT5A/B phosphorylation. The presence of effluxed extracellular inhibitor in the post-HDP medium was confirmed by LC-MS/MS analysis and BCR-ABL-expressing Ba/F3 viability assays. Interestingly, the intracellular accumulation of TKIs is not limited to BCR-ABL inhibitors, suggesting that this is a broader pharmacokinetic property of small molecules (7, 12). Future directions will focus on identifying the molecular mechanism responsible for the intracellular accumulation of BCR-ABL kinase inhibitors. These observations have implications for future drug development efforts. Optimization of a compound with a reduced half-life, but high-intracellular retention, may help avoid unwanted non-specific cytotoxicities.

Resistance to TKI therapy in CML has been thoroughly investigated, but continues to be a clinically relevant issue. The dual ABL/Aurora kinase inhibitors XL228, danusertib (PHA-739358) and MK-0457 (VX-680) were the first to exhibit clinical activity against the T315I-mutation in BCR-ABL; however, the role of Aurora kinase inhibition in the efficacy of these compounds remained unclear (13-19). Therefore, we sought to investigate the mechanism of action of dual ABL/Aurora kinase inhibitors in CML cells. We have generated a murine Ba/F3 cell line harboring a mutation in Aurora B (Y161N) that confers biochemical cross-resistence to all three dual ABL/Aurora kinase inhibitors (chapter 4). Expression of BCR-ABL in Aurora B mutant Ba/F3 cells conferred dasatinib sensitivity, but failed to confer sensitivity to dual ABL/Aurora kinase inhibitor treatment. From these observations, we have concluded that Aurora B is the critical kinase target of XL228, danusertib, and MK-0457 and potentially represents an adjunctive therapeutic target in CML.

In summary, the work presented in this dissertation has focused on understanding BCR-ABL-mediated oncogene addiction through the use of tyrosine kinase inhibitors. We provide evidence that BCR-ABL-dependent negative feedback is a critical aspect of oncogene addiction in CML and is potentially responsible for what differentiates the clinical efficacy of TKI therapy in CML from the clinical efficacy of other kinase inhibitor therapies. Potentiating negative feedback in less responsive kinase-addicted malignancies with the intent of increasing the cells' state of oncogene dependence is an additional hypothesis derived from this work. Future directions could include negative feedback potentiation in BRAF-V600E-dependent or EGFR-dependent cell lines and patient samples *in vitro*.

References

1. Sonoyama J, Matsumura I, Ezoe S, Satoh Y, Zhang X, Kataoka Y*, et al.* Functional cooperation among Ras, STAT5, and phosphatidylinositol 3-kinase is required for full oncogenic activities of BCR/ABL in K562 cells. *J Biol Chem* 2002 Mar 8; **277**(10)**:** 8076-8082.

2. Lito P, Pratilas CA, Joseph EW, Tadi M, Halilovic E, Zubrowski M*, et al.* Relief of profound feedback inhibition of mitogenic signaling by RAF inhibitors attenuates their activity in BRAFV600E melanomas. *Cancer Cell* Nov 13; **22**(5)**:** 668-682.

3. Montero-Conde C, Ruiz-Llorente S, Dominguez JM, Knauf JA, Viale A, Sherman EJ*, et al.* Relief of feedback inhibition of HER3 transcription by RAF and MEK inhibitors attenuates their antitumor effects in BRAF-mutant thyroid carcinomas. *Cancer Discov* 2013 May; **3**(5)**:** 520-533.

4. Prahallad A, Sun C, Huang S, Di Nicolantonio F, Salazar R, Zecchin D*, et al.* Unresponsiveness of colon cancer to BRAF(V600E) inhibition through feedback activation of EGFR. *Nature* Mar 1; **483**(7387)**:** 100-103.

5. Wilson TR, Fridlyand J, Yan Y, Penuel E, Burton L, Chan E*, et al.* Widespread potential for growth-factor-driven resistance to anticancer kinase inhibitors. *Nature* Jul 26; **487**(7408)**:** 505-509.

6. Straussman R, Morikawa T, Shee K, Barzily-Rokni M, Qian ZR, Du J*, et al.* Tumour micro-environment elicits innate resistance to RAF inhibitors through HGF secretion. *Nature* Jul 26; **487**(7408)**:** 500-504.

7. Shah NP, Kasap C, Weier C, Balbas M, Nicoll JM, Bleickardt E*, et al.* Transient potent BCR-ABL inhibition is sufficient to commit chronic myeloid leukemia cells irreversibly to apoptosis. *Cancer Cell* 2008 Dec 9; **14**(6)**:** 485-493.

8. Hiwase DK, White DL, Powell JA, Saunders VA, Zrim SA, Frede AK*, et al.* Blocking cytokine signaling along with intense Bcr-Abl kinase inhibition induces apoptosis in primary CML progenitors. *Leukemia* Apr; **24**(4)**:** 771-778.

9. Snead JL, O'Hare T, Adrian LT, Eide CA, Lange T, Druker BJ*, et al.* Acute dasatinib exposure commits Bcr-Abl-dependent cells to apoptosis. *Blood* 2009 Oct 15; **114**(16)**:** 3459-3463.

10. Steinberg M. Dasatinib: a tyrosine kinase inhibitor for the treatment of chronic myelogenous leukemia and philadelphia chromosome-positive acute lymphoblastic leukemia. *Clin Ther* 2007 Nov; **29**(11)**:** 2289-2308.

11. Christopher LJ, Cui D, Wu C, Luo R, Manning JA, Bonacorsi SJ*, et al.* Metabolism and disposition of dasatinib after oral administration to humans. *Drug Metab Dispos* 2008 Jul; **36**(7)**:** 1357-1364.

12. Gunawardane RN, Nepomuceno RR, Rooks AM, Hunt JP, Ricono JM, Belli B*, et al.* Transient exposure to quizartinib mediates sustained inhibition of FLT3 signaling while specifically inducing apoptosis in FLT3-activated leukemia cells. *Mol Cancer Ther* 2013 Apr; **12**(4)**:** 438-447.

13. Shah NP, Kasap C, Paquette R, Cortes J, Pinilla J, Talpaz M*, et al.* Targeting Drug-Resistant CML and Ph+-ALL with the Spectrum Selective Protein Kinase Inhibitor XL228. *ASH Annual Meeting Abstracts* 2007 December 12, 2007; **110**(11)**:** 474.

14. Cortes J, Paquette R, Talpaz M, Pinilla J, Asatiani E, Wetzler M*, et al.* Preliminary Clinical Activity in a Phase I Trial of the BCR-ABL/IGF- 1R/Aurora Kinase Inhibitor XL228 in Patients with Ph++ Leukemias with Either Failure to Multiple TKI Therapies or with T315I Mutation. *ASH Annual Meeting Abstracts* 2008 December 5, 2008; **112**(11)**:** 3232.

15. Clary DO, Ollmann MM, Detmer SA, Fitzgerald K, Francis R, Kim EO*, et al.* Abstract C192: Characterization of the target profile of XL228, a multi-targeted protein kinase inhibitor in phase 1 clinical development. *Molecular Cancer Therapeutics* 2009 December 10, 2009; **8**(Supplement 1)**:** C192.

16. Paquette RL, Shah NP, Sawyers CL, Martinelli G, John N, Chalukya M*, et al.* PHA-739358, an Aurora Kinase Inhibitor, Induces Clinical Responses in Chronic Myeloid Leukemia Harboring T315I Mutations of BCR-ABL. *ASH Annual Meeting Abstracts* 2007 November 16, 2007; **110**(11)**:** 1030-.

17. Cortes-Franco J, Dombret H, Schafhausen P, Brummendorf TH, Boissel N, Latini F*, et al.* Danusertib Hydrochloride (PHA-739358), a Multi-Kinase Aurora Inhibitor, Elicits Clinical Benefit in Advanced Chronic Myeloid Leukemia and Philadelphia Chromosome Positive Acute Lymphoblastic Leukemia. *ASH Annual Meeting Abstracts* 2009 November 20, 2009; **114**(22)**:** 864-.

18. Giles FJ, Cortes J, Jones D, Bergstrom D, Kantarjian H, Freedman SJ. MK-0457, a novel kinase inhibitor, is active in patients with chronic myeloid leukemia or acute lymphocytic leukemia with the T315I BCR-ABL mutation. *Blood* 2007 Jan 15; **109**(2)**:** 500-502.

19. Carter TA, Wodicka LM, Shah NP, Velasco AM, Fabian MA, Treiber DK*, et al.* Inhibition of drug-resistant mutants of ABL, KIT, and EGF receptor kinases. *Proc Natl Acad Sci U S A* 2005 Aug 2; **102**(31)**:** 11011-11016.

Publishing Agreement

It is the policy of the University to encourage the distribution of all theses, dissertations, and manuscripts. Copies of all UCSF theses, dissertations, and manuscripts will be routed to the library via the Graduate Division. The library will make all theses, dissertations, and manuscripts accessible to the public and will preserve these to the best of their abilities, in perpetuity.

Please sign the following statement:

I hereby grant permission to the Graduate Division of the University of California, San Francisco to release copies of my thesis, dissertation, or manuscript to the Campus Library to provide access and preservation, in whole or in part, in perpetuity.

Jennifer Gugan
Author Signature

8/26/2013
Date